



January 2015

# Characterization Of Dopamine Transporter Palmitoylation

Danielle Elizabeth Rastedt

Follow this and additional works at: <https://commons.und.edu/theses>

---

## Recommended Citation

Rastedt, Danielle Elizabeth, "Characterization Of Dopamine Transporter Palmitoylation" (2015). *Theses and Dissertations*. 1951.  
<https://commons.und.edu/theses/1951>

This Dissertation is brought to you for free and open access by the Theses, Dissertations, and Senior Projects at UND Scholarly Commons. It has been accepted for inclusion in Theses and Dissertations by an authorized administrator of UND Scholarly Commons. For more information, please contact [zeinebyousif@library.und.edu](mailto:zeinebyousif@library.und.edu).

CHARACTERIZATION OF DOPAMINE TRANSPORTER PALMITOYLATION

By

Danielle Elizabeth Rastedt  
Bachelor of Science, Minnesota State University Moorhead, 2010

A Dissertation

Submitted to the Graduate Faculty

of the

University of North Dakota

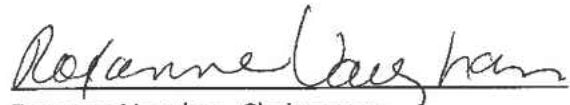
in partial fulfillment of the requirements

for the degree of

Doctor of Philosophy

Grand Forks, North Dakota  
December  
2015

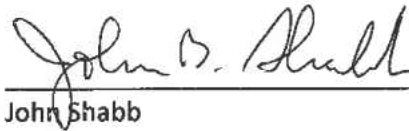
This dissertation, submitted by Danielle Rastedt in partial fulfillment of the requirements for the Degree of Doctor of Philosophy from the University of North Dakota, has been read by the Faculty Advisory Committee under whom the work has been done and is hereby approved.



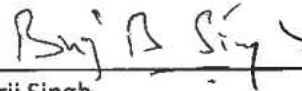
Roxanne Vaughan, Chairperson



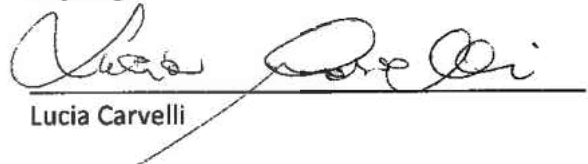
James Foster



John Shabb



Brij Singh



Lucia Carvelli

This dissertation is being submitted by the appointed advisory committee as having met all of the requirements of the School of Graduate Studies at the University of North Dakota and is hereby approved.



Dr. Wayne Swisher,  
Dean of the School of Graduate Studies



Date

## PERMISSION

Title            Characterization of Dopamine Transporter Palmitoylation  
Department    Biochemistry and Molecular Biology  
Degree         Doctor of Philosophy

In presenting this dissertation in partial fulfillment of the requirements for a graduate degree from the University of North Dakota, I agree that the library of this University shall make it freely available for inspection. I further agree that permission for extensive copying for scholarly purposes may be granted by the professor who supervised my dissertation work or, in their absence, by the chairperson of the department or the dean of the School of Graduate Studies. It is understood that any copying or publication or other use of this dissertation or part thereof for financial gain shall not be allowed without my written permission. It is also understood that due recognition shall be given to me and to the University of North Dakota in any scholarly use which may be made of any material in my dissertation.

Name: Danielle Rastedt

Date: 12-2-2015

## TABLE OF CONTENTS

LIST OF FIGURES.....	vi
ABBREVIATIONS.....	viii
ACKNOWLEDGEMENTS.....	x
ABSTRACT.....	xiii
CHAPTER	
I.    INTRODUCTION.....	1
The Synaptic Neurotransmission of Dopamine.....	1
Dopamine Pathways and the Hypothesis of Reward.....	2
The Dopamine Transporter.....	8
The Structure and Transport Mechanism.....	12
Regulation of DAT by Psychostimulants-Blockers and Substrates.....	19
DAT Protein-Protein Interactions.....	21
Regulation of DAT by Lipids.....	26
Protein Palmitoylation.....	27
DAT Palmitoylation.....	33
Purpose of Current Study.....	35
II.   MATERIALS AND METHODS.....	37
Materials.....	37
Equipment.....	38

	Methods.....	40
III.	RESULTS.....	47
	Identification of DAT Palmitoyl Acyl Transferases.....	47
	Palmitoylation Enhances DAT Expression.....	54
	Functional Studies of DAT Palmitoylation in LLCPK <sub>1</sub> Cells.....	57
	Multiple PATs Enhance DAT Palmitoylation and Expression in the N2a Cells.....	59
	Palmitoylation Increase Transporter Capacity via an Alternation of DAT Transport Kinetics.....	62
	DAT Palmitoylation is Present of Surface Transporters....	64
	DAT Palmitoylation at Cys580.....	66
	Lateral Membrane Mobility of DAT.....	69
	Action of Psychostimulants on DAT Palmitoylation.....	71
IV.	DISCUSSION.....	76
	Regulation of DAT Palmitoylation.....	76
	APPENDIX.....	89
	ABE analysis in LLCPK <sub>1</sub> cells.....	89
	ABE analysis in N2a cells.....	91
	REFERENCES.....	92

## LIST OF FIGURES

Figures	Page
1. Schematic diagram of dopaminergic neurotransmission.....	3
2. Dopaminergic pathways in the brain.....	6
3. Schematic diagram of the rat dopamine transporter.....	10
4. Crystal structure of the dopamine transporter.....	14
5. The alternating access mechanism model of the dopamine transporter.....	16
6. DAT protein-protein interactions.....	23
7. Effects of palmitoylation on transmembrane proteins.....	28
8. Domain structure of DHHC enzymes found in the brain.....	30
9. DHHC expression in rDAT LLCPK <sub>1</sub> cells.....	48
10. Acyl-biotinyl exchange method.....	49
11. Multiple DHHC enzymes increase DAT palmitoylation.....	50
12. DHHC-2 induced DAT palmitoylation validated by [ <sup>3</sup> H]palmitic acid labeling.....	52
13. Enzymatic activity of DHHC2 is required for increased DAT palmitoylation.....	53
14. DAT palmitoylation increases total DAT expression.....	55
15. Functional studies in LLCPK <sub>1</sub> cells.....	56
16. DHHC enzymes increase DAT palmitoylation in N2a cells.....	58
17. DAT palmitoylation increases total DAT expression in N2a cells.....	60

18. DAT palmitoylation increases transport $V_{\max}$ in N2a cells .....	61
19. Palmitoylation of DAT does not increase surface expression.....	63
20. Subcellular localization of palmitoylated DATs.....	65
21. Cys580 mediates DHHC2-induced DAT palmitoylation and effects on kinetics.....	67
22. C580A modulates DA transport $V_{\max}$ .....	68
23. Palmitoylation decreases membrane lateral mobility of DAT.....	70
24. Regulation of DAT palmitoylation by psychostimulants in heterologous cells.....	73
25. Regulation of DAT palmitoylation by psychostimulants <i>in vivo</i> .....	74
26. Mechanism of DAT palmitoylation.....	77
27. C-terminal latch of the dopamine transporter.....	81
28. Proposed mechanism of increased DAT expression by DHHC enzymes...	83
29. ABE analysis of co-expressed DHHC enzymes that increased DAT palmitoylation in the LLCPK <sub>1</sub> cells.....	89
30. ABE analysis of co-expressed DHHC enzymes that have no effect on DAT palmitoylation in the LLCPK <sub>1</sub> cells.....	90
31. ABE analysis in the N2a cells.....	91



## ABBREVIATIONS

AADC	Amino acid decarboxylase
ABE	Acyl-Biotinyl Exchange
ADHD	Attention deficit hyperactivity disorder
AMPH	Amphetamine
ANOVA	Analysis of variance
BCA	Bicinchoninic acid
BIM	Bsindolmaleimide
2BP	2-bromo palmitate
BSA	Bovine serum albumin
CaMKII	Calcium-calmodulin dependent kinase II
CFT	2 $\beta$ -carbomethoxy-3 $\beta$ -(4-fluorophenyl) tropane
COC	Cocaine
COMT	Catechol- <i>O</i> -methyltransferase
ConA	Concanavillin A
CRAC motifs	Cholesterol Recognition Amino Acid Consensus
DA	Dopamine
D <sub>2</sub> R	Dopamine D2 receptors
DAT	Dopamine transporter
dDAT	Drosophila dopamine transporter
DHHC	Asp-His-His-Cys
DOPA	Dihydroxyphenylalanine
EL	Extracellular loop
ERK	Extracellular signal-regulated kinase
FRAP	Fluorescence Recovery After Photobleaching
GAT	GABA transporter
GLY	Glycine transporters
GBR 12909	1-[2-[bis(4-fluorophenyl)methoxy]ethyl]-4- 3phenylpropyl)piperazine
GPCR	G protein coupled receptor
HBSS	Hanks balanced salt solution
hDAT	Human dopamine transporter
HPDP	(N-(6-(biotinamido) hexyl)-3-(2'-pyridyldithio)-propionamide
HVA	Homovanillic acid
IL	Intracellular loop

kDA	Kilodalton
KO	Knockout
L-DOPA	3,4-dihydroxyphenylalanine
LeuT	Leucine transporter from <i>Aquifex aeolicus</i>
LLCPK <sub>1</sub> cell	Lewis lung carcinoma porcine kidney cell
MAB	Monoclonal antibody
MAO	Monoamine oxidase
MβCD	Methyl-β-cyclodextrin
METH	Methamohetamine
MMTS	Methyl methanethiosulfonate
NET	Norepinephrine transporter
NH <sub>2</sub> OH	Hydroxylamine
NSS	Neurotransmitter sodium symporter
NTT	Neurotransmitter transporter
PATs	Palmitoyl acyltransferase
PCR	Polymerase chain reaction
PD	Parkinson's disease
PDZ Domain	PSD-95/Discs-large/ZO-1
PICK1	PDZ-domain-containing protein interacting with C-kinase
PKA	Protein kinase A
PKC	Protein kinase C
PMA	Phorbol 12-myristate 13-acetate
PP1	Protein phosphatase 1
PP2A	Protein phosphatase 2A
PPTs	Palmitoyl-protein thioesterases
RACK1	Receptor for active C kinase
rDAT	Rat dopamine transporter
Rin	Ras-like in neurons
SDS-PAGE	Sodium dodecyl sulfate-polyacrylamide gel electrophoresis
SERT	Serotonin transporter
SLC6	Solute carrier 6
SN	Substantia nigra
SNARE	Soluble N-ethylmaleimide-sensitive factor attachment protein receptor
Syn1A	Syntaxin 1A
α-syn	α synuclein
TH	Tyrosine hydroxylase
TMs	Transmembrane
VMAT2	Vesicular monoamine transporter 2
VTA	Ventral tegmental area

## ACKNOWLEDGMENTS

To begin, I would like to thank Dr. Roxanne Vaughan. Her support and encouragement throughout graduate school has made me a better scientist. Dr. Vaughan is the type of mentor that is always wanting you to learn and grow, professionally and personally. Over the years she has helped me design experiments, critically think about the data, and has made me really excited about the discoveries we were making. There were times I would walk into her office with data that I was not thrilled about, and by the end of our meeting she had me eager and motivated to try it again. The high-fives, fist bumps, and OMGs encouraged me more than she will ever know. I would also like to thank her for the countless number of practice presentations she listened to and the never ending abstracts and papers she corrected for me, both have made me a better scientist. Dr. Vaughan has shaped me into a more confident researcher, and for that I will always be grateful.

I would also like to thank Dr. James Foster. He has been a very influential person in my scientific career. He has taught many techniques in the lab, but also how to become a more confident researcher. He always made time for me, even when he had his own lab and students. I would often show up at his door asking if he had a minute and he would always happily say yes. I'm sure he knew every time my questions would never take just a minute. Together, Dr. Vaughan and Dr. Foster have made me the scientist I am today, I am truly privileged to have such great mentors. I would like to thank to my committee

members, Dr. John Shabb, Dr. Brij Singh, and Dr. Lucia Carvelli. They have always provided great feedback and support. I would also like to thank everyone from our former Biochemistry department and our new Basic Sciences department. I especially want to thank Dr. Kathrine Sukalski and Dr. Archana Dhasarathy for their support and guidance over the years. Also I would like to thank Mary and Jenifer for always helping me. From sending a fax or finding a room, they were always there, thank you so much.

I especially want to thank my lab mates Rejwi, Sathya, Margaret, and Mike for being so wonderful. I was lucky to have such wonderful lab mates, they made coming to lab great. We never had a dull moment in the lab, we were always talking! We could be chatting about the “weather” in the lab or important results, there was always something to discuss. Over the years I have gotten to know them all, and I feel they are more than lab mates, they are my friends. I would also like to thank my adopted lab mates Dan and Madhur. They are guys are great! Thank you for always letting me “steal” your chemicals. Also, thank you to all my friends I have made while at grad school, especially, Katie, Liz, Nick, and Danielle. Our happy hours and knit nights were always so much fun, even though I never learned how to knit. Hanging out with them in graduate school kept me sane! I will always remember FLD, FLD! I want to give special thanks to Andrea, she has been by my side since day one. We graduated undergrad together and now we will both become doctors together. She is a great friend. I also have to thank Dr. Joe Provost and Mark Wallert. They gave me the privilege of doing research in high school and fostered my love of science. They both undoubtedly helped make me the scientist I am today.

I want to say thank you to my family. To my parents, that have always showed me unconditional love and support. They have always believed in me, even when I haven't believed in myself. They both taught me to never give up and to always work my hardest. They are the reason I am here today. I owe them everything. I want to thank my sisters, DeeDee and Dacey, for being my inspiration and showing me how to love life. I want to thank the rest of my family and friends for their continued love and support over the years. Finally, I want to thank Mark. He has always supported my goals and dreams, and has pushed me to be a better person. In the last five years we have learned a lot about each other and just how crazy I can get when stressed to the max. His love for me has never wavered. He has always listened when I needed to rant on the bad days, celebrated with me on the good days, and helped me trust in God that things really do happen for a reason. I would have not achieved so much if he wasn't by my side always supporting me.

To my Mom and Dad

## ABSTRACT

The dopamine transporter (DAT) is an integral membrane protein that mediates the reuptake of synaptic dopamine and thus regulates the spatio-temporal dynamics of dopaminergic neurotransmission. DAT is also the target of powerful addictive psychostimulants, including cocaine and methamphetamine that resulted in dysregulation of dopaminergic signaling. Complex control of DAT is exerted by various regulatory processes, including posttranslational modifications. We previously found that DAT is palmitoylated via the addition of a 16-carbon palmitic acid moiety to Cys 580. Pharmacological and mutagenic studies determined that depalmitoylation conditions led to reductions in  $V_{\max}$  and transporter levels, suggesting palmitoylation controls one or more functions of DAT. Palmitoylation is a dynamic and reversible process catalyzed by palmitoyl acyltransferases (PATs) and depalmitoylation is catalyzed by palmitoyl-protein thioesterases (PPTs). PAT enzymes have been further classified as DHHC enzymes based on a conserved cysteine rich domain and the active site sequence Asp-His-His-Cys. Currently, 23 PAT enzymes have been identified in the human genome with some associated with dopaminergic diseases such as schizophrenia; however, the enzymes that act on DAT are unknown. Therefore, we hypothesized that specific PAT enzymes will drive DAT palmitoylation, controlling expression, DA transport, and membrane lateral mobility of the transporter. To address this question, we co-expressed a specific subset of

neuronally-expressed PATs individually with DAT and assessed DAT palmitoylation, total and surface expression, transport activity, and lateral membrane mobility.

Additional studies were also conducted to investigate psychostimulant regulation of DAT palmitoylation.

Palmitoylation assessed by acyl-biotin exchange revealed that the neuronal PATs, DHHC2, DHHC3, DHHC8, DHHC15, and DHHC17 increased DAT palmitoylation at Cys580, while several others had no effect, indicating a level of substrate specificity for actions against DAT. We observed a correlation between increased DAT palmitoylation and increased total DAT expression, consistent with a role for palmitoylation opposing DAT degradation. DAT palmitoylation also led to enhanced DA uptake with no effect on surface levels, suggesting that palmitoylation also increases transport capacity via an alteration of DAT transport kinetics. Our results also indicated that DAT palmitoylation increased the time for recovery after photobleaching, suggesting that increased palmitoylation decreases the membrane lateral mobility of the transporter. Lastly, we observed treatment with methamphetamine but not cocaine resulted in decreased DAT palmitoylation in both heterologous cells and in animal models, suggesting that DAT palmitoylation is regulated by psychostimulants. Palmitoylation thus plays an important role in both short- and long-term regulation of DAT by controlling multiple functions. Therefore, this modification could potentially affect neurotransmitter clearance in dopaminergic disorders where palmitoylation may be impacted.



## **CHAPTER I**

### **INTRODUCTION**

#### **The Synaptic Neurotransmission of Dopamine**

The brain is responsible for physiological and psychological processes of the entire human body. It consists of billions of neurons which communicate by signals from one neuron to another through the release of neurotransmitters. One particular neurotransmitter we are interested in is dopamine (DA). DA was discovered in 1957, by Dr. Arvid Carlsson, when he investigated dopamine in the brains of reserpinized animals treated with L-DOPA (1). Initially, DA was thought to only be the precursor to another neurotransmitter norepinephrine; however, Carlsson discovered that DA was important for physiological function (1–3). DA is important for several physiological roles including movement, reward, and mood. DA like other catecholamines (epinephrine and norepinephrine) is derived from tyrosine which is abundantly found in dietary proteins. Initially, tyrosine is transported into the dopaminergic neuron by amino acid transporters. Once tyrosine enters the neuron, it is converted to L-3, 4-dihydroxyphenylalanine (L-DOPA). This process is catalyzed by cytosolic tyrosine hydroxylase (TH) and the cofactors oxygen, iron, and tetrahydrobiopterin hydroxylates tyrosine. This step in DA synthesis is the rate-limiting step (4). L-DOPA is then decarboxylated to produce DA by aromatic L-amino acid decarboxylase (AADC). Because DA is the starting compound to

generate other neurotransmitters, DA synthesis regulates the synthesis of norepinephrine and epinephrine, the other two catecholamines.

Once DA has been synthesized, the neurotransmitter is transported from the cytoplasm into synaptic vesicles via the vesicular monoamine transporter 2 (VMAT2), where it is stored until release. The concentration of DA in the vesicles is 0.1M, which is 10-1000 times higher than the level in the cytosol (4). Neurotransmitter release of DA is initiated by an action potential that triggers the opening of voltage-gated  $\text{Ca}^{2+}$  channels resulting in a rapid rise in intracellular  $\text{Ca}^{2+}$ . The transient increase in  $\text{Ca}^{2+}$  stimulates the fusion of the synaptic vesicles with the plasma membrane of the presynaptic neuron (synaptic vesicular exocytosis) and the release of the stored DA into the synaptic cleft (5). Once DA is released into the synaptic space it binds to specific receptors found on both the pre and postsynaptic neurons. Neurotransmission is terminated when the excess DA is removed from the synapses by diffusion or reuptake. A small amount of DA is metabolized by catechol-*O*-methyltransferase (COMT) and by monoamine oxidase (MAO) in which homovanillic acid is formed (HVA) (4). However, the primary way DA is removed from the synapse is by the reuptake of DA back into the presynaptic neuron through the action of the dopamine transporter (DAT). DA can then be repackaged into vesicles, awaiting another round of vesicular release. This process is depicted in the schematic diagram in Figure 1.

### Dopamine Pathways and the Hypothesis of Reward

Much of what is known about dopaminergic pathways and behavior comes from anatomical studies that used fluorescence histochemical methods to detect catecholamine

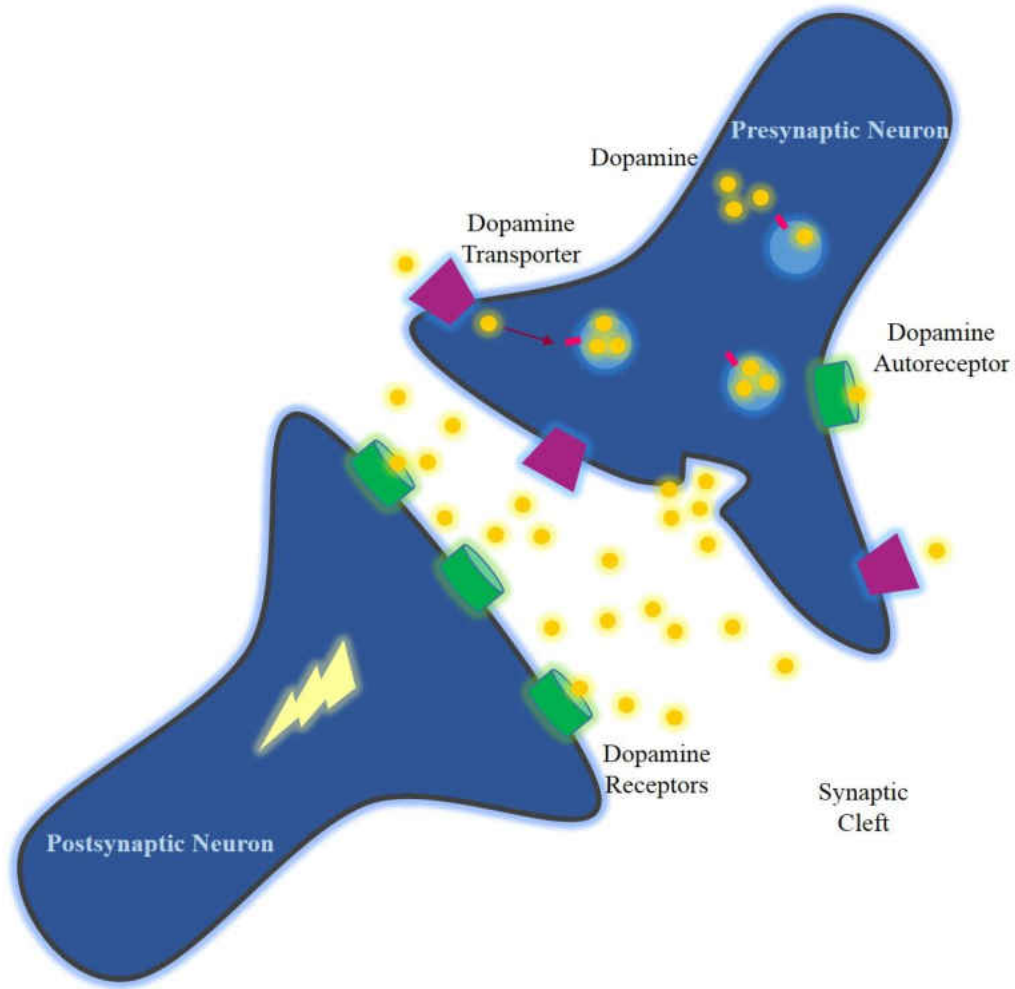


Figure 1: Schematic diagram of dopaminergic neurotransmission. Dopamine (gold circles) is synthesized and packed into synaptic vesicles (light blue) by the vesicular monoamine transporter 2 (VMAT2) (pink rods). Upon an action potential, synaptic vesicles dock at the plasma membrane of the presynaptic neuron and release dopamine into the synaptic cleft. Dopamine then binds to the dopamine receptors (green cylinders) on the postsynaptic neuron, resulting in dopaminergic neurotransmission (yellow lightning bolt). Dopamine can also bind to dopamine autoreceptors on the presynaptic neuron (green cylinders). Dopaminergic neurotransmission is terminated when dopamine is

Figure 1 continued: removed from the synapse by the dopamine transporter (purple trapezoids). Once dopamine is taken up into the presynaptic neuron, it is repackaged into synaptic vesicles waiting for another round of vesicular release.

neurons (6–8). From these studies and others, the major dopamine-mediate pathways were discovered. It was determined that there were four major trajectories of midbrain dopamine neurons, each forming the major dopaminergic pathways (Figure 2). The mesolimbic pathway projects from the ventral tegmental area (VTA) to the limbic system in the nucleus accumbens. These neurons are involved in reward and pleasure pathways and have been associated with diseases such as schizophrenia, attention deficit hyperactivity disorder (ADHD), and addiction. The nigrostriatal pathway projects from the substantia nigra to the striatum in the basal ganglia. These neurons are important for movement and motor control and have been associated with Parkinson’s disease. The tuberinfundibular pathway extends from the hypothalamus to the posterior pituitary. These neurons are important for the inhibition of prolactin secretion, and have been associated with hyperprolactinaemia disorder. Finally, the mesocortical pathway projects from the VTA to the frontal cortex. These neurons are important for motivation, emotion, and attention, therefore associated disorders include schizophrenia, ADHD, and addiction.

Initial electrical stimulation experiments on rats in the 1950s revealed that the brain has specialized centers that control reward functions (9). Additional studies determined that the dopaminergic system was sensitive to electrical self-stimulation in the midbrain from dopaminergic neurons found in the limbic regions. Studies have shown synaptic DA is not only increased by natural rewards such as food, water, and sex, but also by drugs such as cocaine (10, 11). Furthermore, studies have found cocaine self-administration in animals is dependent on the presence of intact mesolimbic neurons (12),

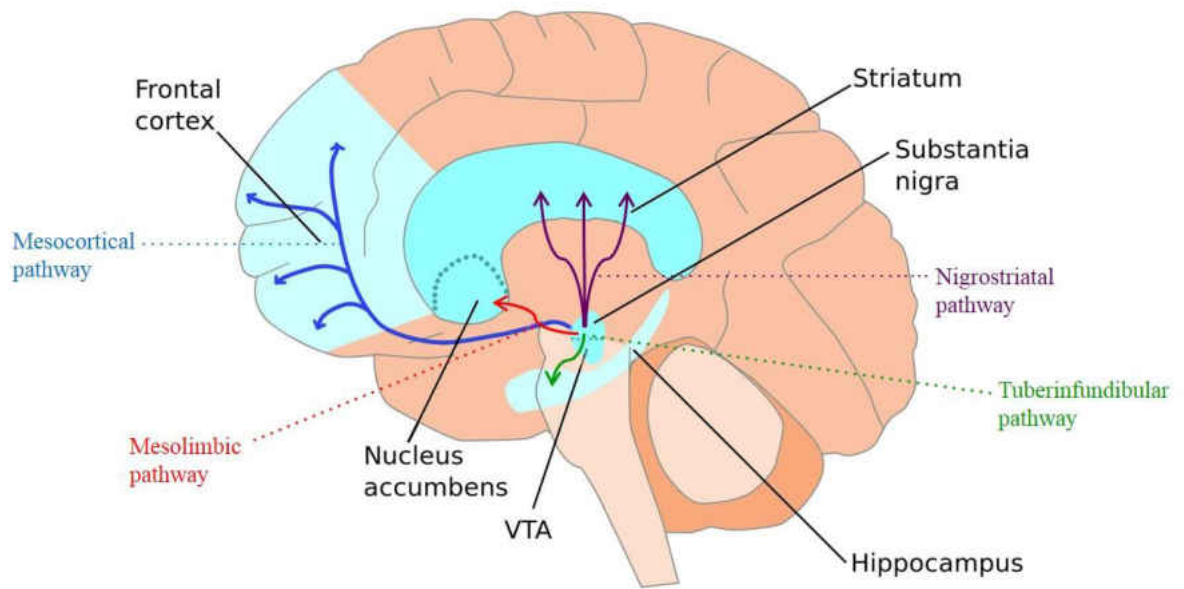


Figure 2: Dopaminergic pathways in the brain. Dopamine neurons projecting from the VTA to the nucleus accumbens form the mesolimbic pathway (red). Dopamine neurons projecting from the VTA to the frontal cortex form the mesocortical pathway (blue). Dopamine neurons projecting from the substantia nigra to the striatum form the nigrostriatal pathway (purple). The tuberinfundibular pathway (green) extends from the hypothalamus to the posterior pituitary. Image modified from Okinawa Institute of Science and Technology (OIST), Okinawa, Japan; with permission

thus it is thought that the mesolimbocortical pathways are important for mediating reinforcement processes of cocaine (13, 14). Together, these studies support the dopamine hypothesis of reward, that suggest drugs of abuse are rewarding due to the increase in DA in the mesolimbic system (13).

To further study the dopamine hypothesis, investigators observed a DAT knockout (KO) mouse (15). In this model, disruption of the mouse DAT gene resulted in spontaneous hyperlocomotion, signifying the importance of DAT in the dopaminergic system (15). In DAT KO mice, DA remained in the extracellular space 100 times longer than wild-type (WT) animals, suggesting clearance by diffusion. Investigators concluded that in the WT animals, DA was cleared faster due to the presence of DAT, suggesting DAT is the key factor in controlling synaptic dopamine levels and ending neurotransmission. From these studies it was also demonstrated that DAT was the target of these psychostimulant drugs including cocaine and amphetamines (15).

However, other studies suggest more than one system may be important for reward. Rocha et al. found DAT KO mice self-administered cocaine (16), while others have found DAT KO mice displayed cocaine-conditioned place preference (17). Together, these studies suggested the possibility of other systems such as the serotonergic system that may be involved in the rewarding effects of cocaine. To further study this concept, serotonin (SERT) KO mice were generated to evaluate the serotonergic system in reward pathways. SERT KO mice also displayed cocaine-conditioned place preference (17), however, the combined DAT/SERT KO mice did not. In contrast, norepinephrine (NET)/SERT KO mice and NET/DAT KO mice still displayed cocaine-conditioned place preference (18), strengthening the argument that SERT may also be involved in the

reward pathways. The DAT KO mice were shown to have many adaptive changes including reduction in DA, tyrosine hydroxylase, and D1 and D2 dopamine receptor levels (15), suggesting adaptive changes may alter the normal reward pathways.

To overcome the adaptive changes observed with the DAT KO mouse, a DAT knock-in mouse line carrying a cocaine-insensitive but functional DAT was created (19). A triple mutations made in TMD 2 resulted in a 69-fold reduction in cocaine inhibition, while nearly 50% of DAT was retained compared to WT DAT (19). Furthermore, the cocaine insensitive knock-in mice displayed abolished cocaine self-administration and cocaine reward as measured by conditioned place preference (20). These results support the dopamine hypothesis, suggesting that DAT is necessary for cocaine reward in mice with a fully functional DAT (20).

### The Dopamine Transporter

The solute carrier 6 (SLC6) are a family of secondary active co-transporters that use extracellular sodium and chloride as a driving force for substrate translocation (21). This family is divided into four subclasses based on sequence similarity and substrate specificity (22). The subfamilies include the neurotransmitter transporters (NTT), the amino acid transporters, creatine transporters, and osmolyte transporters. Specifically, the NTT family includes three  $\gamma$ -aminobutyric acid (GABA) transporters (GAT), two glycine transporters (GLY) and the monoamines, SERT, NET, and DAT.

DAT is a plasma membrane protein expressed in dopaminergic neurons and is essential for regulating dopaminergic neurotransmission. Molecular cloning of DAT has been done in several species including human, rat, mouse, monkey, *Drosophila*



*melanogaster*, and *Caenorhabditis elegans*. From these studies the primary sequence of human (h) and rat (r) DAT is predicted to be 620 and 619 amino acids, respectively, with hDAT containing an extra glycine at position 199 (23). The predicted structure in mammalian DAT includes 12 transmembrane spanning domains, intracellular termini, and a large extracellular loop (EL) between TMD 3 and 4 that contains four glycosylation sites (23–26) (Figure 3). Additionally, four zinc coordinating residues have been identified that are important for stabilizing the outward facing conformation of DAT, acting as a DA uptake inhibitor (27, 28). The zinc coordinating residues found in both EL2 and EL4, are H193 (EL2), D206 (EL2), H375 (EL4), and E396 (EL4) on hDAT (27, 28).

DAT is also modified by many posttranslational modification found throughout the protein. The posttranslational modifications include phosphorylation and ubiquitylation on the N-terminal tail, glycosylation on EL2, and palmitoylation on the C terminus (discussed in future section) (Figure 3). Together these posttranslational modifications affect the regulation, function, and structure of DAT.

Ubiquitylation is a posttranslational modification in which an ubiquitin group is added to a lysine residue. Mass spectrometry analyses of DAT indicated constitutive ubiquitylation of DAT, with an increase in DAT ubiquitylation upon PKC activation. (29). Ubiquitylation of other transmembrane proteins was found to be important as a sorting signal for endocytosis and lysosomal degradation; therefore, experiments were conducted to determine if this was also true for DAT (30). A triple mutation of Lys19, Lys27, and Lys35 in hDAT on the N-terminal tail resulted in abolished PKC dependent

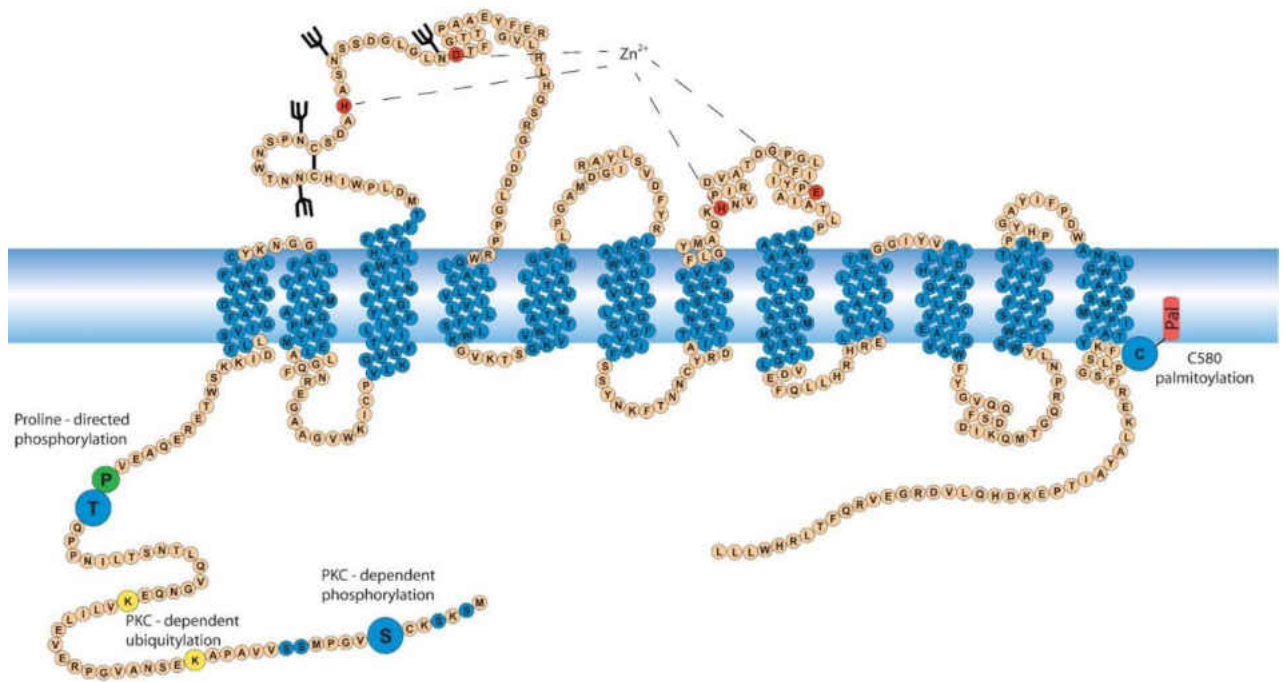


Figure 3: Schematic diagram of the rat dopamine transporter. The structure contains 12 transmembrane domains with N- and C-termini intracellularly oriented. The blue residues represent the transmembrane domains. The large extracellular loop (EL) 2 contains the four glycosylation sites and the N-terminal tail contains two ubiquitylation sites, depicted in yellow. The zinc coordination sites found in EL2 and EL4 are represented by red. The PKC dependent serine phosphorylation sites and the threonine proline-directed phosphorylation site are depicted in blue, with the proline represented by a green residue. The blue cysteine residue on the C-terminus denotes the palmitoylation site on rDAT.

internalization, suggesting the ubiquitin moieties conjugated to DAT are important for interactions with the endocytic machinery (30).

DAT is also heavily glycosylated protein, with the sugars attached to asparagine residues in EL2 (31). Research has shown glycosylation of DAT is important for trafficking and targeting DAT to the cell (32, 33). Furthermore, proper DAT folding was found to be facilitated by a disulfide bond in EL2 between cysteines 180 and 189 (34). This bond was found to be important for proper function of DAT (34).

Studies have also shown that DAT is a phosphoprotein (35–37). This posttranslational modification on DAT affects DAT function and is regulated by protein kinases, suggesting another mechanism for temporal and spatial control of synaptic transmitter levels in dopaminergic signaling. Through phosphoamino acid and protease-based peptide mapping analysis, the direct region of DAT phosphorylation in rat brain tissue was determined (38). Results identified one or more serines on the N terminal tail to be the major sites of both basal and stimulated phosphorylation (38). Additional studies identified the cluster of serines present within the first 21 N-terminal residues to be the site where the majority of basal, PKC-induced, and amphetamine-induced phosphorylation occurs (38–40). Through mutagenic studies, serine 7 was identified as the major site of PKC dependent phosphorylation in both rat striatal DAT and heterologous cells expressing rat and human DAT (41). Interestingly, a mutation at serine 7 resulted in decreased binding affinity for a cocaine analog, further suggesting phosphorylation at serine 7 is important for regulation transporter conformation (41).

An additional phosphorylation site on DAT was also determined to be important for DAT function (37). Studies identified DAT to be phosphorylated at residue Thr53 in

rat and mouse striatum, as well as in heterologous cells (42). Mutagenic studies at position 53 resulted in reduced DA transporter  $V_{max}$ , suggesting the importance of this residue in transporter kinetics (42). This site is different from the PKC phosphorylation site since the Thr53 residue is followed by a proline, making it specific for proline-directed kinases, such as extracellular signal regulated kinase (ERK). Phosphorylation of proline-directed sites are characterized by alterations in protein structure due to the protein being regulated by cis-trans isomerization of the phosphoacceptor-prolyl peptide bond (43), suggesting Thr53 may play a role in the transporter function by affecting the conformation of the protein.

### The Structure and Transport Mechanism

Prior to the first high resolution X-ray crystal structure of the bacterial homolog of the SLC6 transporters, most of the structural understanding was based on observations and mutagenesis studies. However, that changed in 2005, when the leucine transporter (LeuT) from the thermophile bacterium *Aquifex aeolicus* was crystalized with the substrate leucine and two sodium ions bound (44). For the first time, this prokaryotic homolog gave insight into the transporters topology and secondary structure. The crystalized structure confirmed many predictions by revealing 12 TMD connected by short intracellular and extracellular loops, in addition to intracellular N and C termini. The overall LeuT structure is asymmetric with two similar structural motifs arranged by a pseudosymmetric inverted repeat architecture. The 5 + 5 + 2 architecture shows TMDs 1-5 and 6-10 to form helical bundles that are antiparallel, resulting in a pseudo two fold axis symmetry. The TMDs pack together in a helix bundle to form two distinct regions of the transporter, the interior core, and the outer region. The inner core is formed by

TMD1, TMD3, TMD6, and TMD8, together these TMDs form the central substrate binding site (S1) as well as the Na<sup>+</sup> binding sites. Overall, LeuT and SLC6 transporters share 20-25% sequence identity. However, the central core that is important for transport and substrate binding share a high sequence identity of about 55-67% (44, 45). Furthermore, 7 of the 11 residues in LeuT that have direct interactions with the substrate are conserved in all nine mammalian neurotransmitter transporters, suggesting the S1 site is structurally conserved between LeuT and SLC6 transporters (21). This finding is supported by experimental evidence also identifying the S1 residues (45–48).

Although the LeuT structure is the basis for the SLC6 family of transporters it is important to note there are several differences between the prokaryotic and eukaryotic SLC6 transporters (44). The eukaryotic transporter has much longer intracellular N- and C-termini; a longer EL2 loop which contains a disulfide bond and glycosylation sites; and finally several posttranslational modifications that affect the regulation and function of the transporter. Prior to the LeuT crystal structure it was suggested from sequence analysis and biochemical approaches that the monoamine family included these important posttranslational modifications (33, 49). Although models of eukaryotic transporters based on LeuT provided insight into substrate binding, there are still many questions regarding the structure and function. In 2013, the Gouaux lab crystalized the *Drosophila melanogaster* dopamine transporter (dDAT) (50) (Figure 4A). The structure of dDAT was crystallized at a 3.0 Å resolution bound to the tricyclic antidepressant nortriptyline. The dDAT has over 50% sequence homology with the mammalian transporters DAT, NET, and SERT, making it a very useful tool. While dDAT was similar to LeuT there

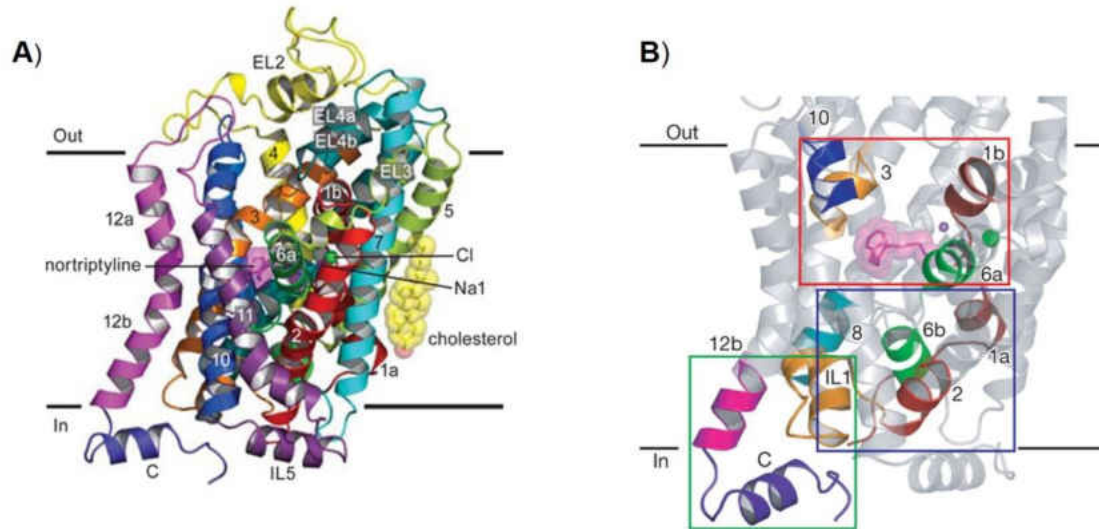


Figure 4. Crystal structure of the dopamine transporter. (A) x-ray crystal structure of the *Drosophila melanogaster* dopamine transporter (dDAT) in complex with the TCA nortriptyline. The structure also shows a cholesterol molecule wedged into a groove formed by TMD1, TMD5, and TMD7. (B) Locations of the open extracellular gate (red box), closed intracellular gate (blue box), and C-terminal latch (green box). Image modified from A. Penmatal, K.H. Wang, and E. Gouaux. 2013. X-ray structure of the dopamine transporter in complex with tricyclic antidepressant. *Nature* 503(7474): 85-90, with permission.

was additional information provided by this structure. The dDAT structure determined that a cholesterol molecule was wedged in a groove formed by TMD1, TMD5, and TMD7, likely important for stabilizing the outward-open conformation (51, 52). The structure also revealed two attributes on the C-terminus. First the crystal structure revealed a kink in TMD12 halfway across the membrane bilayer at Pro572 that causes the intracellular portion of the helix to turn away from the transporter. The structure also revealed a latch-like C-terminal helix thought to be important for interactions with the cytoplasmic face of the transporter. The C-terminal helix was also found to interact with IL1, which interacts with TMD1a (Figure 4B). The close proximal interaction with the cytoplasmic gate suggests the C-terminal helix may be important for modulating transport activity (50). Together, the LeuT and dDAT crystal structures provided important information about the structures and mechanism of SLC6 transporters that was previously unknown.

The process through which DAT transports substrate from the outside of the cell to the inside of the cell is known as the alternating access mechanism. The alternating access mechanism was first coined in 1966 by Dr. Oleg Jardetzky (53). This term was used to describe the conformational changes transporters use to alternate through when transporting substrate from the extracellular space into the cytoplasm. Now with a more complex understanding, it is widely accepted that membrane proteins, including SLC6 proteins, transport their substrate through a series of conformational changes via the alternative access mechanism (21, 54) (Figure 5). The transition of these conformations dictate the transport capacity.

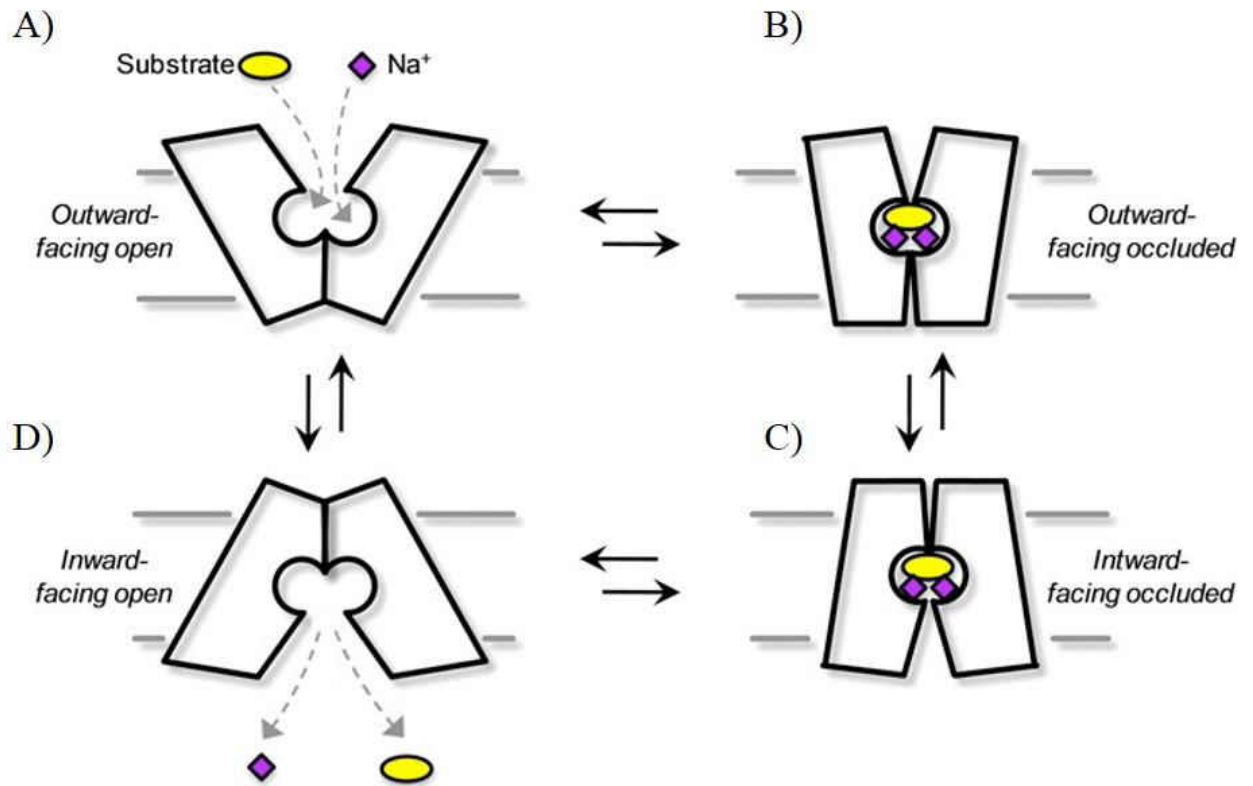


Figure 5: The alternating access mechanism model of the dopamine transporter. A schematic representation of the conformations of DAT important for translocation of substrate from the extracellular space to the cytoplasm. (A) The transporter in an outward facing conformation allowing substrate to bind. The transporter is facing the extracellular space with the extracellular gate open and the intracellular gate closed. (B) The transporter is an outward occluded (C) or inward occluded configuration in which ions and substrate are in there appropriate binding sites, both the extracellular and intracellular gates are closed. (D) Inward facing conformation. The extracellular gate is closed while the intracellular gate opens allowing substrate and ions to be released into the cytoplasm of the cell. Once the substrate is released, the transporter will return to the outward facing



Figure 5 continued: conformation awaiting the next round of translocation. Image modified from Kristensen AS, Andersen J, Jorgensen TN, Sorensen L, Eriksen J, Loland CJ, Stromgaard K, and Gether U. 2011. SLC6 neurotransmitter transporters: structure, function, and regulation *Pharmacol Rev* 63(3):585-640, with permission.

DAT cycles through outward and inward facing conformations that allow for binding of substrates and release into the cytoplasm. Initially, when DAT is in the outward open conformation, the extracellular gate is open allowing substrate to bind. At the same time, the intracellular gate is closed, sealing off the cytoplasmic side from the aqueous extracellular environment (Figure 5A). Once the substrate is bound, the transporter transitions into an occluded state in which both the extracellular and intracellular gates are closed (Figure 5B and C). In a similar manner, the intracellular gate is opened while the extracellular gate is closed thus releasing the substrate into the cell (Figure 5D). Once the substrate has been released the transporter returns to the lowest energy conformation, outward facing, waiting for the next substrate to bind. The gating residues responsible for the transition of conformations are based on the LeuT structure (44). The extracellular gate is formed by the ionic interaction of Arg85 and Asp477. Additionally, Tyr156 and Phe320 form aromatic lids that act as a secondary external gate, preventing access to the central substrate binding site. The intracellular gate is formed by the ionic interaction of Arg60, Ser334, Tyr335, and Asp436. Additionally, Trp63 stabilizes the intracellular halves of TMDs 1 and 6. There have been several proposed models for the translocation of substrate in the transporter core during the outward to inward transition. One model suggests the unwound region in the middle of TMD1 and TMD6 acts as a flexible hinge that can move the intracellular halves independently during a conformational outward to inward transition (21, 44, 55, 56). Another proposed model suggests TMD1 and TMD6, along with TMD2 and TMD7, form a rigid body that rocks back and forth allowing the transition between outward and inward facing conformations (21, 54). The conformation of the transporter is important for kinetics

regulation and functionality. Changes in conformation can result in reverse translocation of substrate (efflux), which requires binding and outward translocation of intracellular DA (57, 58).

### Regulation of DAT by Psychostimulants- Blockers and Substrates

DAT is the target of many clinically used drugs, such as bupropion (Wellbutrin®, an antidepressant), methylphenidate (Ritalin®, ADHD medication), and mazindol (Mazindor®, an appetite suppressant) (21, 59). As well, DAT is also the main site of action for powerful addictive psychostimulants including cocaine and methamphetamine (METH). These drugs work by disrupting normal dopaminergic neurotransmission by either blocking DAT or increasing DA efflux. Both conditions lead to prolonged dopaminergic signaling resulting in the euphoric feeling associated with drug addiction (60). Neurochemical imaging studies have shown chronic use of cocaine or METH can lead to long-term impacts on DAT levels by mechanisms that are not fully understood (61, 62). In addition to the direct effects on DA transports, multiple studies have shown that DAT activity is regulated by blockers and substrates after pretreatment followed by washout, indicating drugs of abuse can affect dopaminergic neurotransmission even after the removal of the drugs.

The two classifications of drugs that act on DAT are substrates and blockers. Drugs like cocaine act as blockers by binding to DAT and inhibiting the reuptake of DA from the synapse, increasing synaptic DA levels. Cocaine has been shown to effect DAT regulation in postmortem samples of human cocaine addicts (63), suggesting chronic abuse of cocaine can cause long term effects in humans. In contrast to blockers, AMPH

and METH act as DAT substrates, competing with endogenous DA for transport and inducing DA efflux through transporter reversal (59, 64–67). METH and AMPH have been shown to have pronounced alterations on DAT trafficking and DA uptake levels (59, 64–68). These effects on transport and surface expression have been shown to be blocked by cocaine, indicating these substrates are activity transported into the cell by DAT (59, 64). Studies show short time exposure (less than 1 minute) to AMPH results in DAT recruitment to the plasma membrane and an increase in transport (69–71). It is thought this rapid recruitment of DAT is important for clearance of extracellular DA induced by the drug (69, 71). In contrast longer exposure to METH and AMPH have resulted in DAT downregulation and endocytosis of DAT (39, 71–73). Downregulation after longer substrate exposure times is thought to be a neuroprotective mechanism by limiting the cytosolic accumulation of DA and its neurotoxic metabolites.

AMPH-stimulated downregulation is thought to occur by both kinetic and endocytotic downregulation mechanisms, because AMPH-induced downregulation has been found in the absence of endocytosis (72, 74). Research has shown that METH-and-AMPH-induced DAT phosphorylation can be blocked by inhibition of PKC, demonstrating PKC is involved in the regulation of DAT by substrates (39, 75, 76). Likewise, METH and PKC induced DAT phosphorylation can be reduced by the truncation of the first 21 residues in DAT, suggesting METH and PKC-mediated phosphorylation occur in the same region of DAT. AMPH and METH have also been shown to stimulate DA efflux (59, 64–67), however this mechanism is poorly understood. Additionally, AMPH stimulated efflux can be impaired when deletions of distal N terminal serines or disruption of the CaMKIIa binding domain occur (77, 78),

though it is not clear how the N-terminus and CaMKIIa operate together for AMPH induced efflux.

### DAT Protein-Protein Interactions

It is well known that DAT is not an isolated protein, but rather a highly regulated multiprotein complex formed by protein-protein interactions (79) that regulate trafficking and function of DAT. Multiple proteins are known to bind and interact with both the N- and C-termini of the transporter (Figure 6). Regulatory partners discovered to interact with the N-terminus include Syntaxin 1A (Syn1A) and D2 receptors. Using a yeast two-hybrid system, Syn1A (80) was revealed to have novel interactions with DAT. Syn1A is a member of the soluble *N*-ethylmaleimide sensitive factor attachment protein receptor (SNARE) protein family and has been shown to mediate AMPH-induced DA efflux in murine synaptosomes and in *C. elegans* to regulate DAT1 ion channel activity (81, 82). Together, these studies have identified the Syn1A binding site on DAT to be on the N-terminus of DAT at residues 1-33. (81, 82). Additional studies aimed at understanding the regulation of Syn1A and DAT found that an overexpression of Syn1A reduces transport  $V_{max}$  and affects surface expression (83). Furthermore, cleavage of Syn1A, with the protease Botulinum Neurotoxin C (BoNT/C) increases DA transport  $V_{max}$  and reduced DAT phosphorylation, suggesting Syn1A interaction with DAT may affect regulatory mechanism important for DAT function (84). Another protein known to directly interact with DAT is the G-protein coupled receptor (GPCR) family member, dopamine receptor, D2. D2 receptors function as autoreceptors allowing an inhibitory feedback mechanism by altering DA synthesis, release, and reuptake in response to increasing levels of extracellular DA found in the synapse. D2 and DAT interactions

involve the N-terminus of DAT and the third intracellular loop of the D2 receptor (85). The physical interaction facilitates the recruitment of DAT to the plasma membrane resulting in enhance DA uptake (85).

Other DAT regulatory partners that interact with DAT near the C-terminus of the transporter include, protein interacting with kinase 1 (PICK1), Rin1 (Ras-like in neurons), flotillin 1 (Flot1), calcium-calmodulin-dependent protein kinase (CaMKIIa), Parkin, and  $\alpha$ -synuclein ( $\alpha$ -syn) (77, 86–91). PICK1 is a PSD-95/Discs-large/ZO-1 (PDZ)-domain containing protein that is important for clustering receptors and ion channels (92). Interestingly, hDAT contains a PDZ binding sequence (LKV) at the end of the C-terminus. PICK1 was a candidate for a regulatory interaction of DAT based on a yeast two-hybrid screening (86). Originally, the interaction between PICK1 and DAT was thought to be important for endoplasmic reticulum (ER) export of DAT. Initial studies, found the truncation of C terminal of DAT resulted in ER retention and impaired surface expression (86). However, it was later demonstrated that the PDZ-binding interactions of DAT was not necessary nor sufficient for DAT surface expression in heterologous cells (93). Additional *in vivo* studies determined DAT knock-in mice with disrupted PDZ-binding motifs had a dramatic loss of DAT expression in the striatum, suggesting PDZ domain interactions were critical for synaptic distribution of DAT in order to maintain DA homeostasis (94).

Rin was identified by yeast two-hybrid screening to interact with DAT was (88). Previous studies determined residues 587-596 (FREKLAYA) encoded an endocytic regulatory domain that modulates both basal and PKC-enhanced DAT internalization rates; (87). Therefore, studies aimed at understanding where Rin binds were performed. It

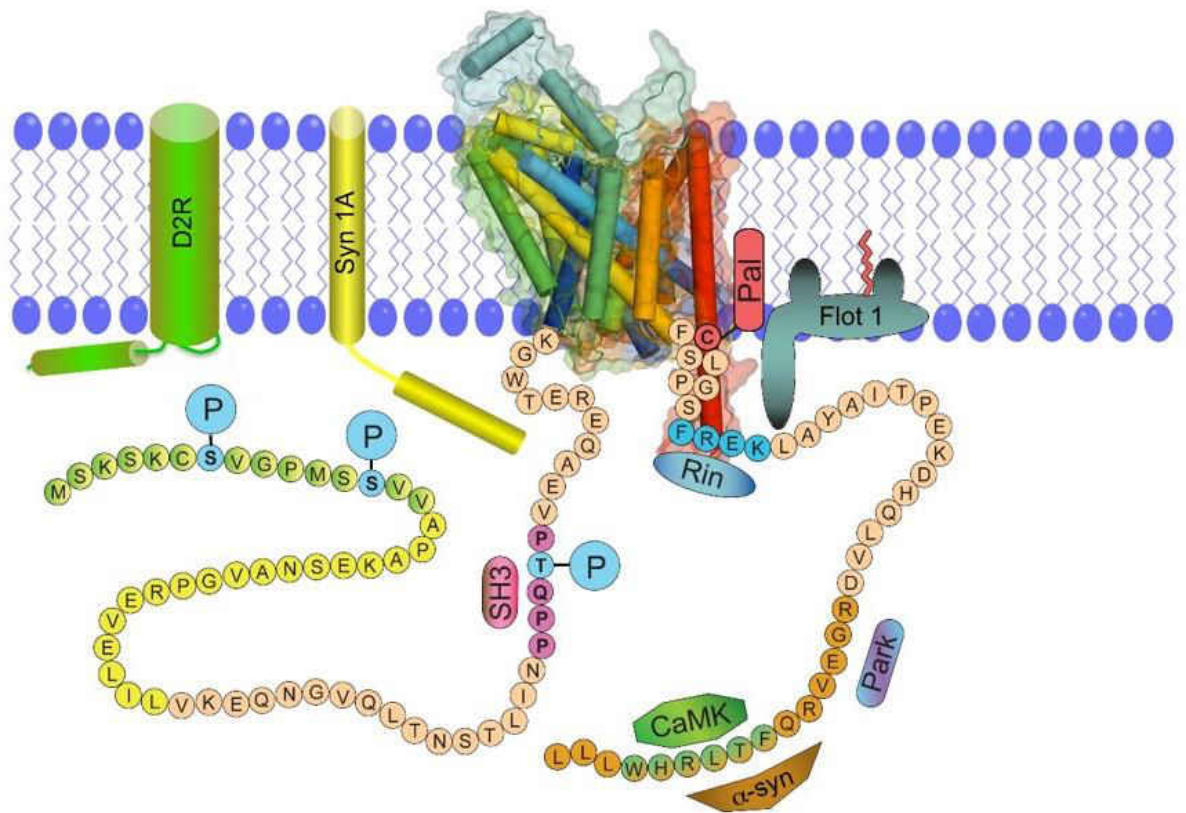


Figure 6: DAT protein-protein interactions. The transporter is positioned in the membrane lipid bilayer with the N-and-C termini. The various binding partners of DAT are depicted based on where they bind or interact with DAT. Syntaxin 1A (Syn1A), dopamine autoreceptor2 (D2), protein interacting with kinase 1 (PICK1), Rin1 (Ras-like in neurons), flotillin 1 (Flot1), calcium-calmodulin-dependent protein kinase (CaMKIIa), Parkin, and  $\alpha$ -synuclein ( $\alpha$ -syn). Modified image from Vaughan RA and Foster JD. Mechanisms of dopamine transporter regulation in normal and disease states 2013. Trends in Pharmacological Sciences 34(9):489-496, with permission

was determined that Rin interacts with DAT at residues 587-590 on the C-terminus in a PKC-regulated manner, which is required for PKC-mediated DAT internalization (88).

Flot1 also known as Reggie 2 is a membrane raft protein whose binding site on DAT is currently unknown (95). Flot1 is highly conserved and expressed in the nervous system and thought to be important for endocytosis (96). This protein associates with the membrane in a cholesterol-dependent manner, resulting in hetero-oligomers and microdomains in the plasma membrane (97). Current studies suggest Flot1 is required for PKC-triggered endocytosis of DAT (95). Furthermore, it was determined that DAT complexes with palmitoylated Flot1 in a PKC-dependent manner and a conserved serine residue of Flot1 is required for PKC-mediated internalization. It was also demonstrated that Flot1 is important to maintain DAT in membrane rafts, suggesting DAT membrane microdomain localization may be important for endocytosis of DAT; however unknown at this time (95).

CaMKII $\alpha$  binds to the distal C-terminus of DAT at residues 612-617 (77) and has been shown to play an important role in AMPH-mediated efflux of DA in heterologous cells and dopaminergic neurons. Fog et. al. demonstrated *in vitro* that CaMKII $\alpha$  is responsible for phosphorylating the serines found on the distal N terminus (77). A mutation made on the C-terminus impaired CaMKII $\alpha$  binding and AMPH-induced efflux. Thus suggesting CaMKII $\alpha$  binding to DAT on the C-terminus facilitates phosphorylation of DAT on the N terminus.

Parkin and  $\alpha$ -syn are two proteins associated with Parkinson's disease. Initial studies determined that  $\alpha$ -syn interacts with the carboxyl tail of hDAT, resulting in the formation of membrane clustering, thereby increasing DA uptake and DA induced



cellular apoptosis (98). This was proposed to be a possible mechanism for the degradation of dopaminergic nerve terminal in Parkinson's disease (98). It was later determined that parkin, an E2-dependent E3 protein ubiquitin ligase, exerts protective effects against DA-induced  $\alpha$ -syn toxicity (90). This study established that parkin impairs the  $\alpha$ -syn and DAT complex by interacting with the carboxyl tail of DAT and blocking  $\alpha$ -syn induced enhancement of DAT surface expression and DA uptake (90).

It is known that neurotransmitter transporters exist as oligomeric complexes in cell, however the function of these complexes are unclear. SERT was initially detected by co-immunoprecipitation to form oligomers (99), and it was later discovered that DAT also forms dimers (33). Additional studies using fluorescence resonance energy transfer (FRET) revealed DAT oligomers are formed in the ER and are continually maintained at the cell surface and during trafficking events between the plasma membrane and endosomes (100). Furthermore, oligomer formation is important for proper targeting of newly synthesized DATs to the plasma membrane (101). The LeuT crystal structure determined the dimer interface was formed by EL2, TM9, and TMD12 (44).

More recently, studies suggest a role for oligomerization in regulating DA transport function. It was discovered that substrates of DAT including DA and amphetamine, are involved in dissociation of DAT oligomers, shifting the distribution of surface DAT from oligomers to more monomers (102). From these studies, it was suggested that substrate induced internalization could be mediated by DAT monomers (102). Additionally, studies have found the formation of oligomers affects the binding properties of DAT, suggesting cooperativity within an oligomer (103).

### Regulation of DAT by lipids

Integral membrane proteins can segregate into plasma microdomains known as membrane rafts. Membrane rafts are small 10-200 nm domains that are highly enriched in cholesterol and sphingolipids (104). These microdomains are important for scaffolding processes such as receptor signaling. These small, highly dynamic rafts can sometimes be stabilized to form larger microdomains through protein-protein and lipid-protein interactions (104). Several membrane proteins are functionally regulated through their association with membrane rafts, including serotonin, norepinephrine, and glutamate transporters (105–107).

DAT has also been found to be associated with membrane microdomains, with a relatively equal distribution between membrane rafts and non-raft domains (108, 109). Studies have shown cholesterol is important for transport activity of DAT. Depletion of cholesterol by methyl  $\beta$  cyclodextrin (m $\beta$ CD) results in a significant decrease in DA uptake (108, 109), lowering both DAT's affinity for DA and the  $V_{\max}$  (109). Membrane mobility and microdomain association of DAT has also studied by fluorescence recovery after photobleaching (FRAP). Adkins et. al demonstrated that cholesterol depletion significantly reduces membrane lateral diffusion of DAT, indicating DAT is more mobile (109). Together these studies indicate association of DAT with lipid microdomains regulates both lateral membrane mobility of the transporter and transport capacity.

Additional studies have focused on the direct interaction of cholesterol and DAT. Research has shown that cholesterol can modulate the transporter into an outward facing conformation with moderate increases in membrane cholesterol content, allowing for increased binding sites for radiolabeled cocaine analogs and enhanced sulfhydryl

accessibility to cysteines (51). Additional studies have shown that disruption of membrane cholesterol by m $\beta$ CD in both raft and non-raft membrane domains results in reduced efflux rate (110). Together, these studies suggest an important role for direct DAT-cholesterol interactions, vital for the regulation of transporter function (51, 110).

Cholesterol can interact with many proteins through Cholesterol Recognition Amino Acid Consensus (CRAC) motifs. The specific sequences L/V-X<sub>(1-5)</sub>-Y-X<sub>(1-5)</sub>-K/R can bind sterols via hydrophobic aromatic and H-bonding interactions (111). These particular CRAC motifs are found in DAT in TMD1, TMD4, TMD6, TMD7, TMD12, and the C terminus (68). These sequences are also highly conserved in NET and SERT. It is unknown if these CRAC motifs are important for interactions between DAT and cholesterol binding, however, it would suggest another mechanism for DAT regulation via cholesterol.

### Protein Palmitoylation

Many proteins, especially those associated with membrane rafts, are modified by palmitoylation. *S*-palmitoylation consists of a thioesterification of a 16-carbon fatty acid (palmitate) on a specific cysteine residue. Palmitoylation increases protein hydrophobicity, mediates protein-lipid bilayer interactions, and can alter protein sorting, function, and regulation (112–116). Specifically for membrane proteins, palmitoylation has been shown to affect the conformation of TMDs by hydrophobic matching, promote association with lipid microdomains, promote the formation of protein complexes, and affect the interplay with other posttranslational modifications (117–121) (Figure 7). Unlike myristoylation and prenylation, which are stable and permanent lipid modifications, the thioester bond that links palmitate to the protein is labile and

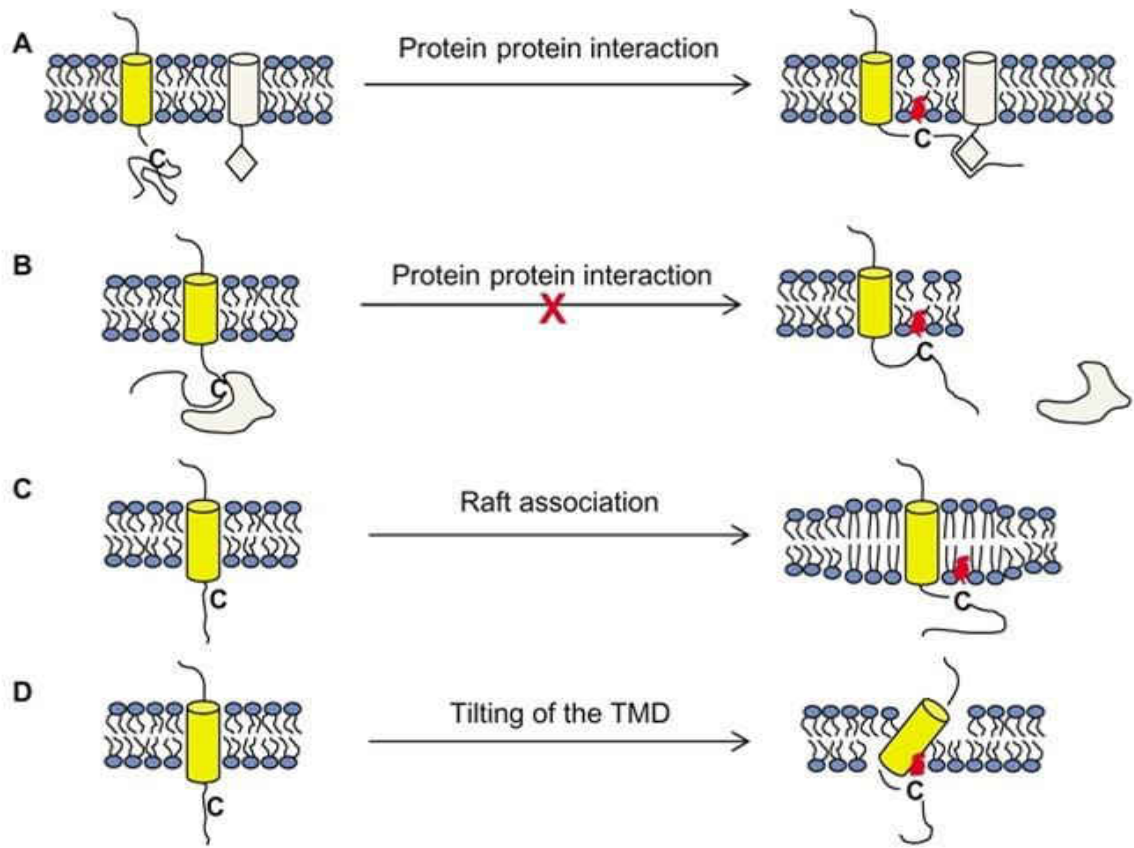


Figure 7: Effects of palmitoylation on transmembrane proteins. (A) Palmitoylation (red rectangle) of transmembrane proteins (yellow cylinder), can promote protein-protein interactions by modifying the conformation of the protein. (B) Palmitoylation can inhibit protein-protein interactions by changing the conformation of the protein. (C). Palmitoylation can promote proteins to associate with specific microdomains. (D) Palmitoylation group change the conformation of the protein by tilting the TMD. Image modified from Charollais J & Van Der Goot GF. 2009: Palmitoylation of membrane proteins *Molecular Membrane Biology*. 26(1-2): 55-66, with permission.

reversible. For many proteins, cycles of palmitoylation and depalmitoylation occur throughout their lifetime (122). Palmitoylation-depalmitoylation cycles can be constitutive or dynamically regulated by signaling events (123, 124), like phosphorylation.

Palmitoylation is catalyzed by palmitoyl acyltransferases (PATs) while depalmitoylation is catalyzed by palmitoyl-protein thioesterases (PPTs). PATs are polytopic membrane proteins (125, 126), suggesting that palmitoylation reactions generally occur near the cytosol membrane interface (127). Systematic screening has recently identified a large family of PAT enzymes in the human genome (112, 125, 128–130), also known as the DHHC enzymes. The PAT enzymes are characterized by the presence of a 50 amino acid cysteine rich domain that contains a conserved amino acid sequence Asp-His-His-Cys (DHHC) in the active site (130). Besides the DHHC core domain, these proteins also contain four or more TMDs, with the DHHC domain usually located between TMD2 and TMD3 (113, 126, 131, 132) (Figure 8). Additionally, some DHHC enzymes have individual protein-protein interacting domains such as a PDZ-binding domain (DHHC3 and DHHC8); SH3 domain (DHHC6); or ankyrin repeats (DHHC13 and DHHC17) (113, 126, 131) (Figure 6). Additionally, The 23 PATs have varied tissue distributions and intracellular localizations, with most being localized to the Golgi apparatus, endoplasmic reticulum, or the plasma membrane (132, 133). The large number of DHHC proteins along with their localization to specific cellular compartments suggests that palmitoylation machinery is tightly regulated and highly controlled.

In contrast to the large number of DHHC enzymes that catalyze palmitoylation, few depalmitoylating enzymes have been discovered. Depalmitoylating enzymes include

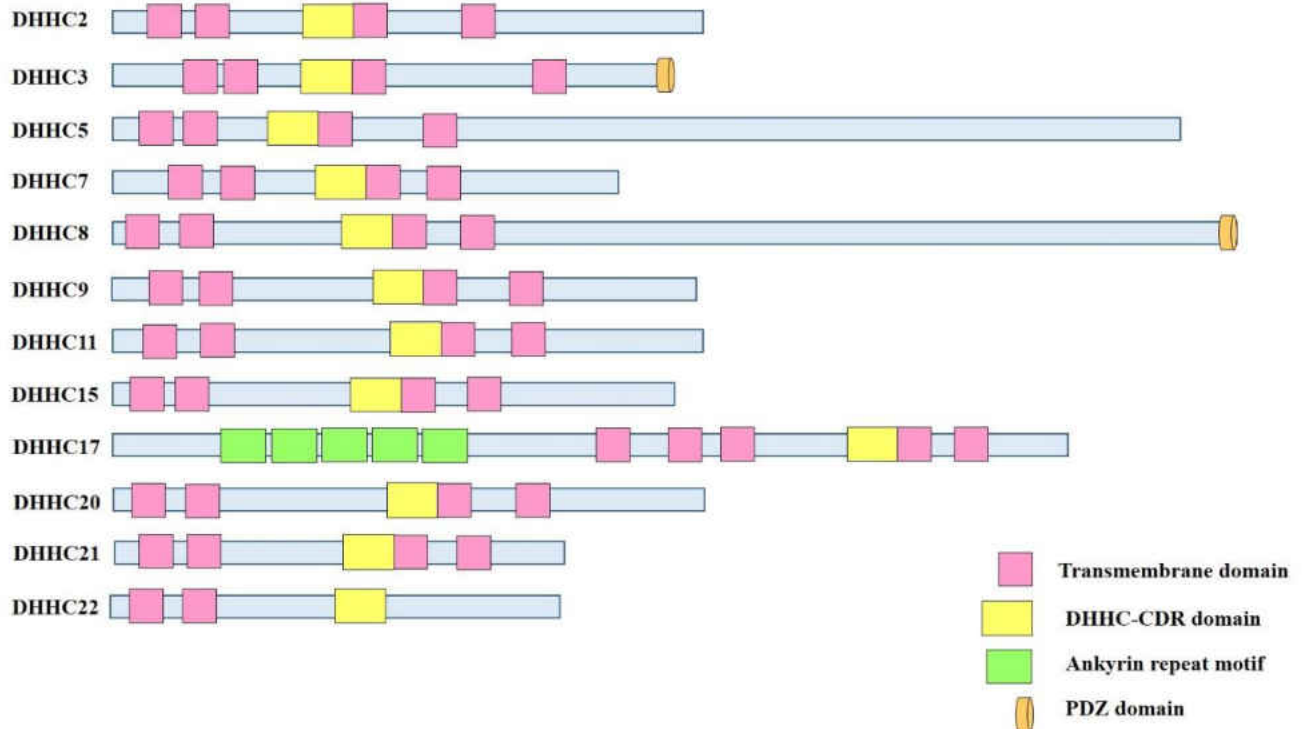


Figure 8: Domain structure of DHHC enzymes found in the brain. A representative diagram of DHHC (Asp-His-His-Cys) proteins. DHHC enzymes contain four or more transmembrane domains (pink squares) and a conserved cysteine rich domain (CRD) containing a DHHC motif (yellow rectangles), which is essential for palmitoylation. Some enzymes have additional motifs including a PDZ binding domain (orange cylinders) at the C terminus for DHHC3 and DHHC8, and ankyrin repeats (green rectangles) for and DHHC17. Image modified from Koryckaa J, Lacha Am Hegerb E, Boguslawskab DM, Wolnya M, Toporkiewixza M, Augoffc K, Korzeniewskid J, and Sikorskia AF 2012. Human DHHC proteins: A spotlight on the hidden player of palmitoylation European Journal of Cell Biology 91: 107-117, with permission

acyl protein thioesterases 1 (APT1), APT2, and APT1-like and and palmitoyl protein thioesterases 1 (PPT1) and PPT2. APTs are cytosolic enzyme that removes palmitate from proteins on the cytosolic membranes (122). PPT1 and PPT2 are lysosomal proteins (134) that are important for depalmitoylating proteins during protein degradation. Because PPT1 and PPT are lysosomal proteins they do not directly act on cytosolic palmitoylated proteins (135). However, PPT1 has been detected in the presynaptic compartments, where it is suggested to be important for maintaining the synaptic vesicle pool (136).

There is no defined consensus sequences for substrate palmitoylation, however, palmitoylated proteins do share common features (127). Palmitoylated proteins often have other lipid modifications such as myristoylation or prenylation, located near the site of palmitoylation. Also palmitoylated Cys residues are located in the cytoplasmic regions surrounding TMDs and are surrounded by amino acids that are basic or hydrophobic. The mechanism by which a substrate protein is palmitoylated occurs in a two-step process (137). First the DHHC enzyme modifies itself with palmitate, in a process known as autoacylation, then the enzyme transfers the palmitate from itself onto the substrate protein (138, 139). Until recently it was unknown where autoacylation occurred. Mass spectrometry studies have now identified the Cys in the DHHC motif as the site of autoacylation (140).

Although the enzymes that control palmitoylation, have been identified, little is currently known regarding mutations or regulatory abnormalities associated with disease states. However, there are a few PAT enzymes that have been associated with neurological disorders. DHHC8 is the most well studied DHHC enzyme and has been

connected to schizophrenia (141, 142). A high risk of developing schizophrenia is associated with microdeletions of human chromosome 22q11.22 locus (141, 142). This deleted region also includes the DHHC8 gene. Interestingly, the deficits linked to the microdeletion could be rescued by expression of the active DHHC8 protein (141), indicating the importance of palmitoylation. Furthermore, PATs represent a potential therapeutic strategy for some diseases.

Huntington's disease is also another neurological disorder linked to DHHC enzymes(143). Huntington's disease is caused by the expansion of polyglutamine (polyQ) repeats in the huntingtin protein (143, 144). Additionally, Huntington's disease is characterized by the accumulation of protein aggregates that are formed by the misfolded polyQ repeat-containing proteins. Normally, the protein huntingtin is palmitoylated by DHHC17, however the polyQ expression of huntingtin disrupts the interaction with DHHC17, resulting in decreased palmitoylation (144). Reduced palmitoylation causes accumulation of protein aggregates in inclusions which may be correlated with cell toxicity (132, 143, 144).

Other DHHC enzymes linked to neurological disease include DHHC9 and DHHC15. Both enzymes have been associated with X-linked intellectual disability in humans (145, 146). Although the exact cause is unknown, mutations in the conserved DHHC9 and DHHC15 genes have been found in families with the X-linked intellectual disability phenotypes. Initial studies suggest proper palmitoylation is required for the temporal and spatial location of proteins in the plasma membrane and Golgi complex. Loss of palmitoylation alters the distribution of target proteins and is sufficient enough to cause X-linked intellectual disability (132, 146).



Depalmitoylation has also been linked to neurodegenerative diseases (147). The autosomal recessive brain disorder, infantile neuronal ceroid lipofuscinosis is caused by a mutation of in PPT1(147, 148). Mutations in the lysosomal PPT1 enzyme impairs the removal of long chain fatty acids from proteins, preventing protein degradation, and resulting in the accumulating of palmitoylated proteins(124, 144, 148).

### DAT Palmitoylation

Our lab demonstrated for the first time that DAT undergoes palmitoylation in both native and heterologously expressed tissues (149). This modification was blocked with the treatment of the irreversible PAT inhibitor 2-bromo palmitate (2BP). In this same study it was determined that 2BP regulates DAT palmitoylation in two distinct ways. A low dose and shorter 2BP treatments resulted in a significant reduction in DA transport  $V_{max}$  with no changes in surface expression. These results indicate reduced DAT palmitoylation decreases transport kinetic efficiency, affecting short-term regulation of DAT. A higher dose and longer treatment with 2BP caused DAT protein losses, indicating DAT palmitoylation is also regulated long-term.

There are five intracellularly oriented cysteines residues that are potential sites of DAT palmitoylation in rDAT (Cys6, Cys135, Cys341, Cys522, and Cys580). Through mutagenic studies, it was determined the major site of DAT palmitoylation is at Cys580 in rDAT. Metabolic Labeling of the C580A mutant with [<sup>3</sup>H]palmitate, reduced DAT palmitoylation by ~60% compared to the WT protein. The [<sup>3</sup>H]palmitate signal remaining on C580A suggests one or more additional site is palmitoylated in rDAT. Additional studies determined the C580A palmitoylation-deficient mutant still had cocaine-displaceable [<sup>3</sup>H]DA transport activity that was proportional to the overall expression.

When immunoblotted, the C580A mutant resulted in low molecular weight degradation fragments that were not visualized in the WT protein. These fragments were enhanced when C580A rDAT cells were treated with 2BP, suggesting palmitoylation is important for opposing DAT degradation. The C580A mutant also displayed increased PMA-induced down-regulation compared to WT, indicating depalmitoylated DAT is more sensitive to PKC-induced down regulation compared to palmitoylated DAT (149).

More recently our lab has shown palmitoylation to play a reciprocal role with phosphorylation (150). To study this process, the C580A palmitoylation mutant and the S7A phosphorylation mutant were assessed for either palmitoylation or phosphorylation levels of DAT. The C580A mutant had significantly enhanced DAT phosphorylation levels in comparison to WT. In reverse experiments, the S7A mutant had increased DAT palmitoylation level when assessed by [<sup>3</sup>H]palmitate labeling. Together, these mutagenic studies suggest that both of these posttranslational modifications may be important in regulating DAT activity. Additional pharmacological experiments were done to confirm the mutagenic results. In these experiments, cells were treated either with PMA, which stimulates PKC and thus DAT phosphorylation, or bisindolmaleimide (BIM), which blocks PMA-stimulated DAT phosphorylation (36). PMA significantly reduced [<sup>3</sup>H]palmitate labeling, while treatment with BIM increased it, suggesting palmitoylation and phosphorylation are working opposite of each other in an unknown mechanism. In reverse experiments, rat striatal synaptosomes were used to determine the DAT phosphorylation state in depalmitoylated conditions. Results showed 2BP treatment caused a significant increase in DAT phosphorylation compared to basal levels. Taken together, the mutational and pharmacological experiments demonstrate that these

posttranslational modifications are reciprocally regulated and important for DAT regulation and function.

### Purpose of Current Study

The dopamine transporter has been found to be palmitoylated on the C-terminus at Cys580 (149). This posttranslational modification is known to regulate diverse aspects of neuronal protein trafficking and function (132, 151), however its role in DAT function is poorly understood. DAT palmitoylation was previously found to be inhibited by the non-specific PAT inhibitor, 2BP. Treatment with 2BP resulted in decreased DA transport activity and an increase in DAT degradation (149), suggesting palmitoylation controls one or more functions of DAT.

There are 23 PAT enzymes currently identified in the human genome (112, 125, 128–130), with some associated with dopaminergic diseases such as schizophrenia (141, 142); however, the enzymes that catalyze DAT palmitoylation still remain unknown. Furthermore, psychostimulant drugs such as METH and cocaine are known to act on DAT, effecting transporter function (69, 70, 73, 75, 76, 152). Nonetheless, the effects of psychostimulant drugs on DAT palmitoylation still remain unknown. Therefore, we hypothesized that specific PAT enzymes will drive DAT palmitoylation, controlling expression, DA transport, and membrane lateral mobility of the transporter. To answer this question, we co-expressed a specific subset of neuronally-expressed PATs individually with DAT and assessed DAT palmitoylation using the acyl-biotinyl exchange method, with some results validated by [<sup>3</sup>H]palmitic acid labeling. Functional changes of DAT were also assessed including, total and surface expression, transport activity, and lateral membrane mobility. Additional studies were also conducted to

investigate psychostimulant regulation of DAT palmitoylation. Identifying the enzymes that drive DAT palmitoylation will allow us to better understand the mechanism of palmitoylation, thus providing critical insight into dysregulation in dopaminergic disorders and drug addiction.

## **CHAPTER II**

### **MATERIALS AND METHODS**

#### **Materials**

##### *Animals*

Male Sprague Dawley rats (200-300g) were obtained from Charles River Laboratories (Wilmington, MA) and were maintained in compliance with the guidelines established by the University of North Dakota Institutional Animal Care and Use committee and the National Institutes of Health.

##### *Reagents*

Methyl methanethiosulfonate (MMTS), (N-(6-(biotinamido) hexyl)-3-(2'-pyridyldithio)-propionamide (HPDP biotin), high capacity Neutravidin resin, Complete Mini Proteases Inhibitors, DHHC2 antibody, X-treme GENE HD, Lipofectamine2000, Opti-MEM, and Trypsin were purchased from Thermofisher Scientific (Waltham, MA). [7,8-<sup>3</sup>H] dopamine (45Ci/mmol) was purchased from Perkin Elmer (Walthman, MA). [9,10-<sup>3</sup>H] palmitic acid was purchased from Moravек (Brea, CA). Protein A Sepharose beads were purchased from GE Healthcare Life Sciences (Piscataway, NJ). (-)-Cocaine, (-) 2 $\beta$ -carbomethoxy-3 $\beta$ -(4-fluorophenyl) tropane ( $\beta$ -CFT), mazindol, dopamine,

hydroxylamine, molecular weight markers were purchased from Sigma-Aldrich (St. Louis, MO). Lewis Lung Carcinoma Porcine Kidney (LLCPK<sub>1</sub>) cells expressing rDAT were kindly provided by Dr. Gary Rudnick (Yale University, New Haven, CT). Neuro-2a (N2a) cells were purchased from American Type Culture Collection (ATTC) (Manassas, VA). The DHHC constructs were kindly provided by Dr. Masaki Fukata from the National Institute for Physiological Sciences, Okazaki, Aich Japan. Hemagglutinin epitope HA.11 monoclonal antibody was purchased from Covance (Emeryville, CA). DHHC3, DHHC8, DHHC9 antibodies were purchased from Santa Cruz Biotechnology (Dallas, TX). Transferrin Receptor (TfR) antibody was purchased from BD Biosciences (San Jose, CA). Alkaline phosphatase conjugated secondary antibody were purchased from Simga-Aldrich (St. Louis, MO). Polyacrylamide gels were purchased from Lonza (Rockland, ME). Alkaline phosphatase developing substrate was purchased from Bio-Rad (Hercules, CA). Site directed mutagenesis Quick Change<sup>®</sup> kit was from Stratagene (La Jolla, CA). Synthesized oligonucleotides were purchased from Eurofin MWG Operon (Huntsville, AL). All other chemicals were purchased from Sigma-Aldrich (St. Louis, MO) or Thermofisher Scientific (Waltham, MA).

## Equipment

### *Centrifuges*

Refrigerated Beckman microfuge R or the bench top Microfuge 18 were used for general lab procedures. The Beckman Avanti J-25, 16.250 and 25.50 rotors were used for synaptosome preparation and harvesting *E.Coli* cells for protein and plasmid isolation purposes. The Beckman J6-MI swinging bucket centrifuge was used to pellet cells and to prepare cross-linked Protein A Sepharose beads.

### *Electrophoresis*

Sodium dodecyl sulfate polyacrylamide gel electrophoresis (SDS-PAGE) and protein transfers were performed using the Bio-Rad Mini-Protein III electrophoresis apparatus and the Bio-Rad Mini trans blot electrophoresis transfer cell, respectively. Electrophoresis and protein transfer was controlled by Fisher Scientific FB300 power supply. Gels were dried using a Bio-Rad Model 583 gel dryer.

### *Spectroscopy*

Bicinchoninic acid (BCA) protein assays were quantified using the Molecular Devices SpectraMax 190 plate reader and DNA quantification was performed using Beckman DU640 spectrophotometer. Incorporation of radioactivity during uptake experiments were counted using a Packard 1900CA or a Beckman LS6500 liquid scintillation counter.

### *Cell Culture and Molecular Biology*

Mammalian cell were maintained in a sterile Nuair Class II A/B3 laminar flow hood, and incubated in a Nuair 2700-30 water jacketed CO<sub>2</sub> incubator. All Polymerase Chain Reactions (PCR) experiments were done in an Eppendorf Mastercycler personal thermal cycler.

### *Microscopy*

Confocal and Fluorescence recovery after photobleaching (FRAP) experiments were done using Zeiss 510 META laser scanning confocal microscope.

## Methods

### *Mammalian Cell Culture*

Lewis lung carcinoma-porcine kidney (LLCPK<sub>1</sub>) cells stably expressing the WT rat dopamine transporter (rDAT) were maintained with  $\alpha$ - minimum essential medium (AMEM) supplemented with 5% fetal bovine serum, 2 mM L-glutamine, 100  $\mu$ g/ml penicillin/streptomycin, and 200ug/ml G418. Neuro-2A cells (N2a) cells were maintained with  $\alpha$ - minimum essential medium (AMEM) supplemented with 10% fetal bovine serum, 2 mM L-glutamine, 100  $\mu$ g/ml penicillin/streptomycin. All cells were grown in T-75 flasks and maintained at 37°C in a 5% CO<sub>2</sub> in the Nuair water-jacketed CO<sub>2</sub> incubator.

### *Transient Transfection and Site Directed Mutagenesis, and Plasmid Transformation*

For transient transfection, LLCPC<sub>1</sub> or N2a cells were grown to ~70 % confluency and transfected using X-tremeGENE HD or lipofectamine 2000 transfection reagent and 2  $\mu$ g of PAT DHHC pEF-BOS-HA tagged plasmid. Cells were incubated for 18-20 hours followed by harvesting. Site-directed mutagenesis of DHHC2 to DHHA2 was performed on pEF-BOS-HA plasmid containing Stratagene design primer software was used to design oligonucleotide primers, which were ordered from MWG operon. QuickChange® method was used to mutant selected residues C156. A 50  $\mu$ L reaction mixture included 5  $\mu$ L of 10X reaction buffer (100 mM KCl, 100 mM NH<sub>4</sub>SO<sub>4</sub>, 200 mM Tris-HCl, 20mM MgSO<sub>4</sub>, 1% Triton X-100, 1 mg/mL nuclease free BSA, pH 8.8), 8  $\mu$ L of template DNA (5 ng/ $\mu$ L), 1.25-1.60  $\mu$ L of oligonucleotide forward and reverse primers (125 ng), 2 $\mu$ L of dNTP mix, 32.5 – 31.8  $\mu$ L of double distilled DNase free H<sub>2</sub>O. Addition of 1  $\mu$ L of pfu Turbo or pfu Ultra DNA Polymerase (2.5 U/ $\mu$ L) initiated the polymerase chain reaction



(PCR). PCR cycling parameters included denaturation, annealing, and primer extension. Denaturation required heating the DNA to 95 °C for 1 min to render it single stranded. The annealing step was performed at 55 °C for 1 min and primer extension was done at 68 °C for 8 min followed by 15 repeated denaturation, annealing, and primer extension cycles. Supercoiled double stranded template DNA was degraded by incubation with 1 µL of DpnI restriction enzyme for 18 h at 37 °C. The generated plasmid was transformed into Stratagene Giga competent *E coli* cells. 1-4 µL of ligation mixture was added to 25 µL of competent cells. Cells were placed on ice for 5 min and heat shocked for 30 sec at 42 °C on a heat block. Tubes were placed on ice for 2 min and 250 µL of SOC media was added and cells were plated on carbenicillin resistant agar plates for > 16 h at 37 °C. The plasmid was isolated using PureYield® Plasmid miniprep System (Promega). DNA was quantified via Epoch microspot spectrometry and sent to MWG operon (Birmingham, AL).

#### *Cell Membrane Isolation*

LLCPK<sub>1</sub> rDAT or N2a cells were grown in 100 mm plates and harvested when reaching 90% confluency. Cells were washed twice (0.25 M sucrose, 10 mM triethanolamine, 10 mM acetic acid, pH 7.8) at 4°C, scraped, and pelleted at 700 X g for 8 mins. Cells were then resuspended in buffer C (0.25 M sucrose, 10 mM triethanolamine, 10 mM acetic acid, 1 mM EDTA, pH 7.8), transferred to a Dounce homogenizer, and homogenized. Homogenate was centrifuged at 700 X g for 10 mins. For membrane isolation the supernatant fraction was further centrifuged and 16,000 X g for 12 min and resuspended in sucrose phosphate buffer (SP) ( 0.32M sucrose).

### *Analysis of DAT Palmitoylation by Acyl-Biotinyl Exchange*

DAT palmitoylation was assessed by ABE using a method modified from Wan et al. (153). LLCPK<sub>1</sub> rDAT or N2a cells were harvested followed by centrifugation at 20,000 x g for 12 mins at 4°C. Cell pellets were solubilized in lysis buffer (50 mM HEPES, pH 7.0, 2% SDS, 1 mM EDTA) containing Mini Complete protease inhibitor and 20 mM MMTS to block free thiols. Lysates were incubated at room temperature for 1 hour with mixing followed by acetone precipitation and resuspension in lysis buffer containing MMTS and incubation again for 1 hour at room temperature followed by acetone precipitation and resuspension in lysis buffer and incubated at room temperature overnight with end-over-end rotation. Excess MMTS was removed by three sequential acetone precipitations followed by resuspension of the precipitated proteins in 300 µl of 4SB (4% SDS, 50 mM Tris, 5 mM EDTA, pH 7.4). Each sample was divided into two equal portions and treated for 2 hours at room temp with 50 mM Tris-HCL, pH 7.4 or 0.7 M hydroxylamine, pH 7.4 to cleave thioester linkages. Hydroxylamine was removed with three sequential acetone precipitations followed by resuspension of pellet in 240 µl of 4SB, and diluted with 50 mM tris containing 0.4 mM sulfhydryl-reactive (N-(6(biotinamido)hexyl)-3'-(2'-pyridyldithio)-pro-pionamide (HPDP) for 1 hour at room temp. Excess HPDP was removed by three sequential acetone precipitations followed by resuspension of pellet in 75 µl of lysis buffer without MMTS. 10 µl of the sample was save for total DAT and the remaining 65 µl was diluted with 50 mM Tris-HCL, pH 7.4 to contain 0.1% SDS. Samples were affinity-purified using Neutravidin resin overnight with end-over-end rotation at 4°C. Proteins were eluted with sample buffer (60 mM Tris, pH 6.8, 20% SDS, 10% glycerol) containing 100 mM DTT and 3% β-mercaptoethanol and

subjected to SDS-PAGE and immunoblotting with DAT monoclonal antibody 16 (mAb16). Palmitoylated DAT protein was normalized to total DAT protein.

*Analysis of DAT Palmitoylation by [<sup>3</sup>H] Metabolic labeling*

LLCPK<sub>1</sub> rDAT cells were metabolically labeled with [9,10-<sup>3</sup>H] palmitic acid (0.5 mCi/ml) for 18 hours at 37°C in AMEM media. After labeling, cells were lysed in radioimmunoprecipitation assay buffer (RIPA: 10 mM sodium phosphate, 150 mM NaCl, 2 mM EDTA, 1% Triton X-100, , 0.1% SDS, pH 7.2). Metabolically labeled samples were normalized to equal amounts of DAT first by immunoblotting with mAb16 then immunoprecipitated with polyclonal Ab16. Precipitated proteins were then resolved on 4-20% SDS-polyacrylamide gels with Rainbow molecular mass markers followed by soaking gels in Fluro-Hance (Research Products International) fluorographic reagent for 30 min, dried, and exposed to pre-flashed x-ray film for 30-90 days. Band intensities were quantified using Quantity One software (Bio-Rad), and values were normalized to total DAT levels.

*Immunoprecipitation and SDS-PAGE Western Blot*

DAT immunoprecipitation and immunoblotting were performed using polyclonal or monoclonal antibody 16 (154, 155). Samples were resolved on 4-20% SDS-PAGE gels with Rainbow molecular mass markers then proteins were transferred to PVDF membranes. Immunoreactive bands were visualized using Immuno-Star AP substrate and quantified using Bio-Rad Chem Doc XRS and Quantity One 4.6.7 software.

### *Surface Biotinylation*

For surface biotinylation LLCPK<sub>1</sub> or N2a cells were transiently transfected with co-expressed rDAT and DHHC enzymes. Cells were washed three times with ice cold Hank's buffer salt solution (HBSS) Mg-Ca (HBSS, 1mM MgSo<sub>4</sub>, 0.1 mM CaCl<sub>2</sub>, Ph 7.4), incubated twice with 0.5mg/mL of membrane-impermeable reagent, sulfo-NHS-SS-biotin for 25 min each at 4°C. The biotinylation reagent was removed and the reaction was quenched by two sequential incubations with 100 mM glycine in HBSS Mg-Ca for 20 min each at 4°C. Cells were then washed with HBSS Mg-Ca and lysed with RIPA containing a Complete Mini protease inhibitor tablet/10 ml. Equal cell lyses (100 ug protein) samples were affinity-purified using Neutravidin resin overnight with end-over-end rotation at 4°C. The beads were washed three times with RIPA buffer and the bound protein was eluted with 32 µl of sample buffer followed by immunoblotting with mAb16. Surface localization of biotinylated DAT protein was confirmed by probing blot for intracellular protein using anti protein-phosphatase 1 α (PP1α) antibody. For some experiments samples were probed for anti-transferrin receptor. Surface expression was normalized to total DAT or total transferrin receptor.

### *[<sup>3</sup>H] DA Uptake Assay*

LLCPK<sub>1</sub> expressing WT rDAT or N2a cells transiently transfected with WT rDAT and DHHC enzymes were grown to 80-90% confluence. Cells were washed twice with Krebs-Ringer HEPES (KRH) buffer (25 mM HEPES, 125 mM NaCl, 4.8 mM KCl, 1.2 mM KH<sub>2</sub>PO<sub>4</sub>, 1.3 mM CaCl<sub>2</sub>, 1.2 mM MgSO<sub>4</sub>, 5.6 mM glucose, pH 7.4). Interval DA uptake was initiated by adding 10 µl of a 100X DA stock solution to bring the final concentration of [<sup>3</sup>H] DA to 10 nM and that of total DA to 3 µM. Nonspecific uptake

was determined by addition of 100  $\mu$ M (—) –cocaine. Uptake assay was performed at 37°C for 8 minutes and terminated by rapidly washing the cells two times with ice-cold KRH buffer. Cells were solubilized in RIPA containing protease inhibitor tablet. Radioactivity contained in lysates was measured by liquid scintillation counting. Uptake activity was normalized to total protein as determined by BCA assay.

#### *Subcellular localization of palmitoylated DATs*

Subcellular fractions were generated by differential centrifugation LLC<sub>PK</sub><sub>1</sub> cells stably expressing WT rDAT were cultured in 150 mm dishes, grown to ~90%. Cells were washed, scraped, and pelleted by centrifugation at 700 x g for 5 min at 4 °C. Pelleted cells were resuspended in Buffer C (0.25M sucrose, 10 mM triethanolamine, 10 mM acetic acid, 1 mM EDTA, pH 7.8) and homogenized in ice-cold Buffer C with 30 strokes in a Dounce homogenizer. Homogenates were centrifuged at 700 x g to remove nuclei, and post- nuclear supernatants (totals), were centrifuged sequentially at 16,000 x g for 12 min (16,000 x g membranes), and at 200,000 x g for 1h (200,000 x g membranes). Resulting pellets were resuspended at the original volume in RIPA buffer containing protease inhibitors. Fractions were immunoblotted for DAT, Na<sup>+</sup>/K<sup>+</sup> ATPase, Rab5A, Rab7, and Rab11, or analyzed by ABE for detection of DAT palmitoylation.

#### *Fluorescence Recovery After Photobleaching (FRAP)*

FRAP studies were done with a Zeiss 510 META laser scanning confocal microscope. N2a cells were grown to ~50% on 1 mm glass coverslips and transiently transfected with EYFP WT rDAT and individual HA-tagged DHHC enzymes. Spot photobleaching using circular regions of interest 30  $\mu$ m in diameter were placed on the

membrane of the visualized cell, followed by bleaching of the region using the 514 nm laser at 100% power to obtain 50-70% bleaching. Images were collected at 2% laser power in 3.93 sec intervals for a duration of 5 mins totaling 100 images. The images were processed in ImageJ and recovery curves were calculated. The rate of recovery ( $t_{1/2}$ ) was calculated from an exponential recovery function ( $F(x) = F_{\infty} + A(\exp(-x/T))$ ) fitted to the fluorescence recovery data.

#### *In vivo Analysis of DAT Palmitoylation in Rats*

Male Sprague Dawley rats (175-350g) were subcutaneously (SC) injected with saline (control), METH (15 mg/kg), or cocaine (15 mg/kg) for 10, 30, 60 min post SC injection. The animals were decapitated and the striata rapidly removed, weighed and placed in ice-cold 0.32 M SP buffer. Striatal tissue was homogenized with a Polytron PT1200 homogenizer (Kinematica, Basel, Switzerland) for 8 seconds and centrifuged at 3,000 x g for 3 min at 4 °C. The supernatant was then centrifuged at 16,000 x g for 12 min. The resulting pellet was resuspended in modified Krebs phosphate buffer (126 mM NaCl, 4.8 mM KCl, 16 mM KPO<sub>4</sub>, 1.4 mM MgSO<sub>4</sub>, 10 mM glucose, 1.1 mM ascorbic acid, and 1.3 mM CaCl<sub>2</sub>, pH 7.4) to 20 mg/ml original wet weight. The membranes were then analyzed for palmitoylation by ABE as previously described.

## **CHAPTER III**

### **RESULTS**

#### **Identification of DAT Palmitoyl Acyl Transferases**

Protein palmitoylation is known to regulate many diverse aspects of neuronal protein trafficking and function (112, 113, 120, 156), however its role in DAT function is poorly understood. Furthermore, 23 PAT enzymes that have been identified in the human genome (112, 125, 128–130), yet the enzymes that catalyze DAT palmitoylation still remain unknown. Previous studies have shown that DAT is palmitoylated and that inhibition of DAT palmitoylation affects the function of the transporter (149), therefore identifying the enzymes that drive palmitoylation is of great interest. The mammalian PAT enzymes have varying tissue and subcellular distribution, and a few, if any, specific pharmacological activators or inhibitors for these enzymes, making the identification of PATs that catalyze DAT palmitoylation difficult. To determine which PATs play a role in DAT palmitoylation we choose a specific subset of DHHC 2, 3, 5, 7, 8, 9, 11, 15, 17, 20, 21, and 22, known to be expressed in a neuronal context or those associated with neurological disorders. In our initial studies, we wanted to determine in a model cell system if we could co-express the DHHC enzymes with DAT. For these studies, LLCPK<sub>1</sub> cells expressing wild type (WT) rDAT were transiently transfected with individual HA-tagged human (h) DHHC coding plasmids kindly provided by Dr. Masaki Fukata from

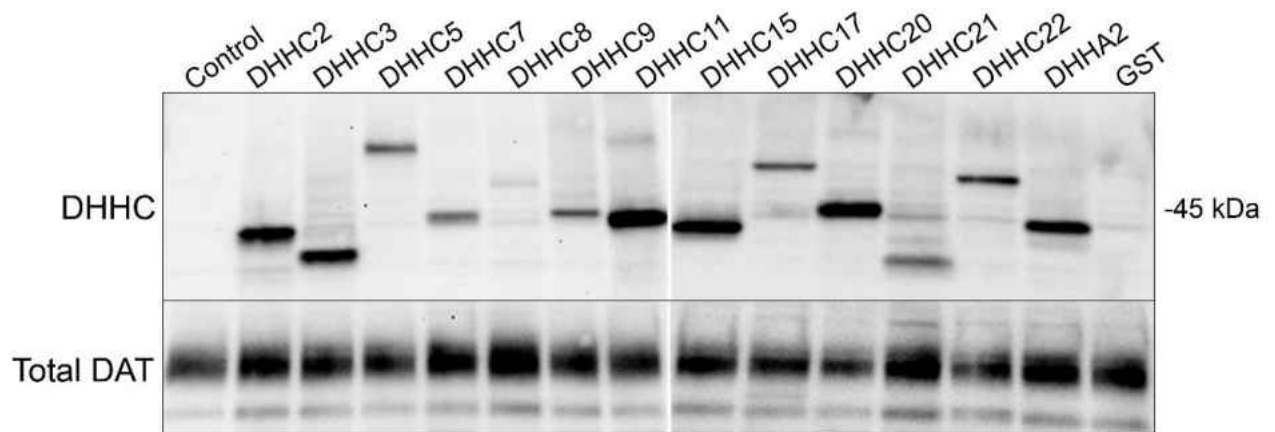


Figure 9: DHHC expression in rDAT LLCPK<sub>1</sub> cells. rDAT LLCPK<sub>1</sub> cells were transiently transfected with the indicated HA-tagged DHHC coding plasmids for 18 h. Cells were immunoblotted for DAT (mAB16) and DHHC expression (anti-HA). GST tagged plasmid was used as a transfection control. Blots are representative of three independent experiments.



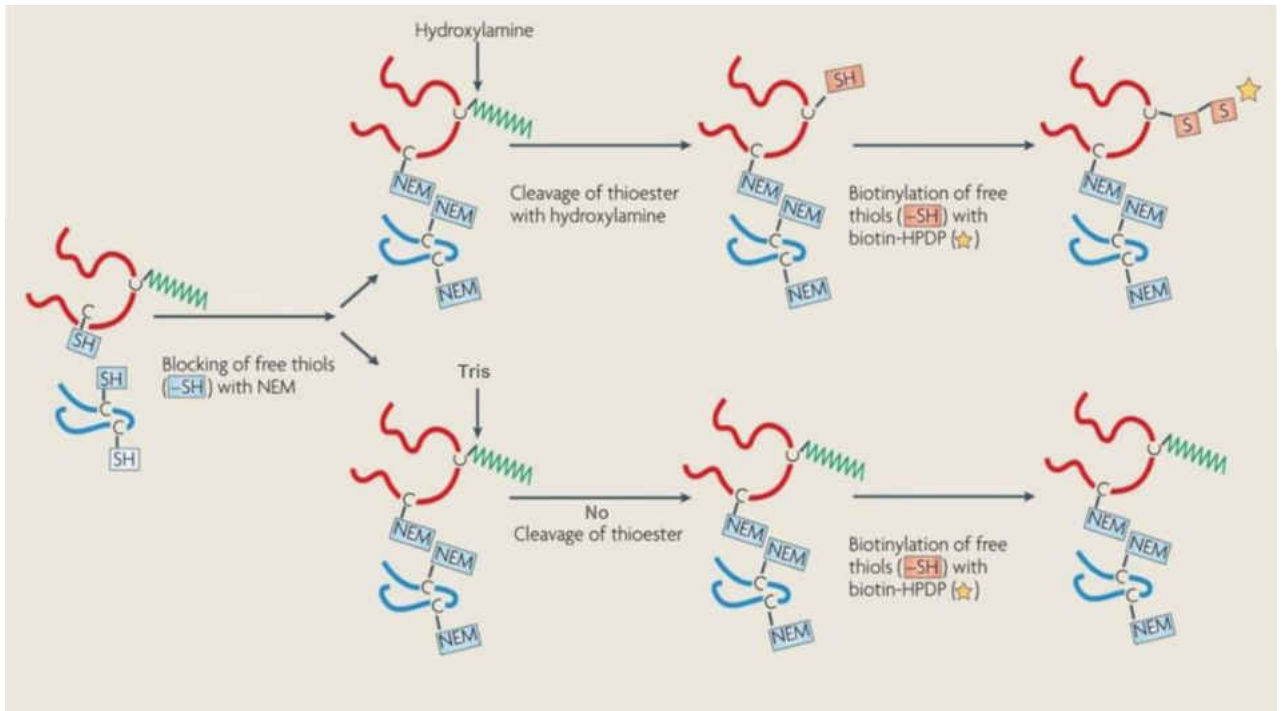


Figure 10: Acyl-biotinyl exchange method. The ABE method consists of three major steps: blockade of unmodified free Cys thiols with MMTS; cleavage of palmitoylation thioester linkages with  $\text{NH}_2\text{OH}$ ; and labeling of newly exposed Cys thiols with a thiol specific biotinylation reagent. Biotinylated proteins are extracted with NeutrAvidin agarose followed by SDS-PAGE and immunoblotting for DAT. Image modified from Yuko Fukata and Masaki Fukata. 2010. Protein palmitoylation in neuronal development and synaptic plasticity *Nature Rev. Neuroscience* 11(3): 161-175, with permission

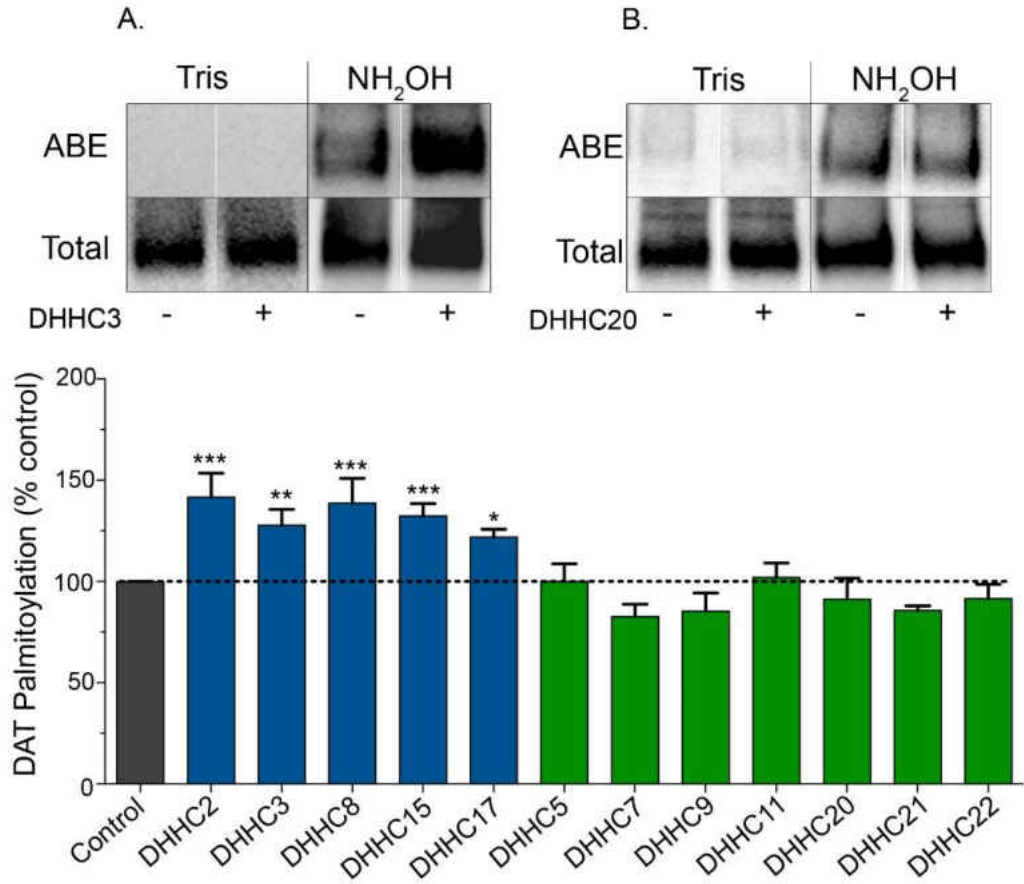


Figure 11: Multiple DHHC enzymes increase DAT palmitoylation. rDAT LLC<sub>PK1</sub> cells transiently transfected with the indicated DHHC coding plasmids were harvested and membranes isolated, followed by assessment of DAT palmitoylation by ABE. Upper panels show representative ABE blots with matching total DAT immunoblots for increased palmitoylation (A and B) and for no effect (C). Histogram represents quantification of palmitoylated DAT normalized for total DAT protein expressed as a fraction of control values normalized to 100% (means  $\pm$  S.E. of 3-4 experiments performed in triplicate). \*  $p < 0.05$ , \*\*  $p < 0.01$  relative to control by (one-way ANOVA with Dunnett's Post hoc test).

the National Institute for Physiological Sciences, Okazaki, Aich Japan. DHHC co-expression was verified by immunoblotting cell lysates 18 h post transfection using an anti-HA antibody (Figure 9). The DHHC enzymes and DAT were easily detectable, indicating successful co-expression of these proteins in our mammalian cell system. The same vector containing the coding sequences for GST was used as a transfection control (Figure 9 far right).

To determine which PATs play a role in DAT palmitoylation, experiments were performed by comparing DAT palmitoylation in the presence of co-transfected DHHCs. For most experiments, DAT palmitoylation was analyzed by the *in vitro* acyl-biotinyl exchange (ABE) method. In this method, samples are treated with methyl methanethiosulfonate (MMTS) to block free thiols, followed by treatment with hydroxylamine (NH<sub>2</sub>OH) to remove thioester-linked palmitate, with parallel samples treated with Tris-HCl (control), and finally the newly exposed cysteine thiols were labeled with a sulfhydryl-reactive biotin for NeutrAvidin extraction followed by SDS-PAGE and immunoblotting for DAT. The method is depicted in Figure 10.

Our findings (Figure 11) show that DAT palmitoylation is enhanced relative to control by over-expression of DHHC2 ( $141.6 \pm 12\%$ ,  $p < 0.001$ ), DHHC3 ( $127.8 \pm 7\%$ ,  $p < 0.01$ ), DHHC8 ( $138.7 \pm 12\%$ ,  $p < 0.001$ ), DHHC15 ( $132.4 \pm 6\%$ ,  $p < 0.001$ ), and DHHC17 ( $121.9 \pm 4\%$ ,  $p < 0.05$ ). Several other co-expressed DHHC enzymes (DHHC5, 7, 9, 11, 20, 21, and 22) however had no effect on DAT palmitoylation ( $p > 0.05$ ), indicating a substrate specific. It is also important to note that the immature form of DAT was also palmitoylated (not shown) in all cases. Taken together, these results indicate that multiple DHHC enzymes may have the capability to modify DAT palmitoylation

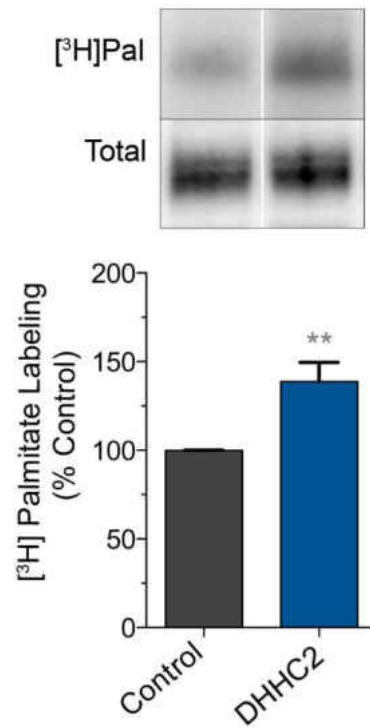


Figure 12: DHHC2-induced DAT palmitoylation validated by [<sup>3</sup>H]palmitic acid labeling. rDAT LLCPK<sub>1</sub> cells were transiently transfected with HA-tagged DHHC2 coding plasmid. After four hours, media was removed and cells were metabolically labeled with [<sup>3</sup>H]palmitic acid for 18 h. Cell lysates were immunoprecipitated followed by SDS-PAGE/fluorography. Upper panel shows representative results for autoradiogram (top) and western blot of total DAT (bottom). Histogram represents quantification of means ± S.E three independent experiments performed in triplicate relative to control normalized to 100%. \*\* p<0.01 DHHC2 versus control (Student's t-test).

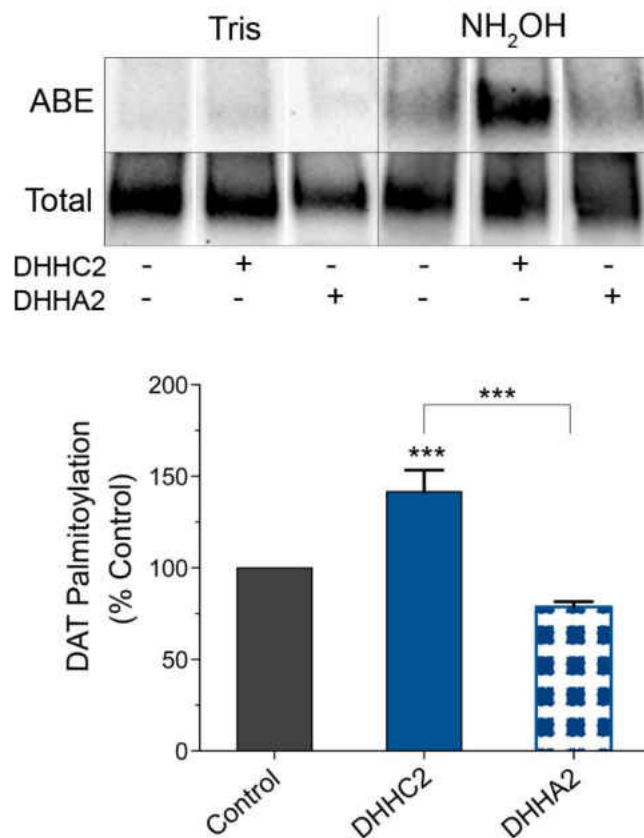


Figure 13: Enzymatic activity of DHHC2 is required for increased DAT palmitoylation. ABE analysis of rDAT LLCPK<sub>1</sub> cells transiently transfected with DHHC2 or C→A mutation DHHA2. Upper panel shows representative results for ABE. Histogram represents quantification of palmitoylated DAT normalized for total DAT protein expressed as a fraction of control values normalized to 100% (means ± S.E. of four independent experiments performed in duplicate). \*\* p< 0.01, \*\*\* p<0.001 relative to control by (one-way ANOVA with Tukey's post hoc test)

To confirm our ABE results, we performed metabolic labeling with [<sup>3</sup>H]palmitic acid (Figure 12). LLCPK<sub>1</sub> cells stably expressing WT rDAT were transiently transfected with HA-tagged DHHC2 and labeled with palmitic acid. Co-expression with DHHC2 significantly increased DAT [<sup>3</sup>H] palmitoylate labeling relative to control (138 ± 11% versus control, p <0.05). Although this method is known to be less sensitive (157), the increases in DAT palmitoylation was similar to the results obtained by ABE. These results confirm that DAT palmitoylation is driven by the overexpression of DHHC enzymes.

To demonstrate that acyl transferase activity in the co-expressed DHHC was necessary for increased DAT palmitoylation, an inactive DHHA2 enzyme was utilized (158). Site directed mutagenesis was used to convert DHHC2 to DHHA2, changing the Cys at position 156 to an Ala, making the enzyme inactive (158). Expression levels of the mutant DHHA2, determined by anti-HA immunoblotting was equivalent to the WT DHHC2 (Figure 9 far right). Co-expression with WT DHHC2 significantly increased DAT palmitoylation (p<0.001) compared to control, however DHHA2 resulted in no change in DAT palmitoylation (DHHA2 78.8 ± 3% relative to control p>0.05), and was significantly different from the WT DHHC2 enzyme (p<0.001) (Figure 13). These results indicate that the enzymatic activity of DHHC2 is required for increased DAT palmitoylation.

### Palmitoylation Enhances DAT Expression

Previous studies have shown acute or chronic inhibition of palmitoylation by 2BP results in increased DAT degradation, as detected by the loss of full-length DAT and appearance of DAT degradation fragments (149). Therefore it was hypothesized that PAT

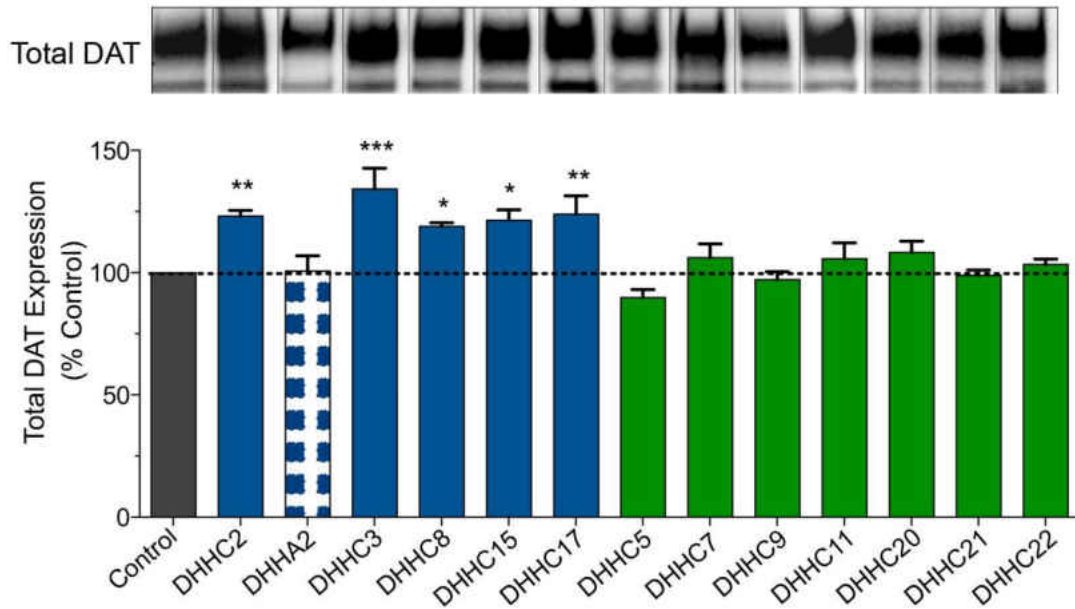


Figure 14: DAT palmitoylation increases total DAT expression. rDAT LLCPK<sub>1</sub> cells were transiently transfected individually with HA-tagged DHHC coding plasmids for 18h equal amounts of protein were immunoblotted for DAT. Top panel shows representative immunoblots and histogram shows band density expressed as a fraction of control values normalized to 100% (means  $\pm$  S.E. of 4 independent experiments performed in duplicate). \*  $p < 0.05$ , \*\*  $p < 0.01$ , \*\*\*  $p < 0.001$  versus control. (one-way ANOVA with Dunnett's post hoc test).

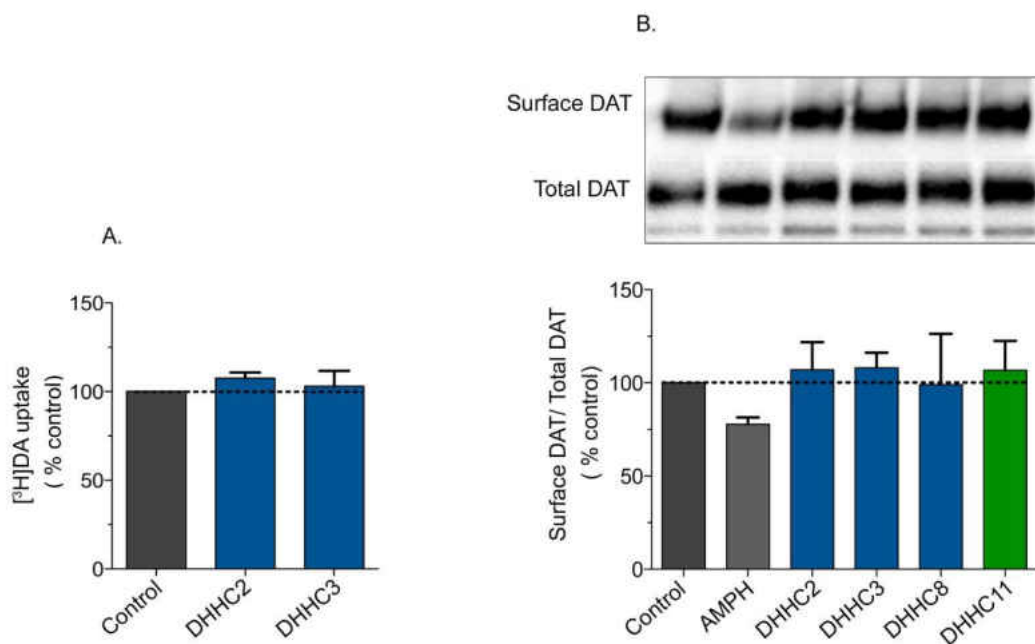


Figure 15: Functional studies in LLCPK<sub>1</sub> cells. rDAT LLCPK<sub>1</sub> cells were transiently transfected with the indicated HA-tagged DHHC coding plasmids and assayed for DA uptake activity and surface expression. (A) DA uptake activity normalized to total protein. Histogram is presented as means  $\pm$  S.E. of 3-4 independent experiments relative to control normalized to 100%  $p > 0.05$  by ANOVA with Dunnett's post hoc test. (B) Surface biotinylation analysis of LLCPK<sub>1</sub> cells co-expressing indicated DHHC enzymes. Representative immunoblots showing equal amounts of protein analyzed for DAT total and surface levels Histogram is presented as means  $\pm$  S.E. 2 independent experiments relative to control normalized to 100%.  $p > 0.05$  by ANOVA with Dunnett's post hoc test.



enzymes that drive DAT palmitoylation would also increase total DAT expression. To test this, LLCPK<sub>1</sub> cells stably expressing WT rDAT were transiently transfected with individual DHHC coding plasmids for 18h, and cell lysates immunoblotted for total DAT (Figure 14). Results show that total DAT levels were increased by co-expression of DHHC enzymes that increase DAT palmitoylation (DHHC2 123 ± 3%, p<0.01; DHHC3 134 ± 9%, p<0.001; DHHC8 119 ± 1%, p<0.05; DHHC15 121 ± 4%, p<0.05, DHH17 ± 8%, p<0.01). The DHHC enzymes that had no effect on DAT palmitoylation did not increase total DAT expression, (DHHC 5, 7, 9, 11, 20, 21, and 22, p>0.05). Co-expression with the inactive enzyme DHHA2, which did not increase DAT palmitoylation, also resulted in no change in total DAT levels (100 ± 6%, p>0.05), supporting the modification of DAT as driving this effect. Together with our previous 2BP finding, these results demonstrate that palmitoylation opposes DAT degradation.

#### Functional Studies of DAT Palmitoylation in LLCPK<sub>1</sub> Cells

To further understand the role of DAT palmitoylation, we investigated the functional effects. Previous studies demonstrated that inhibition of DAT palmitoylation with 2BP decreased DA transport activity (149), therefore we hypothesized that increased palmitoylation would result in increased DAT activity. To test this LLCPK<sub>1</sub> cells stably expressing WT rDAT were transiently transfected with indicated DHHC enzymes for 18 h, followed by assessment for [<sup>3</sup>H]DA uptake (Figure 15A). Surprisingly, we found that DA transport activity was not altered when co-expressed with DHHC enzymes that increased DAT palmitoylation (DHHC2 and DHDHC3 p>0.05). Because we did not see a change in transport activity we assessed plasma membrane levels by surface

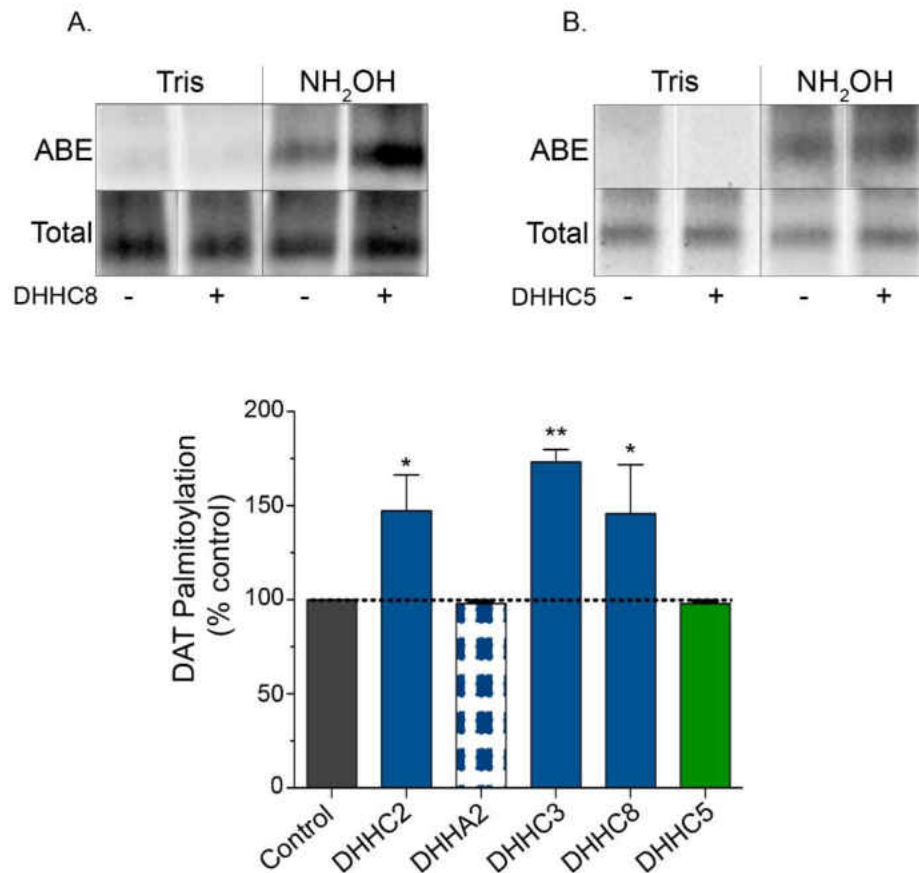


Figure 16: DHHC enzymes increase DAT palmitoylation in N2a cells. N2a cells transiently transfected with WT rDAT and indicated DHHC coding plasmids were harvested and membranes isolated, followed by assessment of DAT palmitoylation by ABE. Upper panels show representative ABE blots and matching total immunoblots for increased palmitoylation (A) and for no effect (B). Histogram shows quantification of palmitoylated DAT normalized for total DAT protein expressed as a fraction of control values normalized to 100% (mean  $\pm$  S.E. of 3-5 experiments performed in duplicate). \*  $p < 0.05$ , \*\*  $p < 0.01$  relative to control by (one-way ANOVA with Dunnett's Post hoc test)

biotinylation to determine if changes in surface expression were occurring (Figure 15B). Results indicated no change in surface DAT when normalized to total DAT for all DHHC enzymes assessed (DHHC2, 3, 8, and 11 ( $p > 0.05$ )). Control experiment with AMPH resulted in decreased surface biotinylation, indicating internalization of DAT (Figure 15B lane 2). These results were unexpected, demonstrating increased DAT palmitoylation does not change transport activity or surface expression. Based on previous results (149) we predicted changes in DAT palmitoylation would be accompanied by functional changes. Studies have suggested functional differences between neuronal and non-neuronal cell lines (109). Therefore we decided to perform the analyses in the Neuro-2A (N2a) neuroblastoma cell line derived from mouse to determine if a neuronal cell provided a better model system.

#### Multiple PATs Enhance DAT Palmitoylation and Expression in the N2a Cells

Because we already determined a specific subset of DHHC enzymes drive DAT palmitoylation in the LLC $PK_1$  cells, we chose to evaluate a limited number of DHHC enzymes in the N2a cells, to determine if the previous results followed a similar pattern. To test this, N2a cells were transiently transfected with WT rDAT and/or select DHHC enzymes for 18 h and analyzed by ABE (Figure 16). In these experiments we found significant increases in DAT palmitoylation relative to control with the over-expression of DHHC2 ( $147.3 \pm 19\%$ ,  $p < 0.05$ ), DHHC3 ( $173.1 \pm 6\%$ ,  $p < 0.01$ ), and DHHC8 ( $145.7 \pm 26\%$ ,  $p < 0.05$ ), whereas DHHC5 ( $98.1 \pm 1\%$ ) and DHHA2 ( $97.9 \pm 2\%$ ) had no effect ( $p > 0.05$ ) on DAT palmitoylation, parallel to our findings the LLC $PK_1$  cells.

Additional experiments were performed to determine if the N2a cells also showed an increase in total DAT expression when DHHC enzymes were overexpressed. N2a

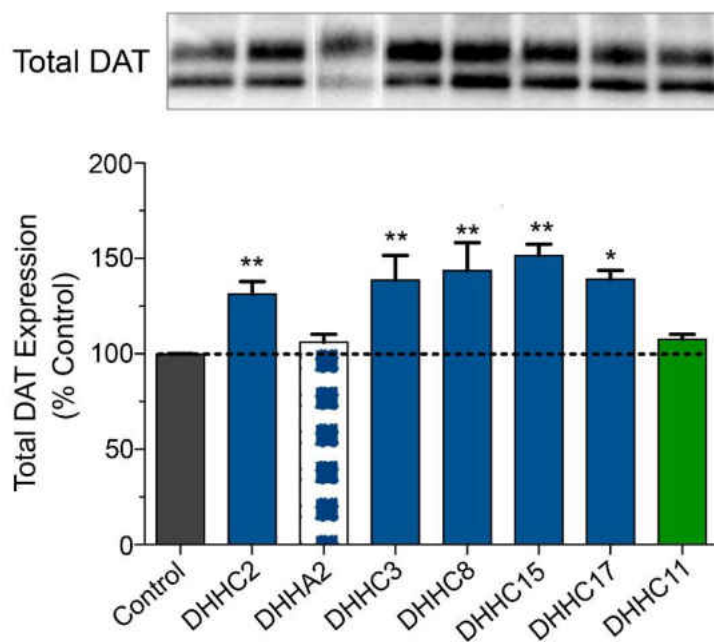


Figure 17: DAT palmitoylation increases total DAT expression in N2a cells. N2a cells were transiently transfected with WT rDAT and indicated HA-tagged DHHC coding plasmids for 18 h and assessed for total DAT expression. Equal amounts of protein were immunoblotted for DAT (representative blot shown) and band density was quantified and expressed as a fraction of control values normalized to 100% (means  $\pm$  S.E. of 2-6 independent experiments performed in duplicate). \*  $P < 0.05$ , \*\*  $P < 0.01$ , \*\*\*  $P < 0.001$  versus control. (one-way ANOVA with Dunnett's post hoc test).

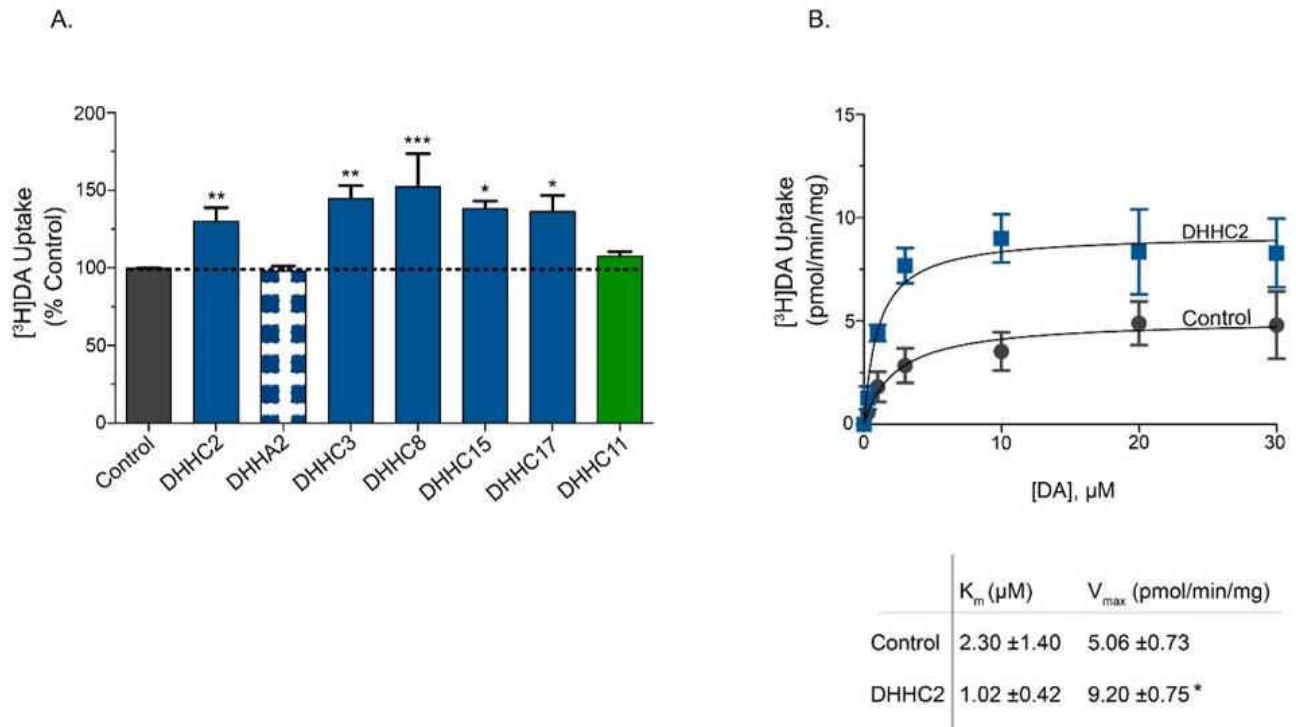


Figure 18: DAT palmitoylation increases transport  $V_{\text{max}}$  in N2a cells. (A) N2a cells were transiently transfected with WT rDAT and the indicated HA-tagged DHHC coding plasmids followed by [ $^3\text{H}$ ]DA uptake. Transport values obtained with co expression of DHHC enzymes were normalized to total protein. Values shown are mean  $\pm$  S.E. of 3-5 independent experiments performed in triplicate relative to controls normalized to 100%. \* $p < 0.05$ , \*\*  $p < 0.01$  versus WT (one-way ANOVA with Dunnett's Post hoc test). (B) DA transport saturation analysis of N2a cells co expressed with rDAT and DHHC2. Results shown are mean  $\pm$  S.E of 3 independent experiments performed in triplicate, \* $p < 0.05$  (Student's t-test).

cells were transiently transfected with WT rDAT and/or select DHHC enzymes for 18 h, cell lysates were subjected to SDS-PAGE, and immunoblotted for total DAT levels. Our results were similar to our previous findings, indicating that total DAT expression is enhanced when DAT is co-expressed with DHHC enzymes that increased DAT palmitoylation (Figure 17). DAT expression was significantly increased with the co-expression of DHHC2 ( $131.2 \pm 7\%$ ,  $p < 0.01$ ); DHHC3 ( $138.6 \pm 13\%$ ,  $p < 0.001$ ); DHHC8 ( $143.6 \pm 15\%$ ,  $p < 0.05$ ); DHHC15 ( $151.5 \pm 6\%$ ,  $p < 0.05$ ), DHH17 ( $139.0 \pm 5\%$ ,  $p < 0.01$ ) whereas DHHC11 and the inactive DHHA2 enzyme had no effect on total expression ( $p > 0.05$ ). These results support our findings in the LLCPK<sub>1</sub> cells, suggesting DAT palmitoylation opposes DAT degradation.

#### Palmitoylation Increases Transporter Capacity via an Alternation of DAT Transport Kinetics

Previous research has shown inhibition of DAT palmitoylation with 2BP results in a significant decrease in transport capacity (149). Therefore we wanted to investigate the functional effects of DAT palmitoylation when driven by the overexpression of DHHC enzymes. To do this, N2a cells were transiently transfected with WT rDAT and individual DHHC enzymes for 18 h, then assessed for [<sup>3</sup>H]DA uptake activity (Figure 18A). We found that DA transport activity was significantly enhanced by all DHHC enzymes that increased DAT palmitoylation (DHHC2  $130 \pm 9\%$ ,  $p < 0.01$ ; DHHC3  $145 \pm 8\%$ ,  $p < 0.01$ ; DHHC8  $152 \pm 21\%$ ,  $p < 0.001$ ; DHHC15  $138 \pm 5\%$ ,  $p < 0.05$ ; and DHHC17  $136 \pm 10\%$   $p < 0.05$ ) but that uptake was not changed with the co-expression of DHHC enzymes that did not enhance DAT palmitoylation (DHHC11  $107 \pm 3\%$  and DHHA2  $98 \pm 3\%$ ,  $p > 0.05$ ). To determine the mechanism underlying increased uptake activity, we performed a [<sup>3</sup>H]DA saturation analysis to determine if the kinetic properties were

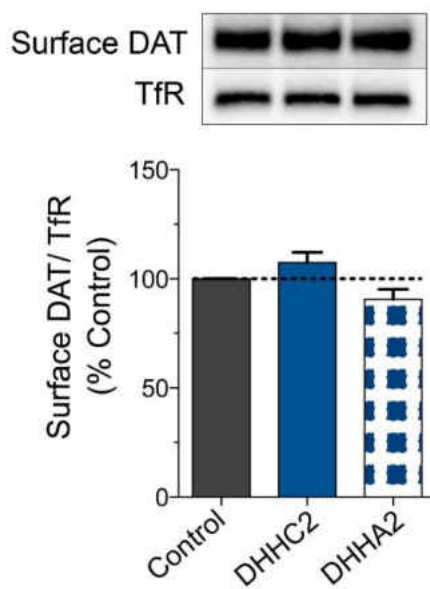


Figure 19: Palmitoylation of DAT does not increase surface expression. N2a cells were transiently transfected with WT rDAT and the indicated HA-tagged DHHC coding plasmids followed by surface biotinylation analysis. Image represents eluted biotinylated fraction (upper panel) normalized to transferrin receptor (TrF) (lower panel). The histogram represents mean  $\pm$  S.E of 5-8 independent experiments relative to controls normalized to 100%.  $p > 0.05$  by ANOVA with Dunnett's post hoc test.

affected by the overexpression of DHHC2 (Figure 18B). Saturation analysis showed DHHC2-induced increases in transport occurred via an increase in  $V_{\max}$  relative to control ( $9.20 \pm 0.75$  versus  $5. \pm 0.73$  pmol/min/mg,  $p < 0.05$ ), with no effect on  $K_m$  ( $1.02 \pm .42$  and  $2.3 \pm 1.40$  nM,  $p > 0.05$ ). Together, these results indicate that DAT palmitoylation affects the transport capacity of the transporter.

To investigate the mechanism of DHHC-induced DA transport increases, we analyzed surface expression of DAT. To do this, N2a cells were transiently transfected with WT rDAT and individually with DHHC2 and DHHA2 followed by analysis by cell surface biotinylation (Figure 19). In five independent experiments performed in duplicate, quantification of surface DAT normalized to the transferrin receptor for each condition showed surface levels of DAT were not different from control levels (DHHC2  $98 \pm 7\%$  DHHA2  $104 \pm 10\%$  compared to control set at 100%,  $p > 0.05$ ), indicating that DAT surface expression is not affected by its palmitoylation status. Together with our [ $^3$ H]DA uptake data, our results indicate that DAT palmitoylation increases transport  $V_{\max}$  via an alternation of surface transport kinetic capacity.

#### Palmitoylation is Present on Surface Transporters

Kinetic regulation of DA transport activity by palmitoylation requires the modification to be present on surface transporters. To examine this, rDAT LLCPK<sub>1</sub> cells were subjected to subcellular fractionation following analysis by ABE of DAT palmitoylation (Figure 20). Post-nuclear supernatants were subjected to differential centrifugation to generate fractions enriched in plasma membranes (16,000 x g pellets) or endosomes (200,000 x g pellets) (26). Immunoblotting showed enrichment of the plasma membrane marker



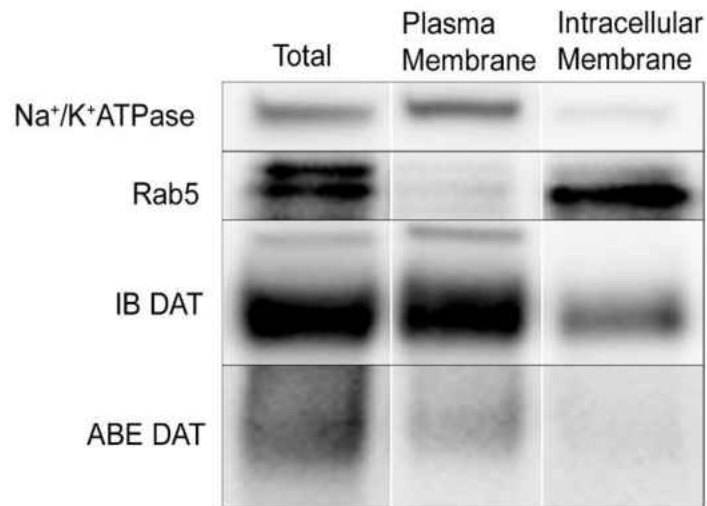


Figure 20: Subcellular localization of palmitoylated DATs. rDAT LLCPK<sub>1</sub> cells were homogenized and post-nuclear supernatants (totals) were subjected to differential centrifugation to produce 16,000 x g membranes and 200,000 x g membranes. Fractions were immunoblotted for Na<sup>+</sup>-K<sup>+</sup>-ATPase, Rab5A, or DAT. Samples were subjected to ABE for detection of DAT palmitoylation. Results are representative of 3-4 independent experiments performed in duplicate.

Na<sup>+</sup>/K<sup>+</sup>-ATPase in the 16,000 x g membranes and the early endosomal marker Rab5A in the 200,000 x g membranes, confirming the separation. ABE analysis showed that palmitoylated transporters were mostly present in the 16,000 x g membranes, with a small amount present in the endosomal fraction. These results support the presence of palmitoylated DATs on the plasma membrane.

#### DAT Palmitoylation at Cys580

We next investigated Cys580, the major site of DAT palmitoylation, and the role this site plays in DHHC-induced DAT palmitoylation. To do this, LLCPK<sub>1</sub> rDAT cells stably expressing the C→A mutation at 580 were transiently transfected with DHHC2 for 18 h followed by analysis of palmitoylation by ABE (Figure 21A). In contrast to WT co-expression of DHHC2 and C580A rDAT resulted in no change in DAT palmitoylation (DHHC2 87.7% ± 6% relative to control p>0.05). Transport activity of Cys580 and co-expression of DHHC2 were also assessed (Figure 21B). In three independent experiments, DA transport activity was significantly increased with the co-expression of DHHC2 in WT expressing cells (p<0.05). Whereas co-expression of DHHC2 in C580A expressing cells resulted in no effect on DA transport activity (DHHC2/C580A relative to control 74 ± 10% p>0.05), indicating Cys580 is required for DHHC2-induced uptake. Taken together, these results indicate that Cys580 mediates DHHC2-induced DAT palmitoylation and increased DA uptake activity.

Previous studies have shown that DA transport V<sub>max</sub> is significantly reduced by conditions that inhibit DAT palmitoylation (149), suggesting that palmitoylation of Cys580 increased transport. To further investigate the role of palmitoylation on transport

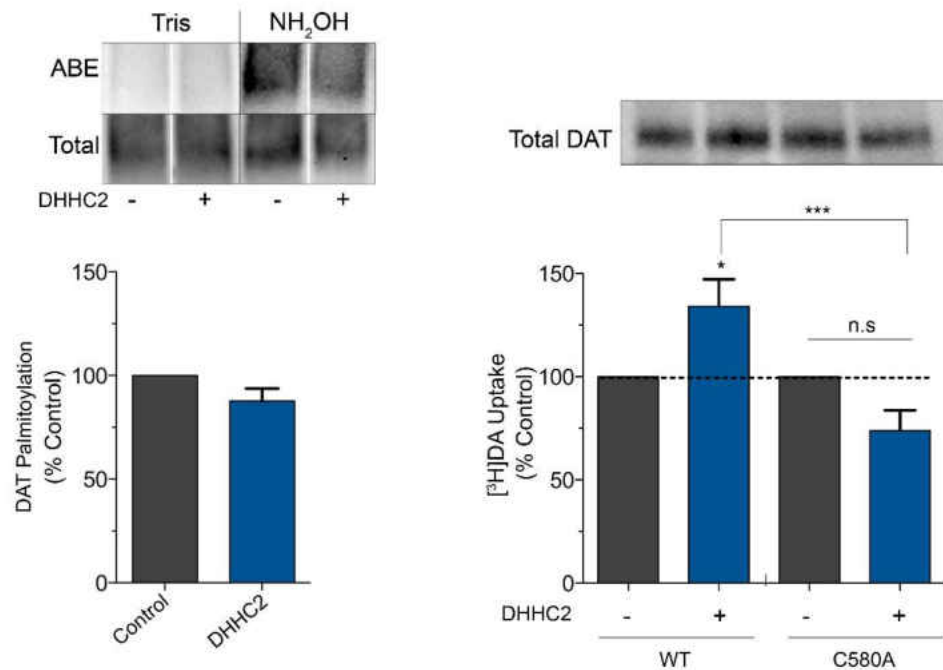


Figure 21: Cys580 mediates DHHC2-induced DAT palmitoylation and effects on kinetics. (A) C580A rDAT LLCPK<sub>1</sub> cells transiently transfected with DHHC2 were analyzed by ABE for DAT palmitoylation. Upper panels show representative results for ABE. Histogram shows quantification of palmitoylated DAT normalized for total DAT protein (means  $\pm$  S.E. of 4 experiments performed in triplicate relative to controls normalized to 100%).  $p > 0.05$ , relative to control by (Student's t test). (B) [<sup>3</sup>H]DA uptake analysis in N2a cells transiently co-transfected with WT or C580A rDAT, and HA-tagged DHHC2 coding plasmid. Transport activity was normalized to total protein. Values shown are mean  $\pm$  S.E. of 3-5 independent experiments relative to controls and C580A normalized to 100%. \* $p < 0.05$  \*\*\* $p < 0.001$  by ANOVA with Tukey's post hoc test.

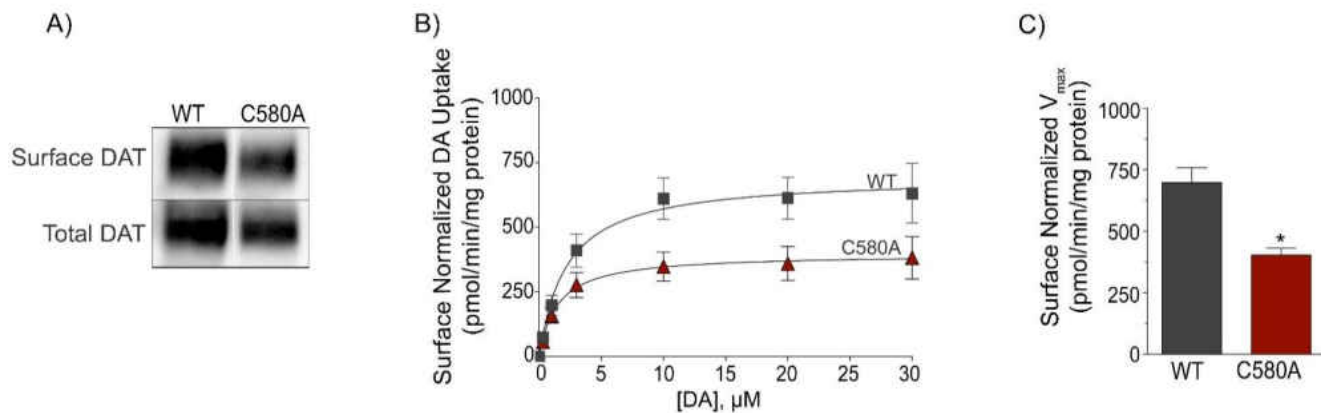


Figure 22: Cys580 modulates DA transport  $V_{max}$ . LLCPK<sub>1</sub> cells expressing WT and C580A were analyzed in parallel for [<sup>3</sup>H] DA saturation transport kinetics, total DAT expression, and DAT cell surface expression. (A) Representative immunoblots showing equal amounts of protein analyzed for DAT total and surface levels. (B) [<sup>3</sup>H] DA saturation analysis normalized for relative transporter surface levels. Uptake values shown are the mean  $\pm$  S.E. of five independent experiments. (C) The histogram shows  $V_{max}$  values for WT and C580A. \*,  $p < 0.05$ . Statistical analyses were performed by ANOVA with a Tukey post-hoc test.

kinetics we performed [<sup>3</sup>H]DA saturation transport analyses for C580A and WT DATs (Figure 22). All experiments were performed in parallel and include analysis of samples for total and surface DAT expression. Relative to the WT transporters values set at 100%, total and surface expression of C580A rDAT was  $55 \pm 5\%$  and  $56 \pm 4\%$ , respectively (Figure 22A). Figure 22B shows uptake saturation values for WT and C580A normalized for surface expression. The  $V_{\max}$  of C580A ( $397 \pm 34$  pmol/min/mg) was significantly less than the WT protein ( $697 \pm 56$  pmol/min/mg;  $p < 0.05$ ) (Figure 22C).  $K_m$  values were not significantly different (WT  $2.3 \pm 0.8$   $\mu$ M, C580A  $1.5 \pm 0.6$   $\mu$ M;  $p > 0.05$ ). Similar total and surface expression levels of C580 DAT indicate alterations in transport are not due to differences in trafficking to the surface.

#### Lateral Membrane Mobility of DAT

We next wanted to investigate the lateral membrane mobility of DAT to better understand the function of DAT palmitoylation. To do this we co-expressed EYFP-DAT and select DHHC enzymes transiently in the N2a cells and analyzed lateral membrane mobility using FRAP (Figure 23). We assayed the lateral mobility of DAT using a circular bleach spot with the average diameter of 3  $\mu$ m. The bleaching was performed at the edge of the membrane, photobleaching approximately 50-70% of the fluorescence signal. Representative images are shown in Figure 23A for DAT and DAT co-expressed with DHHC2. The circles highlight the region of photobleaching and the subsequently recovery recorded over a 5 min period. Our results show, that co-expression with DHHC2, significantly increases the time of recovery as demonstrated by the recovery curves and the histogram (Figure 23B and C) (DHHC2  $107.3 \pm 17$  sec vs control  $30.4 \pm 6$  sec,  $p < 0.001$ ). In contrast, co-expression with DHHC11 and DHHA2 resulted in

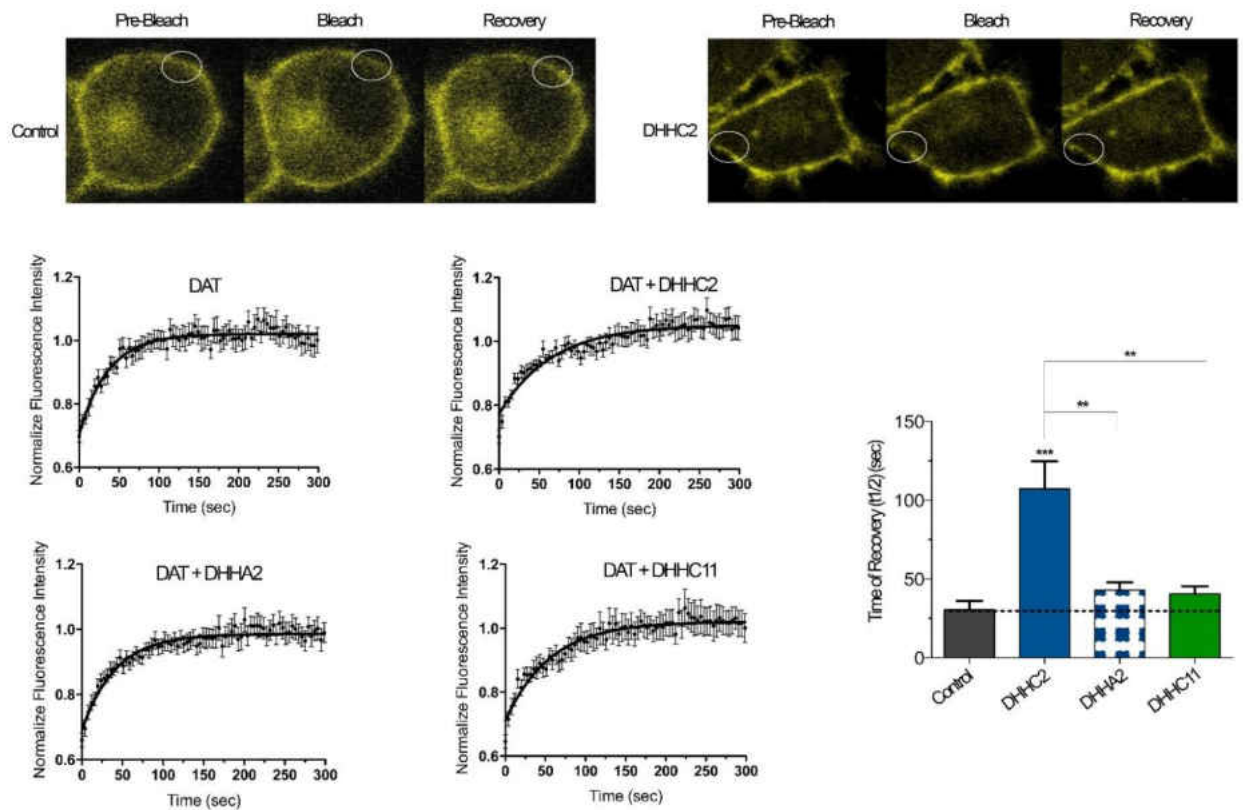


Figure 23: Palmitoylation decreases membrane lateral mobility of DAT. N2a cells transiently transfected with EYFP-rDAT and indicated HA-tagged DHHC coding plasmids were assessed for lateral membrane mobility by FRAP. (A) Representative confocal images showing EYFP-DAT fluorescence concentrated on the plasma membrane at pre-bleach, bleached, and recovery stages. (B) Fluorescence recovery curves for EYFP DAT expressed in N2a cells. Recovery was measured by normalized fluorescence intensity as a function of time (sec). (C) Time of recovery calculated based on FRAP experiments (means  $\pm$  S.E. of 3-5 independent experiments relative to controls) Total number of cells evaluated - control: 35, DHC2: 25, DHC11: 28 and DHHA2: 20. \*\* $p < 0.01$ , \*\*\*  $p < 0.001$  versus control (one-way ANOVA with Dunnett's Post hoc test).

recovery times similar to control (DHHC11  $43.0 \pm 5$  sec and DHHA  $40.6 \pm 5$  sec,  $p > 0.05$ ) (Figure 23B and C). Together these results indicated DAT palmitoylation decreases the lateral membrane mobility.

#### Action of Psychostimulants on DAT palmitoylation

DAT is the target for power addictive psychostimulants, therefore we wanted to investigate the effects of psychostimulants on DAT palmitoylation. To examine DAT palmitoylation, cells were pretreated with COC or METH for 30 min, washed extensively to remove extracellular drug, and assayed for DAT palmitoylation by ABE (Figure 24A). In three independent experiments, COC treatment resulted in no change in palmitoylation compared with untreated controls ( $94.8 \pm 6\%$ ,  $p > 0.05$ ), whereas treatment with METH significantly reduced DAT palmitoylation ( $84.2 \pm 4\%$ ,  $p < 0.05$ ). Time course studies showed decreased DAT palmitoylation at 30 min ( $83.3 \pm 8\%$ ,  $p < 0.05$ ) and 60 min ( $82.1 \pm 4\%$ ,  $p < 0.05$ ) relative to basal (Figure 24B).

To further examine the effect of psychostimulants on DAT palmitoylation, *in vivo* METH studies were performed in male Sprague Dawley rats (Figure 25A). In these studies, the animals were subcutaneously (SC) injected with COC (15mg/kg), METH (15mg/kg) or saline control for 30 min. This dose of drug produces detectable locomotor activity (159). Animals were then decapitated, the striatum was isolated, and membranes were prepared, followed by analysis by ABE. In three independent experiments, COC treatment showed no change in DAT palmitoylation compared with saline controls ( $94.8 \pm 6\%$ ,  $p > 0.05$ ) whereas METH treatment significantly reduced DAT palmitoylation ( $p < 0.05$ ). Time course studies animals were treated with METH (15mg/kg) for 10 min, 30 min, and 60 min post SC injection (Figure 25B). We observed treatment with METH

significantly decreased DAT palmitoylation in as little as 10 min ( $66.8 \pm 10\%$ ,  $p < 0.01$ ), and continued for 30 min ( $50.8 \pm 1\%$ ,  $p < 0.001$ ), and 60 min ( $47.9 \pm 0.3\%$ ,  $p < 0.01$ ). These results are consistent with our previous results which indicated a differential response of psychostimulant substrates versus blockers in both heterologous cells and animals (75, 152). Furthermore, these results indicate DAT palmitoylation is regulated by METH and not COC, which might be important for the clearance of DA in the synapse.



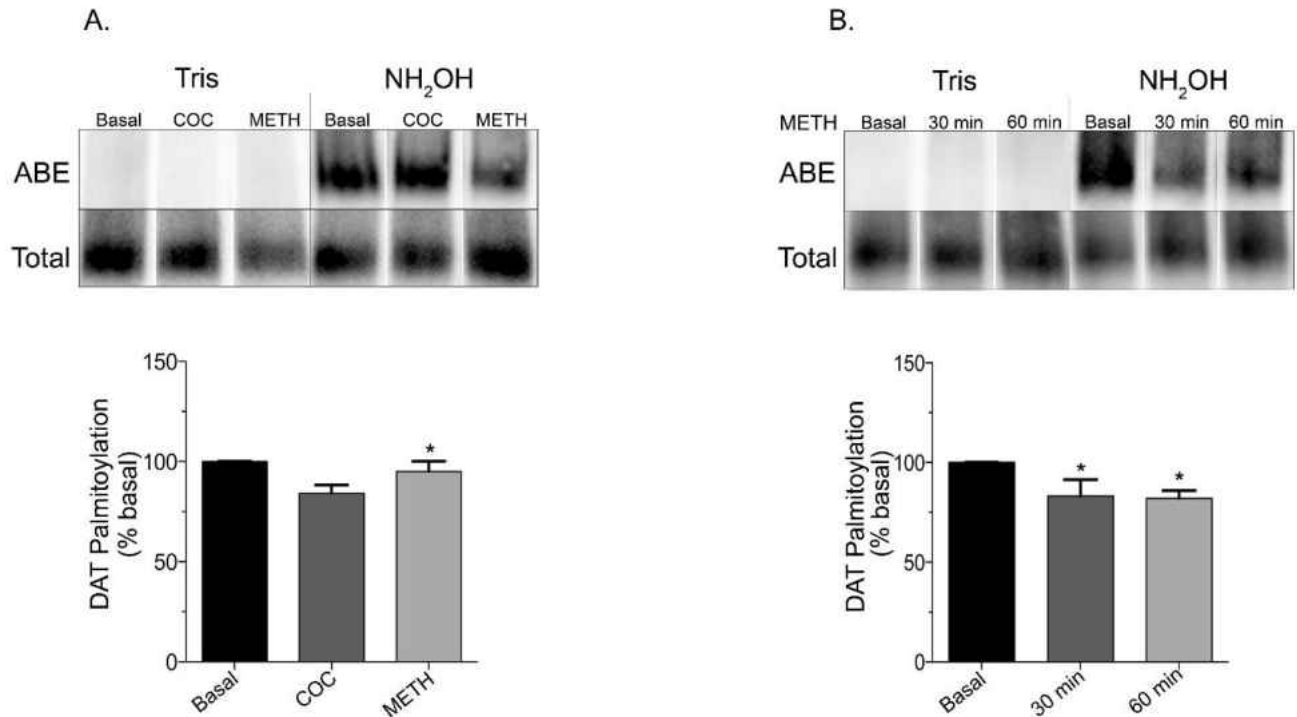


Figure 24: Regulation of DAT palmitoylation by psychostimulants in heterologous cells. LLCPK<sub>1</sub> cells were treated with (A) 10  $\mu$ M METH or 100  $\mu$ M cocaine for 30 min at 37  $^{\circ}$ C followed by assessment by ABE. Histogram represents quantification of palmitoylated DAT normalized for total DAT protein expressed as a fraction of basal values normalized to 100% (means  $\pm$  S.E. of 4 experiments performed in duplicate). \*  $P < 0.05$ , relative to control by (one-way ANOVA with Dunnett's Post hoc test). (B) 10  $\mu$ M methamphetamine (METH) for 30 or 60 min at 37  $^{\circ}$ C, cell membranes made, followed by assessment of DAT palmitoylation by ABE. Upper panels show representative ABE blots with matching total DAT immunoblots. Histogram represents quantification of palmitoylated DAT normalized for total DAT protein expressed as a fraction of basal values normalized to 100% (means  $\pm$  S.E. of 7 experiments performed in duplicate). \*  $P < 0.05$ , relative to control by (one-way ANOVA with Dunnett's Post hoc test).

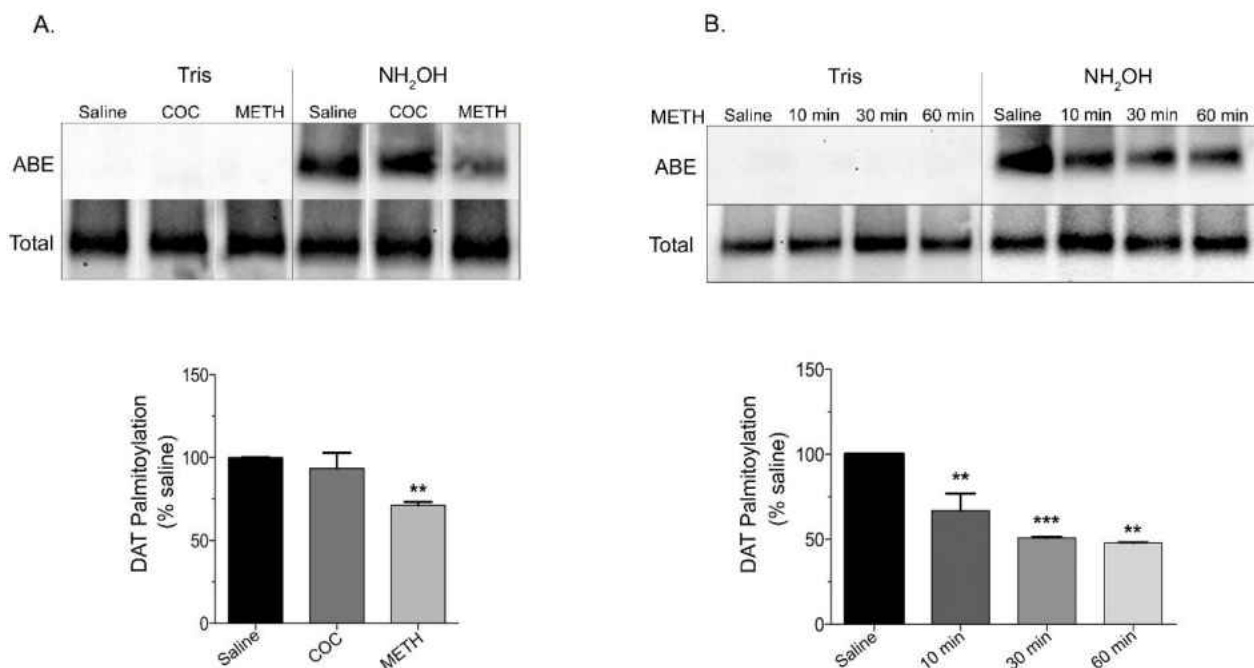


Figure 25: Regulation of DAT palmitoylation by psychostimulants *in vivo*. Male Sprague Dawley rats were SC injected with (A) METH (15 mg/kg), cocaine (COC) (15 mg/kg), or saline control for 30 min. The animals were decapitated and striatal membranes were made following analysis for DAT palmitoylation by ABE. Upper panels show representative ABE blots with matching total DAT immunoblots. Histogram represents quantification of palmitoylated DAT normalized for total DAT protein expressed as a fraction of saline control values normalized to 100% (means  $\pm$  S.E. of 3 experiments performed in triplicate). \*  $p < 0.05$  (one-way ANOVA with Dunnett's Post hoc test). (B) METH (15 mg/kg) or saline control for indicated time points. The animals were decapitated and striatal membranes were made following analysis for DAT palmitoylation by ABE. Upper panels show representative ABE blots with matching total DAT immunoblots. Histogram represents quantification of palmitoylated DAT normalized for total DAT protein expressed as a

Figure 25 continued: fraction of saline control values normalized to 100% (means  $\pm$  S.E. of 2-3 experiments performed in triplicate). \*\*  $p < 0.01$ , \*\*\*  $p < 0.001$  (one-way ANOVA with Tukey's post hoc test)

## **CHAPTER IV**

### **DISCUSSION**

#### **Regulation of DAT Palmitoylation by DHHC Enzymes**

Complex control of DAT is exerted by various regulatory processes, including palmitoylation. Protein palmitoylation increases protein hydrophobicity; mediates protein-lipid bilayers interactions; and can alter protein sorting, function, and regulation (112–116), however its role in DAT function is poorly understood. In this study, we have demonstrated for the first time that multiple DHHC enzymes drive DAT palmitoylation altering the function of the transporter. Figure 26 summarizes the numerous finding from my dissertation work and previous studies supporting DAT palmitoylation. In this model DAT palmitoylation is driven by a specific subset of DHHC enzymes resulting in enhanced DAT palmitoylation. Our findings reveal a connection between the increased DAT palmitoylation and total DAT expression. In all cases we observed enhanced total DAT expression when DAT palmitoylation was increased with the co-expression of DHHC enzymes, supporting an additional role for palmitoylation in opposing DAT degradation. We also found DAT palmitoylation increases transporter capacity with no change in surface expression, indicating changes in transport  $V_{max}$  occur via a kinetic mechanism. With respect to membrane lateral mobility, we found DAT palmitoylation increases the time of recovery, suggesting palmitoylation decreases the membrane lateral mobility of DAT. Additionally, in this study we provide evidence showing DAT

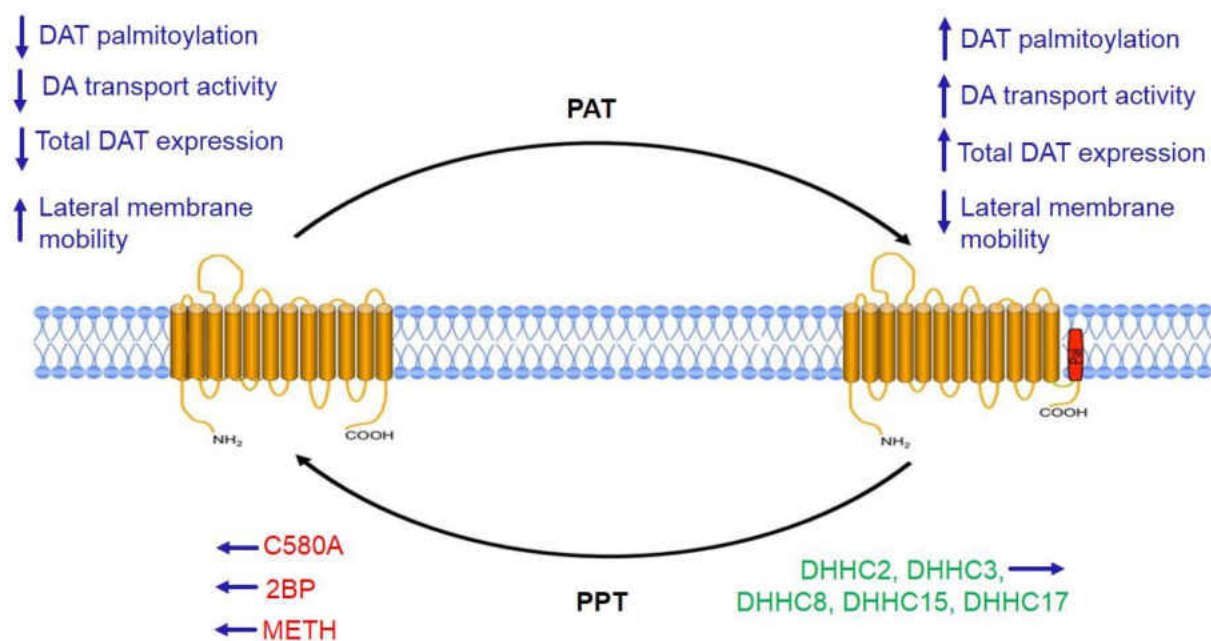


Figure 26: Mechanism of DAT palmitoylation. A Schematic representation of DAT palmitoylation and depalmitoylation cycles. The red palmitate group represents a known site of palmitoylation on the C-terminus near the TM12/cytoplasm interface. Increased DAT palmitoylation catalyzed by select DHHC enzymes results in increased total DAT expression, increased DA transport capacity, and decreased lateral membrane mobility. In contrast depalmitoylation by PPT enzymes results in decreased palmitoylation, decreased transporter expression, decreased DA uptake capacity, and increase in lateral membrane mobility. Methamphetamine (METH), C580A mutant, and 2-bromopalmitate (2BP) all reduce DAT palmitoylation.

palmitoylation is regulated by METH in both native and model systems. Together these findings indicate that palmitoylation of DAT alters the function and regulation of the transporter.

Our studies revealed that DAT palmitoylation can be catalyzed by several but not all, DHHC enzymes evaluated, suggesting a level of substrate specificity in both the LLCPK<sub>1</sub> and N2a cells. Similar findings have been reported for other neuronal proteins (112, 125, 160, 161), suggesting that substrate palmitoylation by multiple DHHC enzymes is important for the mechanism of palmitoylation. The 23 DHHC enzymes are found present in many intracellular localizations including the Golgi apparatus, ER, and plasma membrane (133, 156), however it remains unknown where DAT is being palmitoylated at. From our results we can infer DAT is being palmitoylated in some degree in the Golgi since the immature form of DAT is palmitoylated; however, the multiple DHHC enzymes involved in DAT palmitoylation could suggest palmitoylation is taking place at multiple locations including the plasma membrane. The redundancy in substrate recognition might be important for the turnover of the protein, however remains unknown. The dynamic nature of palmitoylation and depalmitoylation could potentially allow for multiple palmitoylation/ depalmitoylation cycles to occur during the time DAT is synthesized to the time it is degraded. This process could require multiple DHHC enzymes to palmitoylate DAT at different subcellular locations effecting the overall function of the transporter.

Further support for substrate specificity was validated by [<sup>3</sup>H]palmitate labeling and mutagenic studies, confirming DHHC2 significantly increases DAT palmitoylation. Our studies revealed that the enzymatic activity of DHHC2 is required for increased DAT

palmitoylation. Similar mutagenic studies have been reported (125, 130), supporting the idea that the intact DHHC motif is required for palmitoylation (138, 162). Studies have shown mutations of the Cys in the DHHC motif blocks both autoacylation and transfer activity of DHHC enzymes (126), however the exact Cys was unknown. Recently, it was discovered that the Cys of the DHHC motif is specifically required for the two step catalytic mechanisms of palmitoylation (140). Furthermore, the same study found mutation of the highly conserved cysteine rich domain outside of the DHHC motif also results in activity deficits (140), suggesting the importance of this region.

Palmitoylation can alter membrane proteins in various ways, affecting the conformation and regulation (117–121). Therefore we investigated the functional effects of DAT palmitoylation. We found DAT palmitoylation significantly increased DA transport with no changes in surface expression, suggesting changes in DA transport are occurring via a kinetic mechanisms. Several observations support the occurrence of this type of transport. Down-regulation has been shown to still occur when ConA treatment is used to block PMA-induced DAT endocytosis (108). Furthermore, rat striatal synaptosomes prepared in hypertonic sucrose, which is known to inhibit clathrin-mediated endocytosis (163), still resulted in down regulation when treated with PMA and 2BP with surface levels unchanged (149). Our results further provide support that DA transport can undergo regulation at the plasma membrane via a kinetic mechanism.

The mechanism for transport regulation by palmitoylation remains unknown, however it is most likely an indirect effect that is presumably affecting the rate of transport. Palmitoylation has been shown to affect many aspects of membrane proteins that could attribute to changes in transporter function (117–121). Specifically,

palmitoylation can affect the conformation of TMD (119, 164). Palmitoylation has been shown to facilitate the re-orientation of TMDs, by maximizing hydrophobic matching and tilting a TMD peptide (117, 165). Evidence for this was provided by structural studies in artificial lipid membranes, which the addition of a palmitoylation chain induced the tilt of the helix in the membrane plane (165). More recently *in vivo* studies have suggested that this action also occurs in full-length proteins in biological membranes (117). These studies suggest the possibility that tilting of TMD12 of DAT could affect the function of transporter, altering the transport mechanism. The substrate translocation pathways of DAT is formed by TMD1, TMD3, TMD6, and TMD8, (44, 55), while the major site of palmitoylation is found on TMD12, outside the inner core and does not contribute directly to the substrate active site. Substrate translocation occurs via an alternating access mechanism. DAT cycles through outward and inward facing conformations that allow for binding of substrates and release into the cytoplasm (21, 54). These conformations are controlled by extracellular and intracellular gate residues and the equilibrium between these conformations determines the rate of forward transport therefore a slight tilt of the TMD 12 could have major effects on transport activity. The dDAT structure revealed a latch-like C-terminal helix (Figure 27) thought to be important for interactions with the cytoplasmic face of the transporter. The C-terminal helix was found to interact with IL1 (Figure 27B), which interacts with TMD1a. The close proximal interaction with the cytoplasmic gate suggests the C-terminal helix may be important for activity and changes in palmitoylation could modulating transport (50).



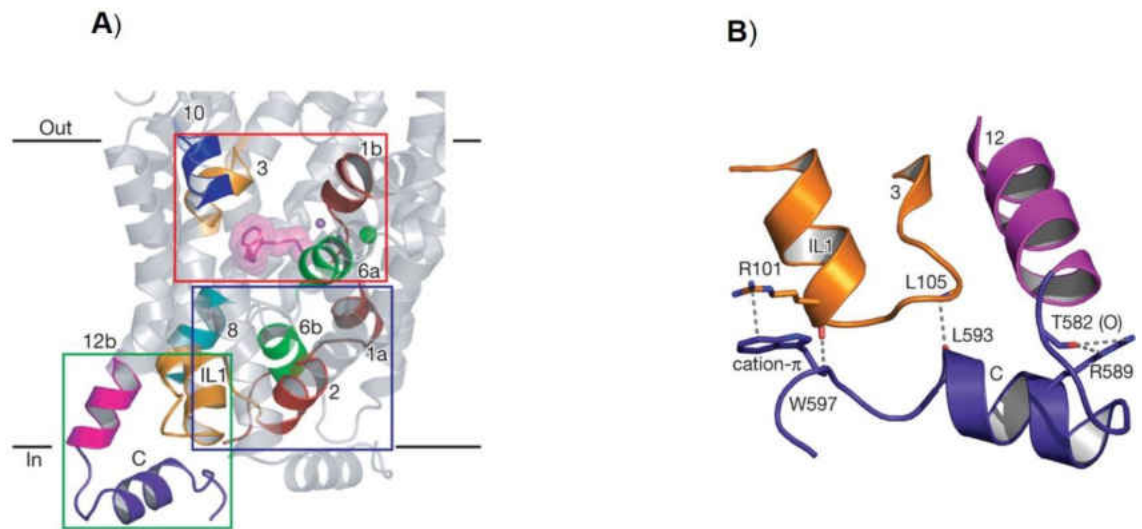


Figure 27. C-terminal latch of the dopamine transporter. A. x-ray crystal structure of the *Drosophila melanogaster* dopamine transporter (dDAT). (A). Locations of the open extracellular gate (red box), closed intracellular gate (blue box), and C-terminal latch (green box). (B). The C-terminal helix following TMD12 is bound to the cytoplasmic face of the transporter via ionic interactions with IL1. Polar and electrostatic bonds are represented by gray dashed lines. Image modified from A. Penmatal, K.H. Wang, and E. Gouaux. 2013. X-ray structure of the dopamine transporter in complex with tricyclic antidepressant. *Nature* 503(7474): 85-90, with permission

Palmitoylation can also alter protein-protein interactions (164). Alterations in protein interactions is thought to occur through either by steric hindrance, changes in conformation, and/or localization to the membrane interface (164). Palmitoylation has been shown to affect interactions of proteins in both positive and negative ways (119, 164). Studies by McCormick et al. found palmitoylation is required for the interaction of the mannose-6-phosphate receptor and a larger multiprotein complex important for lysosomal targeting (166), however others have shown palmitoylation hinders protein-protein interactions (117, 167). DAT interacts with numerous proteins on both the N- and C-termini (77, 79, 86–91, 94) that affect the overall function of the transporter. Proteins like Rin, CaMKII,  $\alpha$ -Syn, Park, and PICK1 all bind all on the C-terminus of DAT (79) and it is unknown if palmitoylation affects the interactions. Furthermore, the important FREKLAYA (residues 587-596) endocytic regulatory domain important for both basal and PKC-enhanced DAT internalization (87) is also near the C-terminus palmitoylation site. At this point it is unknown if DAT palmitoylation affects these important binding partners. It will be important in the future to determine if these interactions are effected in a positive or negative manner and if they are important for regulation of DAT.

Additional validation studies were done to evaluate our palmitoylation deficient mutant, C580A for palmitoylation and activity when co-expressed with DHHC2. In these studies, we found DAT palmitoylation and transport activity was not increased when palmitoylation was driven by DHHC2, suggesting Cys580 mediates DHHC2-induced changes in DAT palmitoylation. As previously mentioned palmitoylation can alter protein-protein interactions a (112–115), affecting the function of other proteins.

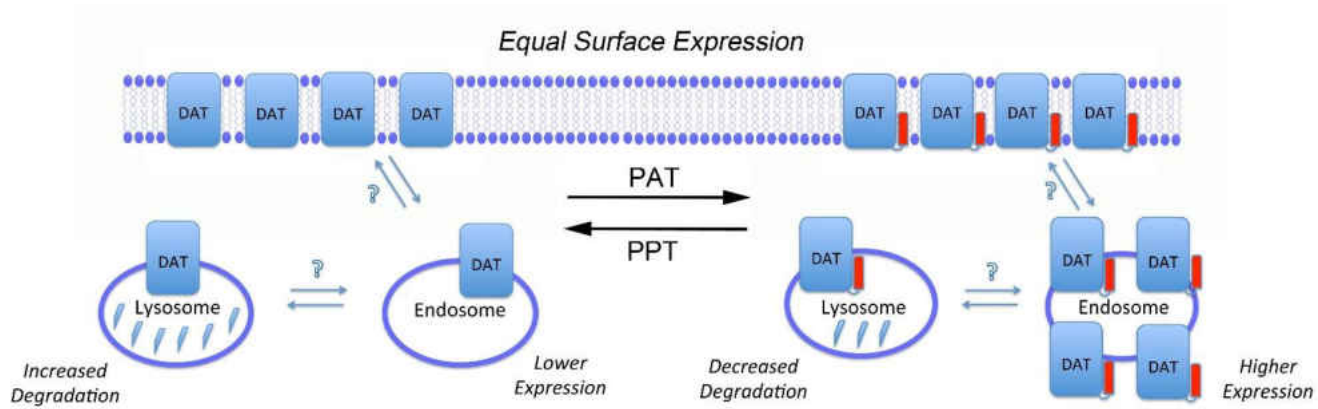


Figure 28. Proposed mechanism of increased DAT expression by DHHC enzymes. Schematic representation of DAT palmitoylation, showing populations possessing decreased palmitoylation (left) or increased palmitoylation (right). Increased palmitoylation is driven by the overexpression of PAT enzymes, whereas depalmitoylation is catalyzed by PPT enzymes. Conditions that increase palmitoylation and total DAT expression are predicted to retain DAT in endosomes resulting in reduced lysosomal degradation. In contrast, decreased palmitoylation and total DAT expression is predicted to have reduced DATs in endosomes with increased lysosomal degradation

However, our results indicate DHHC2 is increasing DAT palmitoylation and transport activity, by palmitoylating the transporter directly at Cys580.

To further support increased DAT palmitoylation effects transporter function, we investigated total DAT expression. Our studies revealed that increased DAT palmitoylation results in increased total DAT expression, suggesting palmitoylation opposes DAT degradation. These results are consistent with our previous studies, which have shown that acute or chronic inhibition of palmitoylation by 2BP results in increased DAT degradation as detected by loss of full-length DAT and the appearance of DAT degradation fragments (149). We know that increased DAT expression is not found at the surface as demonstrated by the surface biotinylation experiments, suggesting increased expression is the result of decreased DAT degradation (Figure 28). We suggest that increased palmitoylation stabilizes DAT in the endosome and reduces DAT targeting to the lysosome, resulting in higher expression and reduced degradation. A small amount of palmitoylated DAT was found in the 200,000 x g fraction of the subcellular fractionation, indicating DAT is in fact in the endosomes. Multiple studies have shown that palmitoylation is important for regulating protein turnover (127). Increased protein turnover and reduced stability has also been found for palmitoylation defective mutants of multiple proteins including, viral membrane glycoprotein of Rous sarcoma virus, the A1 adenosine receptor, and the chemokine receptor CCR5 (168–170). Furthermore, we found C580A DAT has a higher rate of turnover compared to the WT protein, suggesting palmitoylation stabilizes DAT (Amy Mortiz, University of North Dakota, personal communication). Our results provide additional support that palmitoylation opposes DAT degradation.

Palmitoylation has also been shown to alter protein function by targeting palmitoylated proteins to lipid microdomains (164). It has been proposed that increased palmitoylation enhances the affinity of proteins for cholesterol-rich microdomains (164, 171). The affinity of a protein for a lipid microdomain is dependent on multiple factors including: the amino acid composition of the TMD, the interaction of multiple TMD in homo-or hetero-multimers forms, and the interaction with protein binding partners that also have strong associates with lipids (164). Furthermore, it has been shown that disruption of cholesterol in microdomains with m $\beta$ CD results in a significantly faster lateral diffusion of DAT in the plasma membrane (109). In addition, control experiments were performed in our lab in which the C580A palmitoylation deficient mutant and treatment with 2BP both resulted in decreased lateral membrane mobility (Madhur Shetty, University of North Dakota, personal communication). From our studies we speculate palmitoylation could be reducing the membrane lateral mobility of DAT in various ways. The obvious mechanism is palmitoylated DAT is targeted to lipid microdomains, thus reducing lateral membrane mobility and affecting the function of the transporter. However, recent data from our lab suggests reduced palmitoylation actually targets DAT to rafts domains (Madhur Shetty, University of North Dakota, personal communication), suggesting increased palmitoylation does not target DAT to lipid membrane rafts. Another mechanism which might result in reduced lateral mobility of DAT is protein-protein interactions. It is well known that DAT has multiple binding partners that affect its function (79) as previously mentioned. Furthermore, palmitoylation can promote protein-protein interactions by modifying the conformation of the protein (164). Therefore enhanced DAT palmitoylation could promote interactions

with known DAT binding partners, resulting in reduced lateral membrane mobility. DAT palmitoylation could also be promoting DAT oligomerization, again reducing lateral membrane mobility

In this study we provided the first evidence that DAT palmitoylation is regulated by METH. We found treatment with METH for 30 and 60 min in LLCPK<sub>1</sub> cells resulted in a significant decrease in DAT palmitoylation. In addition, animals SC injected with METH for 10, 30, and 60 min were also found to have decreased DAT palmitoylation, demonstrating an important similarity between native and model systems. Interestingly, cocaine treatment had no effect on DAT palmitoylation, suggesting a difference in regulation between the two drugs. Similar studies have been done; however, phosphorylation was measured after METH treatment (39). In these studies, Cervinski et. al. found treatment with AMPH or METH resulted in a significant increase in DAT phosphorylation. The DAT blocker cocaine, however did not affect DAT phosphorylation but prevent the phosphorylation increase induced by METH (39). Together, these studies suggest palmitoylation and phosphorylation may be working opposite of each other in an unknown mechanism.

Several observation support the occurrence of reciprocal regulation of DAT palmitoylation and phosphorylation after METH treatment. Most recently, our lab has demonstrated that the palmitoylation deficient mutant, C580A had enhanced basal DAT phosphorylation levels in comparison to WT (150). In reverse experiments, the phosphorylation mutant, S7A had increased DAT palmitoylation when assessed by [<sup>3</sup>H] palmitate labeling. Further pharmacological experiments were done and confirmed the mutagenic results. Additionally, regulation of DAT palmitoylation by DHHC enzymes

supports the reciprocity between DAT palmitoylation and phosphorylation. Studies have shown, treatment with METH, which increases DAT phosphorylation (39), results in DAT downregulation and endocytosis (39, 71–73). In contrast, our studies demonstrate enhanced palmitoylation by the over expression of DHHC enzymes drive DAT palmitoylation, resulting in increased DA transport capacity. Together these studies provide further evidence that palmitoylation and phosphorylation are reciprocally regulated and important for DAT regulation and function

Similar mechanisms have been shown for other proteins as well (121, 172–174). Examples of this include the  $\beta$ 2-adrenergic receptor in which palmitoylation of Cys341 interferes with PKC-mediated phosphorylation of Ser345 and Ser346, modulating the capacity which the receptors interacts with Gs (172). Another example is phosphodiesterase 10A, in which phosphorylation of Thr16 regulates trafficking and localization by preventing palmitoylation of Cys11 (121). Although similar in mechanism, these examples are different from DAT because the phosphorylation and palmitoylation sites of  $\beta$ 2-adrenergic receptor and phosphodiesterase 10A are in close proximity in the primary sequence, while DAT's sites are far apart in the primary sequences. This could suggest that the N-and-C termini are in close proximity in the tertiary structure, however based on the current crystal structures, (44, 52) little is known about the N and C termini interactions.

Disruption in dopaminergic signaling is thought to be the consequence of dysregulation of DAT resulting in abnormal DA clearance (175). Studies have shown non-coding single nucleotide polymorphisms and variable-number tandem repeats in the DAT1 gene to correlate with predisposition to various neurological and psychiatric

disorders (176). More recently, rare coding polymorphisms have been identified in patients diagnosed with ADHD, bipolar disorder, and autism spectrum disorder (68, 177–180). These mutations have been shown to affect DAT function in numerous ways including elevated efflux and increased transporter phosphorylation (178–180). Likewise, we know from numerous studies that DHHC enzymes have been associated with dopaminergic and neuropsychiatric diseases such as schizophrenia, X-linked intellectual disability, Alzheimer disease, and Huntington disease (113, 141, 142, 146, 147, 181, 182), highlighting the importance of this modification in proper neuronal function. Mutations in enzymes regulating palmitate removal can also result in disease (147, 148), indicating that palmitoylation is relevant to disease processes. Imbalances in DA in dopaminergic diseases may result from alterations in palmitoylation, therefore, DHHC enzymes that catalyze DAT palmitoylation could represent potential therapeutic targets for dopaminergic disorders and drug addiction. Overall, these results suggest that palmitoylation plays a critical role in promoting both short- and long-term regulation of DAT by controlling important functions of the transporter, thereby potentially impacting neurotransmitter clearance in dopaminergic disorders.



## APPENDIX

### ABE analysis in the LLCPK<sub>1</sub> cells

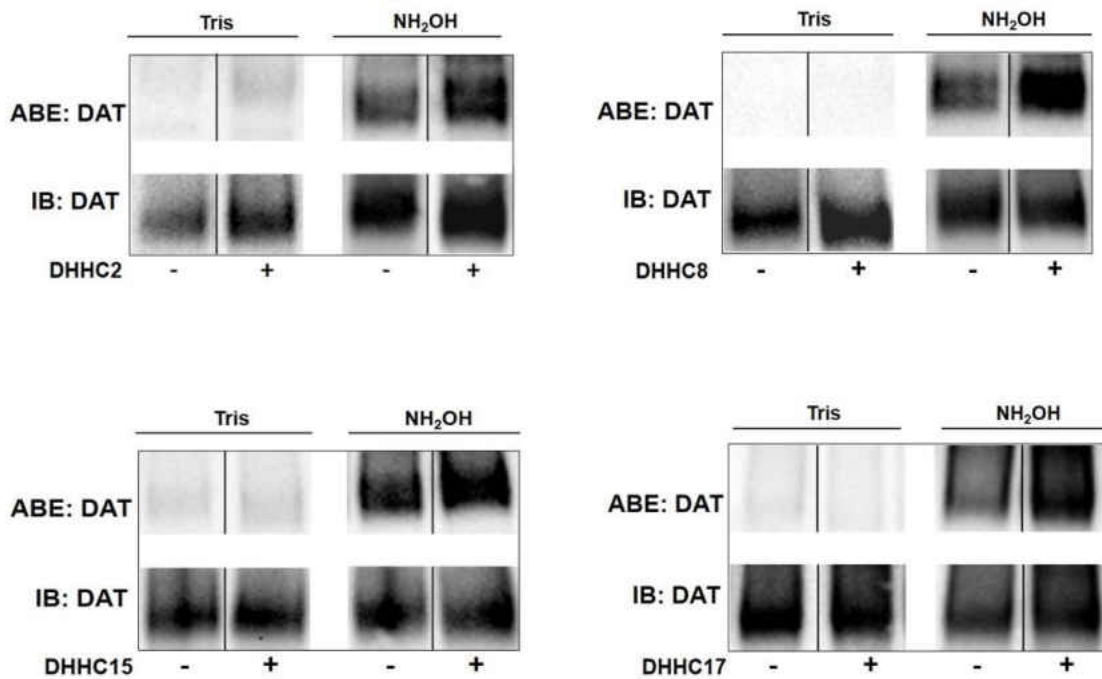


Figure 29: ABE analysis of increased DAT palmitoylation in the LLCPK<sub>1</sub> cells. rDAT LLCPK<sub>1</sub> cells transiently transfected with the indicated DHHC coding plasmids were harvested and membranes isolated, followed by assessment of DAT palmitoylation by ABE. Upper panels show representative ABE blots with matching total DAT immunoblots.

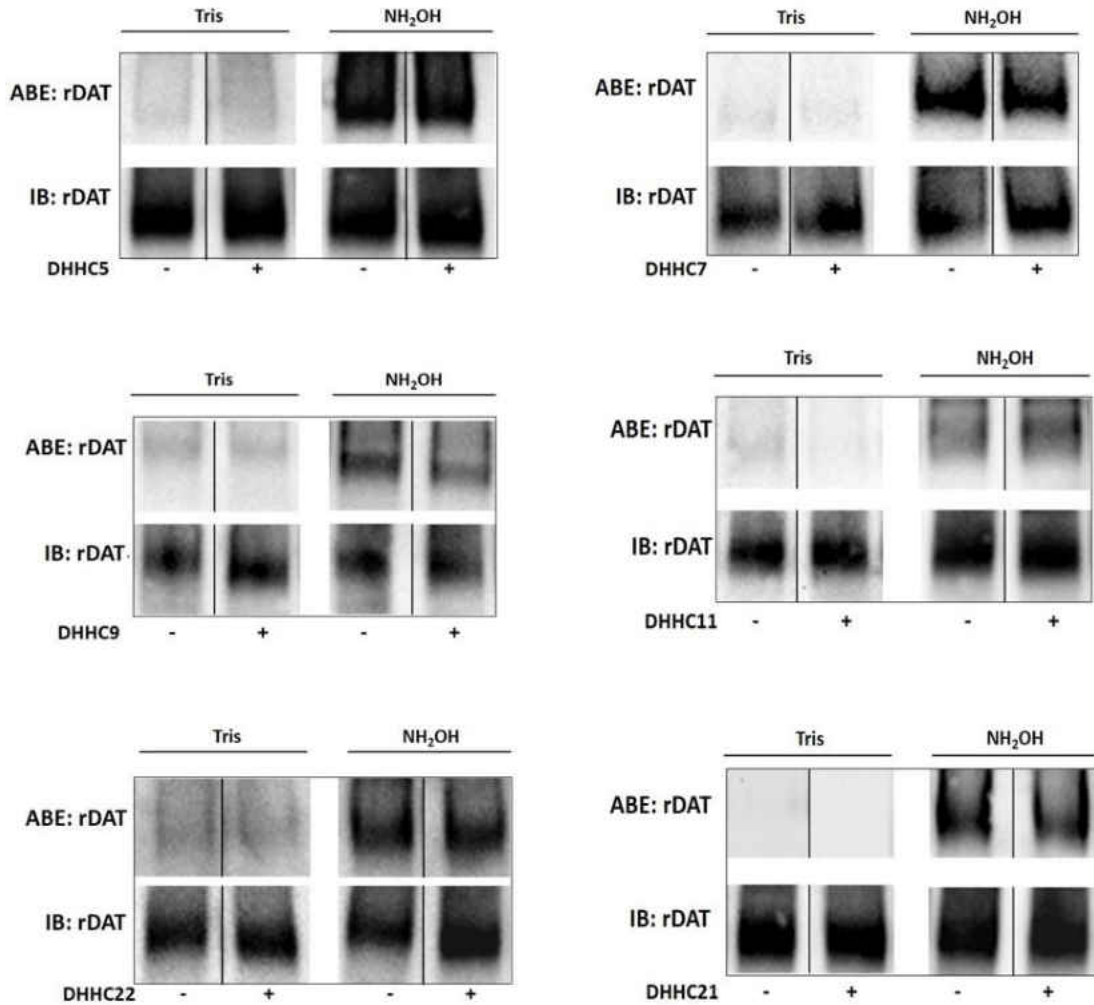


Figure 30: ABE analysis of co-expressed DHHC enzymes that have no effect on DAT palmitoylation in the LLCPK<sub>1</sub> cells. rDAT LLCPK<sub>1</sub> cells transiently transfected with the indicated DHHC coding plasmids were harvested and membranes isolated, followed by assessment of DAT palmitoylation by ABE. Upper panels show representative ABE blots with matching total DAT immunoblots.

ABE analysis in the N2a cells

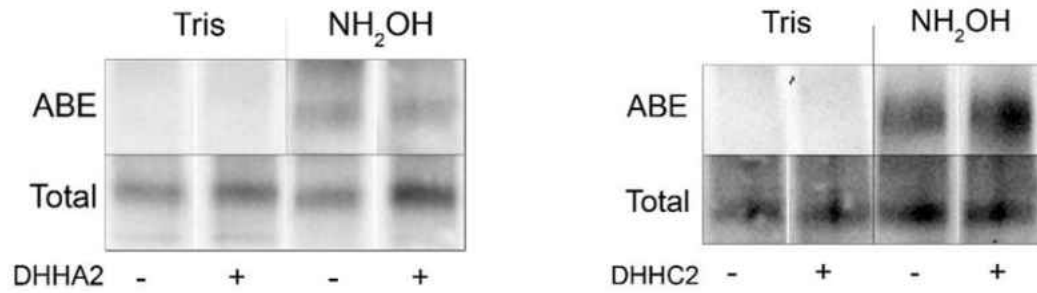


Figure 31: ABE analysis in the N2a cells. N2a- cells transiently transfected with the indicated DHHC coding plasmids were harvested and membranes isolated, followed by assessment of DAT palmitoylation by ABE. Upper panels show representative ABE blots with matching total DAT immunoblots.

## REFERENCES

1. Carlsson, a (1959) The occurrence, distribution and physiological role of catecholamines in the nervous system. *Pharmacol. Rev.* **11**, 490–493
2. Yeragani, V. K., Tancer, M., Chokka, P., & Baker, G. B. (2010) Arvid Carlsson, and the story of dopamine. *Indian J. Psychiatry.* **52**, 87–88
3. Iversen, S. D., and Iversen, L. L. (2007) Dopamine: 50 years in perspective. *Trends Neurosci.* **30**, 188–93
4. Elsworth, J. D., and Roth, R. H. (1997) Dopamine synthesis, uptake, metabolism, and receptors: relevance to gene therapy of Parkinson’s disease. *Exp. Neurol.* **144**, 4–9
5. Südhof, T. C. (2013) Neurotransmitter release: the last millisecond in the life of a synaptic vesicle. *Neuron.* **80**, 675–90
6. Ungerstedt, U. (1971) Stereotaxic mapping of the monoamine pathways in the rat brain. *Acta Physiol. Scand.* **367**, 1–48
7. Moore, R.Y. and Bloom, F. . (1978) Central catecholamine neuron systems: anatomy and physiology of the dopamine systems. *Annu. Rev. Neurosci.* **1**, 129–69
8. Schultz, W. (1999) The Reward Signal of Midbrain Dopamine Neurons. *News Physiol. Sci.* **14**, 249–255
9. Olds, J., and Milnkr, P. (1954) Postive reinforcement produced by electrical stimulation of septal area and other regions of rat brain. *Public Health*
10. Di Chiara, G., and Imperato, a (1988) Drugs abused by humans preferentially increase synaptic dopamine concentrations in the mesolimbic system of freely moving rats. *Proc. Natl. Acad. Sci. U. S. A.* **85**, 5274–5278
11. Pontieri, F. E., Tanda, G., and Di Chiara, G. (1995) Intravenous cocaine, morphine, and amphetamine preferentially increase extracellular dopamine in the “shell” as compared with the “core” of the rat nucleus accumbens. *Proc. Natl. Acad. Sci. U. S. A.* **92**, 12304–12308

12. Roberts, D. C. S., Corcoran, M. E., and Fibiger, H. C. (1977) On the role of ascending catecholaminergic systems in intravenous self administration of cocaine. *Pharmacol. Biochem. Behav.* **6**, 615–620
13. Kuhar, M. J., Ritz, M. C., and Boja, J. W. (1991) The dopamine hypothesis of the reinforcing properties of cocaine. *Trends Neurosci.* **14**, 299–302
14. Spanagel, R., and Weiss, F. (1999) The dopamine hypothesis of reward: past and current status. *Trends Neurosci.* **22**, 521–527
15. Giros, B., Jaber, M., Jones, S. R., Wightman, R. M., and Caron, M. G. (1996) Hyperlocomotion and indifference to cocaine and amphetamine in mice lacking the dopamine transporter. *Nature.* **379**, 606–612
16. Rocha, B. A., Fumagalli, F., Gainetdinov, R. R., Jones, S. R., Ator, R., Giros, B., Miller, G. W., Caron, M. G., Address, P., and Inseem, U. (1998) Cocaine self-administration in dopamine-transporter knockout mice
17. Sora, I., Wichems, C., Takahashi, N., Li, X. F., Zeng, Z., Revay, R., Lesch, K. P., Murphy, D. L., and Uhl, G. R. (1998) Cocaine reward models: conditioned place preference can be established in dopamine- and in serotonin-transporter knockout mice. *Proc. Natl. Acad. Sci. U. S. A.* **95**, 7699–7704
18. Hall, F. S., Sora, I., Drgonova, J., Li, X.-F., Goeb, M., and Uhl, G. R. (2004) Molecular mechanisms underlying the rewarding effects of cocaine. *Ann. N. Y. Acad. Sci.* **1025**, 47–56
19. Chen, R., Han, D. D., and Gu, H. H. (2005) A triple mutation in the second transmembrane domain of mouse dopamine transporter markedly decreases sensitivity to cocaine and methylphenidate. *J. Neurochem.* **94**, 352–359
20. Chen, R., Tilley, M. R., Wei, H., Zhou, F., Zhou, F.-M., Ching, S., Quan, N., Stephens, R. L., Hill, E. R., Nottoli, T., Han, D. D., and Gu, H. H. (2006) Abolished cocaine reward in mice with a cocaine-insensitive dopamine transporter. *Proc. Natl. Acad. Sci. U. S. A.* **103**, 9333–9338
21. Kristensen, A. S., Andersen, J., Jørgensen, T. N., Sørensen, L., Eriksen, J., Loland, C. J., Strømgaard, K., and Gether, U. (2011) SLC6 neurotransmitter transporters: structure, function, and regulation. *Pharmacol. Rev.* **63**, 585–640
22. Bröer, S. (2006) The SLC6 orphans are forming a family of amino acid transporters. *Neurochem. Int.* **48**, 559–567
23. Giros, B., el Mestikawy, S., Godinot, N., Zheng, K., Han, H., Yang-Feng, T., and Caron, M. G. (1992) Cloning, pharmacological characterization, and chromosome assignment of the human dopamine transporter. *Mol. Pharmacol.* **42**, 383–390

24. Giros, B., El Mestikawy, S., Bertrand, L., and Caron, M. G. (1991) Cloning and functional characterization of a cocaine-sensitive dopamine transporter. *FEBS Lett.* **295**, 149–154
25. Chen, J. G., Liu-Chen, S., and Rudnick, G. (1998) Determination of external loop topology in the serotonin transporter by site-directed chemical labeling. *J. Biol. Chem.* **273**, 12675–12681
26. Kilty, J. E., Lorang, D., and Amara, S. G. (1991) Cloning and expression of a cocaine-sensitive rat dopamine transporter. *Science.* **254**, 578–579
27. Stockner, T., Montgomery, T. R., Kudlacek, O., Weissensteiner, R., Ecker, G. F., Freissmuth, M., and Sitte, H. H. (2013) Mutational Analysis of the High-Affinity Zinc Binding Site Validates a Refined Human Dopamine Transporter Homology Model. *PLoS Comput. Biol.* 10.1371/journal.pcbi.1002909
28. Norgaard-Nielsen, K., Norregaard, L., Hastrup, H., Javitch, J. a., and Gether, U. (2002) Zn<sup>2+</sup> site engineering at the oligomeric interface of the dopamine transporter. *FEBS Lett.* **524**, 87–91
29. Miranda, M., Wu, C. C., Sorkina, T., Korstjens, D. R., and Sorkin, A. (2005) Enhanced ubiquitylation and accelerated degradation of the dopamine transporter mediated by protein kinase C. *J. Biol. Chem.* **280**, 35617–24
30. Miranda, M., Dionne, K. R., Sorkina, T., and Sorkin, A. (2007) Three ubiquitin conjugation sites in the amino terminus of the dopamine transporter mediate protein kinase C-dependent endocytosis of the transporter. *Mol. Biol. Cell.* **18**, 313–23
31. Vaughan, R. a, and Kuhar, M. J. (1996) Dopamine transporter ligand binding domains. Structural and functional properties revealed by limited proteolysis. *J.Biol.Chem.* **271**, 21672–21680
32. Li, L.-B., Chen, N., Ramamoorthy, S., Chi, L., Cui, X.-N., Wang, L. C., and Reith, M. E. a (2004) The role of N-glycosylation in function and surface trafficking of the human dopamine transporter. *J. Biol. Chem.* **279**, 21012–21020
33. Torres, G. E., Carneiro, A., Seamans, K., Fiorentini, C., Sweeney, A., Yao, W. D., and Caron, M. G. (2003) Oligomerization and trafficking of the human dopamine transporter: Mutational analysis identifies critical domains important for the functional expression of the transporter. *J. Biol. Chem.* **278**, 2731–2739
34. Chen, R., Wei, H., Hill, E. R., Chen, L., Jiang, L., Han, D. D., and Gu, H. H. (2007) Direct evidence that two cysteines in the dopamine transporter form a disulfide bond. *Mol. Cell. Biochem.* **298**, 41–48

35. Huff, R. A., Vaughan, R. A., Kuhar, M. J., and Uhl, G. R. (1997) Phorbol esters increase dopamine transporter phosphorylation and decrease transport Vmax. *J. Neurochem.* **68**, 225–32
36. Vaughan, R. A., Huff, R. A., Uhl, G. R., and Kuhar, M. J. (1997) Protein kinase C-mediated phosphorylation and functional regulation of dopamine transporters in striatal synaptosomes. *J. Biol. Chem.* **272**, 15541–6
37. Gorentla, B. K., Moritz, A. E., Foster, J. D., and Vaughan, R. A. (2009) Proline-directed phosphorylation of the dopamine transporter N-terminal domain. *Biochemistry.* **48**, 1067–76
38. Foster, J. D., Pananusorn, B., and Vaughan, R. A. (2002) Dopamine transporters are phosphorylated on N-terminal serines in rat striatum. *J. Biol. Chem.* **277**, 25178–86
39. Cervinski, M. A., Foster, J. D., and Vaughan, R. A. (2005) Psychoactive substrates stimulate dopamine transporter phosphorylation and down-regulation by cocaine-sensitive and protein kinase C-dependent mechanisms. *J. Biol. Chem.* **280**, 40442–40449
40. Granas, C., Ferrer, J., Loland, C. J., Javitch, J. A., and Gether, U. (2003) N-terminal truncation of the dopamine transporter abolishes phorbol ester- and substance P receptor-stimulated phosphorylation without impairing transporter internalization. *J. Biol. Chem.* **278**, 4990–5000
41. Moritz, A. E., Foster, J. D., Gorentla, B. K., Mazei-Robison, M. S., Yang, J.-W., Sitte, H. H., Blakely, R. D., and Vaughan, R. A. (2013) Phosphorylation of dopamine transporter serine 7 modulates cocaine analog binding. *J. Biol. Chem.* **288**, 20–32
42. Foster, J. D., Yang, J.-W., Moritz, A. E., Challasivakanaka, S., Smith, M. A., Holy, M., Wilebski, K., Sitte, H. H., and Vaughan, R. A. (2012) Dopamine transporter phosphorylation site threonine 53 regulates substrate reuptake and amphetamine-stimulated efflux. *J. Biol. Chem.* **287**, 29702–12
43. Lu, K. P., Liou, Y., and Zhou, X. Z. (2002) Pinning down phosphorylation signaling. *Trends Cell Biol.* **12**, 164–172
44. Yamashita, A., Singh, S. K., Kawate, T., Jin, Y., and Gouaux, E. (2005) Crystal structure of a bacterial homologue of Na<sup>+</sup>/Cl<sup>-</sup>-dependent neurotransmitter transporters. *Nature.* **437**, 215–223

45. Beuming, T., Shi, L., Javitch, J. A., and Weinstein, H. (2006) A comprehensive structure-based alignment of prokaryotic and eukaryotic neurotransmitter/Na<sup>+</sup> symporters (NSS) aids in the use of the LeuT structure to probe NSS structure and function. *Mol. Pharmacol.* **70**, 1630–42
46. Henry, L. K., Meiler, J., and Blakely, R. D. (2007) Bound to be different: neurotransmitter transporters meet their bacterial cousins. *Mol. Interv.* **7**, 306–309
47. Rudnick, G. (2006) Serotonin transporters--structure and function. *J. Membr. Biol.* **213**, 101–110
48. Kanner, B. I., and Zomot, E. (2008) Sodium-coupled neurotransmitter transporters. *Chem. Rev.* **108**, 1654–1668
49. Torres, G. E., Gainetdinov, R. R., and Caron, M. G. (2003) Plasma membrane monoamine transporters: structure, regulation and function. *Nat. Rev. Neurosci.* **4**, 13–25
50. Penmatsa, A., Wang, K. H., and Gouaux, E. (2013) X-ray structure of dopamine transporter elucidates antidepressant mechanism. *Nature.* **503**, 85–90
51. Hong, W. C., and Amara, S. G. (2010) Membrane cholesterol modulates the outward facing conformation of the dopamine transporter and alters cocaine binding. *J. Biol. Chem.* **285**, 32616–32626
52. Penmatsa, A., Wang, K. H., and Gouaux, E. (2013) X-ray structure of dopamine transporter elucidates antidepressant mechanism. *Nature.* **503**, 85–90
53. Jardetzky, O. (1966) Simple allosteric model for membrane pumps. *Nature.* **211**, 969–70
54. Forrest, L. R., Zhang, Y.-W., Jacobs, M. T., Gesmonde, J., Xie, L., Honig, B. H., and Rudnick, G. (2008) Mechanism for alternating access in neurotransmitter transporters. *Proc. Natl. Acad. Sci. U. S. A.* **105**, 10338–10343
55. Krishnamurthy, H., Piscitelli, C. L., and Gouaux, E. (2009) Unlocking the molecular secrets of sodium-coupled transporters. *Nature.* **459**, 347–355
56. Singh, S. K., Piscitelli, C. L., Yamashita, A., and Gouaux, E. (2008) A competitive inhibitor traps LeuT in an open-to-out conformation. *Science.* **322**, 1655–1661
57. Kahlig, K. M., and Galli, A. (2003) Regulation of dopamine transporter function and plasma membrane expression by dopamine, amphetamine, and cocaine. *Eur. J. Pharmacol.* **479**, 153–158



58. Shan, Javitch, Shi, and Weinstein (2011) The substrate-driven transition to an inward-facing conformation in the functional mechanism of the dopamine transporter. *PLoS One*. **6**, e16350
59. Schmitt, K. C., and Reith, M. E. A. (2010) Regulation of the dopamine transporter: aspects relevant to psychostimulant drugs of abuse. *Ann. N. Y. Acad. Sci.* **1187**, 316–40
60. Ritz, M. C., and Kuhar, M. J. (1989) Relationship between self-administration of amphetamine and monoamine receptors in brain: comparison with cocaine. *J. Pharmacol. Exp. Ther.* **248**, 1010–7
61. Mash, D. C., Pablo, J., Ouyang, Q., Hearn, W. L., and Izenwasse, S. (2002) Dopamine transport function is elevated in cocaine users. *J. Neurochem.* **81**, 292–300
62. Urban, N. B. L., and Martinez, D. (2012) Neurobiology of Addiction. Insight from Neurochemical Imaging. *Psychiatr. Clin. North Am.* **35**, 521–541
63. Little, K. Y., Zhang, L., Desmond, T., Frey, K. a, Dalack, G. W., and Cassin, B. J. (1999) Striatal dopaminergic abnormalities in human cocaine users. *Am. J. Psychiatry.* **156**, 238–245
64. Jayanthi, L. D., and Ramamoorthy, S. (2005) Regulation of monoamine transporters: influence of psychostimulants and therapeutic antidepressants. *AAPS J.* **7**, E728–38
65. Eshleman, a J., Henningsen, R. a, Neve, K. a, and Janowsky, a (1994) Release of dopamine via the human transporter. *Mol. Pharmacol.* **45**, 312–316
66. Sulzer, D., Chen, T. K., Lau, Y. Y., Kristensen, H., Rayport, S., and Ewing, a (1995) Amphetamine redistributes dopamine from synaptic vesicles to the cytosol and promotes reverse transport. *J. Neurosci.* **15**, 4102–4108
67. Sulzer, D., Sonders, M. S., Poulsen, N. W., and Galli, A. (2005) Mechanisms of neurotransmitter release by amphetamines: a review. *Prog. Neurobiol.* **75**, 406–33
68. Vaughan, R. A., and Foster, J. D. (2013) Mechanisms of dopamine transporter regulation in normal and disease states. *Trends Pharmacol. Sci.* **34**, 489–96
69. Johnson, L. A., Guptaroy, B., Lund, D., Shamban, S., and Gnegy, M. E. (2005) Regulation of amphetamine-stimulated dopamine efflux by protein kinase C beta. *J. Biol. Chem.* **280**, 10914–9

70. Furman, C. A., Chen, R., Guptaroy, B., Zhang, M., Holz, R. W., and Gnegy, M. (2009) Dopamine and amphetamine rapidly increase dopamine transporter trafficking to the surface: live-cell imaging using total internal reflection fluorescence microscopy. *J. Neurosci.* **29**, 3328–36
71. Chen, R., Furman, C. a, Zhang, M., Kim, M. N., Gereau, R. W., Leitges, M., and Gnegy, M. E. (2009) Protein kinase Cbeta is a critical regulator of dopamine transporter trafficking and regulates the behavioral response to amphetamine in mice. *J. Pharmacol. Exp. Ther.* **328**, 912–920
72. Richards, T. L., and Zahniser, N. R. (2009) Rapid substrate-induced down-regulation in function and surface localization of dopamine transporters: rat dorsal striatum versus nucleus accumbens. *J. Neurochem.* **108**, 1575–84
73. Saunders, C., Ferrer, J. V, Shi, L., Chen, J., Merrill, G., Lamb, M. E., Leeb-Lundberg, L. M., Carvelli, L., Javitch, J. a, and Galli, a (2000) Amphetamine-induced loss of human dopamine transporter activity: an internalization-dependent and cocaine-sensitive mechanism. *Proc. Natl. Acad. Sci. U. S. A.* **97**, 6850–6855
74. German, C. L., Hanson, G. R., and Fleckenstein, A. E. (2012) Amphetamine and methamphetamine reduce striatal dopamine transporter function without concurrent dopamine transporter relocation. *J. Neurochem.* **123**, 288–297
75. Gorentla, B. K., and Vaughan, R. A. (2005) Differential effects of dopamine and psychoactive drugs on dopamine transporter phosphorylation and regulation. *Neuropharmacology.* **49**, 759–68
76. Richards, T. L., and Zahniser, N. R. (2009) Rapid substrate-induced down-regulation in function and surface localization of dopamine transporters: Rat dorsal striatum versus nucleus accumbens. *J. Neurochem.* **108**, 1575–1584
77. Fog, J. U., Khoshbouei, H., Holy, M., Owens, W. A., Vaegter, C. B., Sen, N., Nikandrova, Y., Bowton, E., McMahon, D. G., Colbran, R. J., Daws, L. C., Sitte, H. H., Javitch, J. A., Galli, A., and Gether, U. (2006) Calmodulin kinase II interacts with the dopamine transporter C terminus to regulate amphetamine-induced reverse transport. *Neuron.* **51**, 417–29
78. Khoshbouei, H., Sen, N., Guptaroy, B., Johnson, L., Lund, D., Gnegy, M. E., Galli, A., and Javitch, J. a. (2004) N-terminal phosphorylation of the dopamine transporter is required for amphetamine-induced efflux. *PLoS Biol.* **2**, 387–393
79. Torres, G. E. (2006) The dopamine transporter proteome. *J. Neurochem.* **97 Suppl 1**, 3–10

80. Lee, K. H., Kim, M. Y., Kim, D. H., and Lee, Y. S. (2004) Syntaxin 1A and receptor for activated C kinase interact with the N-terminal region of human dopamine transporter. *Neurochem. Res.* **29**, 1405–1409
81. Binda, F., Dipace, C., Bowton, E., Robertson, S. D., Lute, B. J., Fog, J. U., Zhang, M., Sen, N., Colbran, R. J., Gnegy, M. E., Gether, U., Javitch, J. A., Erreger, K., and Galli, A. (2008) Syntaxin 1A interaction with the dopamine transporter promotes amphetamine-induced dopamine efflux. *Mol. Pharmacol.* **74**, 1101–8
82. Carvelli, L., Blakely, R. D., and DeFelice, L. J. (2008) Dopamine transporter/syntaxin 1A interactions regulate transporter channel activity and dopaminergic synaptic transmission. *Proc. Natl. Acad. Sci. U. S. A.* **105**, 14192–7
83. Cervinski, M. a., Foster, J. D., and Vaughan, R. a. (2010) Syntaxin 1A regulates dopamine transporter activity, phosphorylation and surface expression. *Neuroscience.* **170**, 408–416
84. Cervinski, M. a., Foster, J. D., and Vaughan, R. a. (2010) Syntaxin 1A regulates dopamine transporter activity, phosphorylation and surface expression. *Neuroscience.* **170**, 408–416
85. Lee, F. J. S., Pei, L., Moszczynska, A., Vukusic, B., Fletcher, P. J., and Liu, F. (2007) Dopamine transporter cell surface localization facilitated by a direct interaction with the dopamine D2 receptor. *EMBO J.* **26**, 2127–2136
86. Torres, G. E., Yao, W. D., Mohn, A. R., Quan, H., Kim, K. M., Levey, A. I., Staudinger, J., and Caron, M. G. (2001) Functional interaction between monoamine plasma membrane transporters and the synaptic PDZ domain-containing protein PICK1. *Neuron.* **30**, 121–34
87. Boudanova, E., Navaroli, D. M., Stevens, Z., and Melikian, H. E. (2008) Dopamine transporter endocytic determinants: carboxy terminal residues critical for basal and PKC-stimulated internalization. *Mol. Cell. Neurosci.* **39**, 211–7
88. Navaroli, D. M., Stevens, Z. H., Uzelac, Z., Gabriel, L., King, M. J., Lifshitz, L. M., Sitte, H. H., and Melikian, H. E. (2011) The Plasma Membrane-Associated GTPase Rin Interacts with the Dopamine Transporter and Is Required for Protein Kinase C-Regulated Dopamine Transporter Trafficking. *J. Neurosci.* **31**, 13758–13770
89. Cremona, M. L., Matthies, H. J. G., Pau, K., Bowton, E., Speed, N., Lute, B. J., Anderson, M., Sen, N., Robertson, S. D., Vaughan, R. a, Rothman, J. E., Galli, A., Javitch, J. a, and Yamamoto, A. (2011) Flotillin-1 is essential for PKC-triggered endocytosis and membrane microdomain localization of DAT. *Nat. Neurosci.* **14**, 469–477

90. Moszczynska, A., Saleh, J., Zhang, H., Vukusic, B., Lee, F. J. S., and Liu, F. (2007) Parkin disrupts the  $\alpha$ -synuclein/dopamine transporter interaction: Consequences toward dopamine-induced toxicity. *J. Mol. Neurosci.* **32**, 217–227
91. Lee, F. J. S., Liu, F., Pristupa, Z. B., and Niznik, H. B. (2001) Direct binding and functional coupling of  $\alpha$ -synuclein to the dopamine transporters accelerate dopamine-induced apoptosis. *FASEB J.* **15**, 916–926
92. Harris, B. Z., and Lim, W. a (2001) Mechanism and role of PDZ domains in signaling complex assembly. *J. Cell Sci.* **114**, 3219–3231
93. Bjerggaard, C., Fog, J. U., Hastrup, H., Madsen, K., Loland, C. J., Javitch, J. a, and Gether, U. (2004) Surface targeting of the dopamine transporter involves discrete epitopes in the distal C terminus but does not require canonical PDZ domain interactions. *J. Neurosci.* **24**, 7024–7036
94. Rickhag, M., Hansen, F. H., Sørensen, G., Strandfelt, K. N., Andresen, B., Gotfryd, K., Madsen, K. L., Vestergaard-Klewe, I., Ammendrup-Johnsen, I., Eriksen, J., Newman, A. H., Füchtbauer, E.-M., Gomeza, J., Woldbye, D. P. D., Wörtwein, G., and Gether, U. (2013) A C-terminal PDZ domain-binding sequence is required for striatal distribution of the dopamine transporter. *Nat. Commun.* **4**, 1580
95. Pizzo, A. B., Karam, C. S., Zhang, Y., Yano, H., Freyberg, R. J., Karam, D. S., Freyberg, Z., Yamamoto, A., McCabe, B. D., and Javitch, J. A. (2013) The membrane raft protein Flotillin-1 is essential in dopamine neurons for amphetamine-induced behavior in *Drosophila*. *Mol. Psychiatry.* **18**, 824–33
96. Glebov, O. O., Bright, N. a, and Nichols, B. J. (2006) Flotillin-1 defines a clathrin-independent endocytic pathway in mammalian cells. *Nat. Cell Biol.* **8**, 46–54
97. Frick, M., Bright, N. a., Riento, K., Bray, A., Merrified, C., and Nichols, B. J. (2007) Coassembly of Flotillins Induces Formation of Membrane Microdomains, Membrane Curvature, and Vesicle Budding. *Curr. Biol.* **17**, 1151–1156
98. Lee, F. J. S., Liu, F., Pristupa, Z. B., and Niznik, H. B. (2001) Direct binding and functional coupling of  $\alpha$ -synuclein to the dopamine transporters accelerate dopamine-induced apoptosis. *FASEB J.* **15**, 916–926
99. Kilic, F., and Rudnick, G. (2000) Oligomerization of serotonin transporter and its functional consequences. *Proc. Natl. Acad. Sci. U. S. A.* **97**, 3106–3111
100. Sorkina, T., Doolen, S., Galperin, E., Zahniser, N. R., and Sorkin, A. (2003) Oligomerization of dopamine transporters visualized in living cells by fluorescence resonance energy transfer microscopy. *J. Biol. Chem.* **278**, 28274–28283

101. Scholze, P., Freissmuth, M., and Sitte, H. H. (2002) Mutations within an intramembrane leucine heptad repeat disrupt oligomer formation of the rat GABA transporter 1. *J. Biol. Chem.* **277**, 43682–43690
102. Chen, N., and Reith, M. E. a (2008) Substrates dissociate dopamine transporter oligomers. *J. Neurochem.* **105**, 910–920
103. Zhen, J., Antonio, T., Cheng, S.-Y., Ali, S., Jones, K. T., and Reith, M. E. a. (2015) Dopamine transporter oligomerization: impact of combining protomers with differential cocaine analog binding affinities. *J. Neurochem.* 10.1111/jnc.13025
104. Pike, L. J. (2006) Rafts defined: a report on the Keystone Symposium on Lipid Rafts and Cell Function. *J. Lipid Res.* **47**, 1597–1598
105. Magnani, F., Tatell, C. G., Wynne, S., Williams, C., and Haase, J. (2004) Partitioning of the serotonin transporter into lipid microdomains modulates transport of serotonin. *J. Biol. Chem.* **279**, 38770–38778
106. Jayanthi, L. D., Samuvel, D. J., and Ramamoorthy, S. (2004) Regulated Internalization and Phosphorylation of the Native Norepinephrine Transporter in Response to Phorbol Esters: Evidence for localization in lipid rafts and lipid raft-mediated internalization. *J. Biol. Chem.* **279**, 19315–19326
107. Butchbach, M. E. R., Tian, G., Guo, H., and Lin, C. L. G. (2004) Association of excitatory amino acid transporters, especially EAAT2, with cholesterol-rich lipid raft microdomains: Importance for excitatory amino acid transporter localization and function. *J. Biol. Chem.* **279**, 34388–34396
108. Foster, J. D., Adkins, S. D., Lever, J. R., and Vaughan, R. A. (2008) Phorbol ester induced trafficking-independent regulation and enhanced phosphorylation of the dopamine transporter associated with membrane rafts and cholesterol. *J. Neurochem.* **105**, 1683–99
109. Adkins, E. M., Samuvel, D. J., Fog, J. U., Eriksen, J., Jayanthi, L. D., Vaegter, C. B., Ramamoorthy, S., and Gether, U. (2007) Membrane mobility and microdomain association of the dopamine transporter studied with fluorescence correlation spectroscopy and fluorescence recovery after photobleaching. *Biochemistry.* **46**, 10484–10497
110. Jones, K. T., Zhen, J., and Reith, M. E. a (2012) Importance of cholesterol in dopamine transporter function. *J. Neurochem.* **123**, 700–715
111. Epand, R. M. (2008) Proteins and cholesterol-rich domains. *Biochim. Biophys. Acta - Biomembr.* **1778**, 1576–1582

112. Fang, C., Deng, L., Keller, C. A., Fukata, M., Fukata, Y., Chen, G., and Lüscher, B. (2006) GODZ-mediated palmitoylation of GABA(A) receptors is required for normal assembly and function of GABAergic inhibitory synapses. *J. Neurosci.* **26**, 12758–68
113. Greaves, J., and Chamberlain, L. H. (2011) DHHC palmitoyl transferases: substrate interactions and (patho)physiology. *Trends Biochem. Sci.* **36**, 245–53
114. Lai, J., and Linder, M. E. (2013) Oligomerization of DHHC protein S-acyltransferases. *J. Biol. Chem.* **288**, 22862–70
115. Greaves, J., Carmichael, J. A., and Chamberlain, L. H. (2011) The palmitoyl transferase DHHC2 targets a dynamic membrane cycling pathway: regulation by a C-terminal domain. *Mol. Biol. Cell.* **22**, 1887–95
116. el-Husseini, A. el-D., and Brecht, D. S. (2002) Protein palmitoylation: a regulator of neuronal development and function. *Nat. Rev. Neurosci.* **3**, 791–802
117. Abrami, L., Kunz, B., Iacovache, I., and van der Goot, F. G. (2008) Palmitoylation and ubiquitination regulate exit of the Wnt signaling protein LRP6 from the endoplasmic reticulum. *Proc. Natl. Acad. Sci. U. S. A.* **105**, 5384–9
118. Levental, I., Lingwood, D., Grzybek, M., Coskun, U., and Simons, K. (2010) Palmitoylation regulates raft affinity for the majority of integral raft proteins. *Proc. Natl. Acad. Sci. U. S. A.* **107**, 22050–4
119. Blaskovic, S., Blanc, M., and van der Goot, F. G. (2013) What does S-palmitoylation do to membrane proteins? *FEBS J.* **280**, 2766–74
120. Iwanaga, T., Tsutsumi, R., Noritake, J., Fukata, Y., and Fukata, M. Dynamic protein palmitoylation in cellular signaling. *Prog. Lipid Res.* **48**, 117–27
121. Charych, E. I., Jiang, L.-X., Lo, F., Sullivan, K., and Brandon, N. J. (2010) Interplay of palmitoylation and phosphorylation in the trafficking and localization of phosphodiesterase 10A: implications for the treatment of schizophrenia. *J. Neurosci.* **30**, 9027–37
122. Linder, M. E., and Deschenes, R. J. (2007) Palmitoylation: policing protein stability and traffic. *Nat. Rev. Mol. Cell Biol.* **8**, 74–84
123. Smotrys, J. E., and Linder, M. E. (2004) Palmitoylation of intracellular signaling proteins: regulation and function. *Annu. Rev. Biochem.* **73**, 559–87
124. Fukata, Y., and Fukata, M. (2010) Protein palmitoylation in neuronal development and synaptic plasticity. *Nat. Rev. Neurosci.* **11**, 161–175

125. Fukata, M., Fukata, Y., Adesnik, H., Nicoll, R. A., and Brecht, D. S. (2004) Identification of PSD-95 palmitoylating enzymes. *Neuron*. **44**, 987–96
126. Mitchell, D. A., Vasudevan, A., Linder, M. E., and Deschenes, R. J. (2006) Protein palmitoylation by a family of DHHC protein S-acyltransferases. *J. Lipid Res.* **47**, 1118–27
127. Salaun, C., Greaves, J., and Chamberlain, L. H. (2010) The intracellular dynamic of protein palmitoylation. *J. Cell Biol.* **191**, 1229–38
128. Tsutsumi, R., Fukata, Y., and Fukata, M. (2008) Discovery of protein-palmitoylating enzymes. *Pflugers Arch.* **456**, 1199–206
129. Fukata, Y., Iwanaga, T., and Fukata, M. (2006) Systematic screening for palmitoyl transferase activity of the DHHC protein family in mammalian cells. *Methods*. **40**, 177–82
130. Roth, A. F., Feng, Y., Chen, L., and Davis, N. G. (2002) The yeast DHHC cysteine-rich domain protein Akr1p is a palmitoyl transferase. *J. Cell Biol.* **159**, 23–8
131. Planey, S. L., and Zacharias, D. A. (2009) Palmitoyl acyltransferases, their substrates, and novel assays to connect them (Review). *Mol. Membr. Biol.* **26**, 14–31
132. Korycka, J., Łach, A., Heger, E., Bogusławska, D. M., Wolny, M., Toporkiewicz, M., Augoff, K., Korzeniewski, J., and Sikorski, A. F. (2012) Human DHHC proteins: a spotlight on the hidden player of palmitoylation. *Eur. J. Cell Biol.* **91**, 107–17
133. Ohno, Y., Kihara, A., Sano, T., and Igarashi, Y. (2006) Intracellular localization and tissue-specific distribution of human and yeast DHHC cysteine-rich domain-containing proteins. *Biochim. Biophys. Acta.* **1761**, 474–83
134. Verkruyse, L. a., and Hofmann, S. L. (1996) Lysosomal Targeting of Palmitoyl-protein Thioesterase. *J. Biol. Chem.* **271**, 15831–15836
135. Fukata, Y., and Fukata, M. (2010) Protein palmitoylation in neuronal development and synaptic plasticity. *Nat. Rev. Neurosci.* **11**, 161–75
136. Kim, S., Zhang, Z., Sarkar, C., Tsai, P., Lee, Y., Dye, L., and Mukherjee, A. B. (2008) Palmitoyl protein thioesterase-1 deficiency impairs synaptic vesicle recycling at nerve terminals, contributing to neuropathology in humans and mice. *J. Clin. Invest.* **118**, 3075–3086

137. Mitchell, D. a. (2006) Protein palmitoylation by a family of DHHC protein S-acyltransferases. *J. Lipid Res.* **47**, 1118–1127
138. Jennings, B. C., and Linder, M. E. (2012) DHHC protein S-acyltransferases use similar ping-pong kinetic mechanisms but display different acyl-CoA specificities. *J. Biol. Chem.* **287**, 7236–45
139. Linder, M. E., and Jennings, B. C. (2013) Mechanism and function of DHHC S-acyltransferases. *Biochem. Soc. Trans.* **41**, 29–34
140. Gottlieb, C. D., Zhang, S., and Linder, M. E. (2015) The Cysteine-rich Domain of the DHHC3 Palmitoyltransferase is Palmitoylated and Contains Tightly Bound Zinc. *J. Biol. Chem.* 10.1074/jbc.M115.691147
141. Mukai, J., Dhillia, A., Drew, L. J., Stark, K. L., Cao, L., MacDermott, A. B., Karayiorgou, M., and Gogos, J. A. (2008) Palmitoylation-dependent neurodevelopmental deficits in a mouse model of 22q11 microdeletion. *Nat. Neurosci.* **11**, 1302–10
142. Mukai, J., Liu, H., Burt, R. A., Swor, D. E., Lai, W.-S., Karayiorgou, M., and Gogos, J. A. (2004) Evidence that the gene encoding ZDHHC8 contributes to the risk of schizophrenia. *Nat. Genet.* **36**, 725–731
143. Butland, S. L., Sanders, S. S., Schmidt, M. E., Riechers, S. P., Lin, D. T. S., Martin, D. D. O., Vaid, K., Graham, R. K., Singaraja, R. R., Wanker, E. E., Conibear, E., and Hayden, M. R. (2014) The palmitoyl acyltransferase HIP14 shares a high proportion of interactors with huntingtin: Implications for a role in the pathogenesis of Huntington’s disease. *Hum. Mol. Genet.* **23**, 4142–4160
144. Young, F. B., Butland, S. L., Sanders, S. S., Sutton, L. M., and Hayden, M. R. (2012) Putting proteins in their place: palmitoylation in Huntington disease and other neuropsychiatric diseases. *Prog. Neurobiol.* **97**, 220–38
145. Mansouri, M. R., Marklund, L., Gustavsson, P., Davey, E., Carlsson, B., Larsson, C., White, I., Gustavson, K.-H., and Dahl, N. (2005) *Loss of ZDHHC15 expression in a woman with a balanced translocation t(X;15)(q13.3;cen) and severe mental retardation.*, 10.1038/sj.ejhg.5201445



146. Raymond, F. L., Tarpey, P. S., Edkins, S., Tofts, C., O'Meara, S., Teague, J., Butler, A., Stevens, C., Barthorpe, S., Buck, G., Cole, J., Dicks, E., Gray, K., Halliday, K., Hills, K., Hinton, J., Jones, D., Menzies, A., Perry, J., Raine, K., Shepherd, R., Small, A., Varian, J., Widaa, S., Mallya, U., Moon, J., Luo, Y., Shaw, M., Boyle, J., Kerr, B., Turner, G., Quarrell, O., Cole, T., Easton, D. F., Wooster, R., Bobrow, M., Schwartz, C. E., Gecz, J., Stratton, M. R., and Futreal, P. A. (2007) Mutations in ZDHHC9, which encodes a palmitoyltransferase of NRAS and HRAS, cause X-linked mental retardation associated with a Marfanoid habitus. *Am. J. Hum. Genet.* **80**, 982–7
147. Young, F. B., Butland, S. L., Sanders, S. S., Sutton, L. M., and Hayden, M. R. (2012) Putting proteins in their place: palmitoylation in Huntington disease and other neuropsychiatric diseases. *Prog. Neurobiol.* **97**, 220–38
148. Gupta, P., Soyombo, a a, Atashband, a, Wisniewski, K. E., Shelton, J. M., Richardson, J. a, Hammer, R. E., and Hofmann, S. L. (2001) Disruption of PPT1 or PPT2 causes neuronal ceroid lipofuscinosis in knockout mice. *Proc. Natl. Acad. Sci. U. S. A.* **98**, 13566–13571
149. Foster, J. D., and Vaughan, R. a (2011) Palmitoylation controls dopamine transporter kinetics, degradation, and protein kinase C-dependent regulation. *J. Biol. Chem.* **286**, 5175–5186
150. Moritz, A. E., Rastedt, D. E., Stanislawski, D. J., Shetty, M., Smith, M. a., Vaughan, R. a., and Foster, J. D. (2015) Reciprocal Phosphorylation and Palmitoylation Control Dopamine Transporter Kinetics. *J. Biol. Chem.* 10.1074/jbc.M115.667055
151. Noritake, J., Fukata, Y., Iwanaga, T., Hosomi, N., Tsutsumi, R., Matsuda, N., Tani, H., Iwanari, H., Mochizuki, Y., Kodama, T., Matsuura, Y., Bredt, D. S., Hamakubo, T., and Fukata, M. (2009) Mobile DHHC palmitoylating enzyme mediates activity-sensitive synaptic targeting of PSD-95. *J. Cell Biol.* **186**, 147–60
152. Cervinski, M. a, Foster, J. D., and Vaughan, R. a (2005) Psychoactive substrates stimulate dopamine transporter phosphorylation and down-regulation by cocaine-sensitive and protein kinase C-dependent mechanisms. *J. Biol. Chem.* **280**, 40442–40449
153. Wan, J., Roth, A. F., Bailey, A. O., and Davis, N. G. (2007) Palmitoylated proteins: purification and identification. *Nat. Protoc.* **2**, 1573–84
154. Vaughan, R. A. (1995) Photoaffinity-labeled ligand binding domains on dopamine transporters identified by peptide mapping. *Mol. Pharmacol.*

155. Gaffaney, J. D., and Vaughan, R. A. (2004) Uptake inhibitors but not substrates induce protease resistance in extracellular loop two of the dopamine transporter. *Mol. Pharmacol.* 10.1124/mol.65.3.692
156. Korycka, J., Łach, A., Heger, E., Bogusławska, D. M., Wolny, M., Toporkiewicz, M., Augoff, K., Korzeniewski, J., and Sikorski, A. F. (2012) Human DHHC proteins: A spotlight on the hidden player of palmitoylation. *Eur. J. Cell Biol.* **91**, 107–117
157. Drisdell, R. C., and Green, W. N. (2004) Labeling and quantifying sites of protein palmitoylation. *Biotechniques.* **36**, 276–85
158. Noritake, J., Fukata, Y., Iwanaga, T., Hosomi, N., Tsutsumi, R., Matsuda, N., Tani, H., Iwanari, H., Mochizuki, Y., Kodama, T., Matsuura, Y., Bredt, D. S., Hamakubo, T., and Fukata, M. (2009) Mobile DHHC palmitoylating enzyme mediates activity-sensitive synaptic targeting of PSD-95. *J. Cell Biol.* **186**, 147–60
159. Fleckenstein, a E., Metzger, R. R., Wilkins, D. G., Gibb, J. W., and Hanson, G. R. (1997) Rapid and reversible effects of methamphetamine on dopamine transporters. *J. Pharmacol. Exp. Ther.* **282**, 834–838
160. Greaves, J., Salaun, C., Fukata, Y., Fukata, M., and Chamberlain, L. H. (2008) Palmitoylation and membrane interactions of the neuroprotective chaperone cysteine-string protein. *J. Biol. Chem.* **283**, 25014–26
161. Tsutsumi, R., Fukata, Y., Noritake, J., Iwanaga, T., Perez, F., and Fukata, M. (2009) Identification of G protein alpha subunit-palmitoylating enzyme. *Mol. Cell. Biol.* **29**, 435–47
162. Blaskovic, S., Adibekian, A., Blanc, M., and van der Goot, G. F. (2014) Mechanistic effects of protein palmitoylation and the cellular consequences thereof. *Chem. Phys. Lipids.* **180**, 44–52
163. Heuser, J. E., and Anderson, R. G. W. (1989) Hypertonic media inhibit receptor-mediated endocytosis by blocking clathrin-coated pit formation. *J. Cell Biol.* **108**, 389–400
164. Charollais, J., and Van Der Goot, F. G. (2009) Palmitoylation of membrane proteins (Review). *Mol. Membr. Biol.* **26**, 55–66
165. Joseph, M., and Nagaraj, R. (1995) Conformations of peptides corresponding to fatty acylation sites in proteins. A circular dichroism study. *J. Biol. Chem.* **270**, 19439–19445

166. McCormick, P. J., Dumaresq-Doiron, K., Pluvisse, A. S., Pichette, V., Tosato, G., and Lefrancois, S. (2008) Palmitoylation controls recycling in lysosomal sorting and trafficking. *Traffic*. **9**, 1984–1997
167. Hayashi, T., Rumbaugh, G., and Huganir, R. L. (2005) Differential Regulation of AMPA Receptor Subunit Trafficking by Palmitoylation of Two Distinct Sites. *Neuron*. **47**, 709–723
168. Gao, Z., Ni, Y., Szabo, G., and Linden, J. (1999) Palmitoylation of the recombinant human A1 adenosine receptor: enhanced proteolysis of palmitoylation-deficient mutant receptors. *Biochem. J.* **342** ( Pt 2, 387–395
169. Ochsenbauer-Jambor, C., Miller, D. C., Roberts, C. R., Rhee, S. S., and Hunter, E. (2001) Palmitoylation of the Rous sarcoma virus transmembrane glycoprotein is required for protein stability and virus infectivity. *J. Virol.* **75**, 11544–11554
170. Percherancier, Y., Planchenault, T., Valenzuela-Fernandez, A., Virelizier, J. L., Arenzana-Seisdedos, F., and Bachelier, F. (2001) Palmitoylation-dependent Control of Degradation, Life Span, and Membrane Expression of the CCR5 Receptor. *J. Biol. Chem.* **276**, 31936–31944
171. Parton, R. G., and Hancock, J. F. (2004) Lipid rafts and plasma membrane microorganization: Insights from Ras. *Trends Cell Biol.* **14**, 141–147
172. Moffett, S., Adam, L., Bonin, H., Loisel, T. P., Bouvier, M., and Mouillac, B. (1996) Palmitoylated cysteine 341 modulates phosphorylation of the beta2-adrenergic receptor by the cAMP-dependent protein kinase. *J. Biol. Chem.* **271**, 21490–7
173. Dorfleutner, A., and Ruf, W. (2003) Regulation of tissue factor cytoplasmic domain phosphorylation by palmitoylation. *Blood*. **102**, 3998–4005
174. Lin, D.-T., Makino, Y., Sharma, K., Hayashi, T., Neve, R., Takamiya, K., and Huganir, R. L. (2009) Regulation of AMPA receptor extrasynaptic insertion by 4.1N, phosphorylation and palmitoylation. *Nat. Neurosci.* **12**, 879–887
175. Miller, G. W., Gainetdinov, R. R., Levey, a I., and Caron, M. G. (1999) Dopamine transporters and neuronal injury. *Trends Pharmacol. Sci.* **20**, 424–9
176. Haddley, K., Vasiliou, a. S., Ali, F. R., Paredes, U. M., Bubb, V. J., and Quinn, J. P. (2008) Molecular Genetics of Monoamine Transporters: Relevance to Brain Disorders. *Neurochem. Res.* **33**, 652–667
177. Hahn, M. K., and Blakely, R. D. (2007) The functional impact of SLC6 transporter genetic variation. *Annu. Rev. Pharmacol. Toxicol.* **47**, 401–441

178. Mazei-Robison, M. S., Bowton, E., Holy, M., Schmudermaier, M., Freissmuth, M., Sitte, H. H., Galli, A., and Blakely, R. D. (2008) Anomalous dopamine release associated with a human dopamine transporter coding variant. *J. Neurosci.* **28**, 7040–6
179. Bowton, E., Saunders, C., Erreger, K., Sakrikar, D., Matthies, H. J., Sen, N., Jessen, T., Colbran, R. J., Caron, M. G., Javitch, J. A., Blakely, R. D., and Galli, A. (2010) Dysregulation of dopamine transporters via dopamine D2 autoreceptors triggers anomalous dopamine efflux associated with attention-deficit hyperactivity disorder. *J. Neurosci.* **30**, 6048–57
180. Sakrikar, D., Mazei-Robison, M. S., Mergy, M. A., Richtand, N. W., Han, Q., Hamilton, P. J., Bowton, E., Galli, A., Veenstra-Vanderweele, J., Gill, M., and Blakely, R. D. (2012) Attention deficit/hyperactivity disorder-derived coding variation in the dopamine transporter disrupts microdomain targeting and trafficking regulation. *J. Neurosci.* **32**, 5385–97
181. Maynard, T. M., Meechan, D. W., Dudevoir, M. L., Gopalakrishna, D., Peters, A. Z., Heindel, C. C., Sugimoto, T. J., Wu, Y., Lieberman, J. A., and Lamantia, A.-S. (2008) Mitochondrial localization and function of a subset of 22q11 deletion syndrome candidate genes. *Mol. Cell. Neurosci.* **39**, 439–51
182. Shin, H. D., Park, B. L., Bae, J. S., Park, T. J., Chun, J. Y., Park, C. S., Sohn, J.-W., Kim, B.-J., Kang, Y.-H., Kim, J. W., Kim, K.-H., Shin, T.-M., and Woo, S.-I. (2010) Association of ZDHHC8 polymorphisms with smooth pursuit eye movement abnormality. *Am. J. Med. Genet. B. Neuropsychiatr. Genet.* **153B**, 1167–72